Photocatalytic Aerobic Oxidative Cleavage of Olefins in Pure Water

Tengfei Niu*, Yang Yang, Feiyan Zhang, Shengjun Chen, Yingxin Guo, Yan Li, Bangqing Ni, Yuming Dong*

Prof. Dr. T. Niu, Ms. Y. Yang, Ms. F. Zhang, Mr. S. Chen, Dr. Y. Guo, Ms. Y. Li, Prof. B. Ni, Prof. Dr. Y. Dong

International Joint Research Center for Photo-responsive Molecules and Materials, Key Laboratory of Synthetic and Biological Colloids, School of Chemical and Material Engineering, Jiangnan University, Wuxi 214122, P. R. China

*E-mail: dongym@jiangnan.edu.cn; niutf@jiangnan.edu.cn

Content Table

General Methods

All chemicals were commercially available and used without further purification. Analytical thin-layer chromatography was performed on glass plates precoated with silica gel impregnated with a fluorescent indicator (254 nm). The plates were visualized by exposure to ultraviolet light. ^{1}H NMR spectra were recorded on Bruker DRX (400 MHz) and ^{13}C NMR spectra on Bruker DRX (100 MHz) spectrometer. Mass spectra were taken on a Finnigan TSQ Quantum-MS instrument in the electrospray ionization (ESI) mode. Elemental analyses were performed on a Yanagimoto MT3CHN recorder.

Materials

Melamine ($C_3H_6N_6$, 99%), hydrochloric acid (HCl 37%), iron (Ⅱ) sulfate heptahydrate ($FeSO_4·7H_2O$, 99%), sodium iodate ($NaIO_3$, 99%), iron (Ⅲ) chloride hexahydrate ($FeCl_3·6H_2O$, 99%), sodium acetate anhydrous (CH_3COONa, 99%), absolute ethyl alcohol (C_2H_5OH), and deionized water. All reagents were used without further purification.

Synthesis of p-g-C_3N_4 composites

Porous g-C_3N_4 (p-g-C_3N_4) were synthesized according to the methods in the literature.[19] First melamine hydrochloride was synthesized by reacting melamine with hydrochloric acid. Then melamine hydrochloride was heated at 500 °C for 2 h in static air with a ramp rate of 20 °C min^{-1}. After that, the powder followed by a further heat treatment at 520 °C for 2 h. The resultant yellow powder was named as p-g-C_3N_4.

Synthesis of the photo-catalyst composites

FeO_x/C_3N_4-P was produced by photo-oxidation deposition. In detail, 20 mg of p-g-C_3N_4 was added in a mixture solution of 2 mL $FeSO_4$ aqueous solution (0.1 M), 2 mL $NaIO_3$ aqueous solution (0.2 M) and 16 mL deionized water. Then, the mixture was degassed by nitrogen about 40 min. Subsequently, this suspension was stirred and irradiated with a 300 W Xe lamp. At last, the product was washed several times with water and alcohol, and dried with nitrogen gas. The final samples by photo-deposition for 1 h, 2 h, 3 h, 4 h were denoted as FeO_x/C_3N_4-P1, FeO_x/C_3N_4-P2, FeO_x/C_3N_4-P3, FeO_x/C_3N_4-P4, respectively. The synthesis pathways of CoO_x/C_3N_4-P3 and MnO_x/C_3N_4-P3 were as the same as FeOx/C_3N_4-P, using $CoSO_4·7H_2O$ and $MnSO_4·H_2O$ as reagent instead of $FeSO_4$.The FeO_x/C_3N_4-H was synthesized through oil bath. The synthesis pathways of this sample were as the same as FeO_x/C_3N_4-P, except for illumination. The experiment was heated at 50 °C. And then the product was washed several times and dried with nitrogen gas. The final samples were named as

FeO_x /C_3N_4-HThe FeO_x/C_3N_4-C nanoplates were fabricated based on the literature report. [2] First, 8.0 mmol of $FeCl_3$ was dissolved into a beaker which containing 80 mL ethanol and 5.6 mL water under stirring. Then 6.4 g of sodium acetate was added into the $FeCl_3$ solution with stirring. Subsequently, the homogenous solution was transferred into a 100 mL Teflon-lined and heated at 180 °C for 12 h. The resulting product was washed with water and ethanol several times, and dried at 80 °C overnight.

The photocatalytic oxidative cleavage of C=C bonds

A 25 mL clean and dry Schlenk reaction tube with a magnetic stirring rotor was equipped with styrene (1 mmol), FeO_x/C_3N_4-P (20 mg) and water (2 mL). The mixture was irradiated under sunlight or Xe lamp (250 W) (the distance of the reaction vial from the lamp is about 6 centimeters) with an oxygen ball for 6 h. The reaction vial cooled by an electric fan at room temperature (approximately 27 °C). After the reaction, the solvent was removed under reduced pressure. Purification of the crude product was achieved by flash column chromatography using petrol n-hexane/ethyl acetate (8:1~16:1) as eluent, and the collected product was evaporated and concentrated in the oven (60 ℃) for further drying and weighing.

In situ attenuated total reflection infrared spectroscopy experimental method

The as-prepared photocatalyst (5 mg) was uniformly dispersed in a Nafion-ethanol solution via ultrasonication for 15 min. Subsequently, 0.1 mL of the suspension was drop-cast onto the in-situ IR reaction cell and dried under ambient conditions. The photocatalyst-loaded cell was then filled with 20 mL of O_2-saturated aqueous styrene solution (0.1 M). Prior to light irradiation, background spectra were recorded in the dark (64 scans, 8 cm^{-1} resolution) under continuous O_2 purging (5 mL/min). Photocatalytic reactions were initiated using a 300 W Xe lamp (λ > 420 nm, 100 mW/cm^2) with simultaneous O_2 flow (5 mL/min). Time-dependent IR spectra were acquired at 5-min intervals for 30 min to monitor the evolution of characteristic vibrational bands. Control experiments were systematically performed using FeOx-free g-C_3N_4 and catalyst-free blank systems under identical conditions. All spectral data were processed using Kubelka-Munk transformation to ensure quantitative comparability.

Sample characterization

The X-ray powder diffraction (XRD) patterns were measured on a D8 X-ray diffractometer (Bruker AXS, German). The UV-vis absorption spectra were evaluated by the UV-3600 spectrophotometer (Shimadzu, Japan). X-ray photoelectron spectroscopy (XPS) was carried out by the ESCALAB 250 Xi (Thermo, USA) X-

ray photoelectron spectrometer with the Al Kα line as the excitation source (hv = 1484.8 eV). TEM (HRTEM) images of samples were determined by JEM-2100 transmission electron microscope (JEOL, Japan) to research the size and lattice stripes of photo-catalyst. The pore size distribution and specific surface area data were measured by N_2 physisorption isotherms on a Micromeritics ASAP 2020 instrument. The photoluminescence (PL) spectra was measured by using the fluorescence spectrophotometer (Cary Eclipse, Varian, USA). The surface photo-voltage (SPV) was collected by a self-developed device. The time-resolved PL emission spectra (375 nm excitation) was performed on a fluorescence spectrophotometer (Edinburgh Instruments, FLS980). The actual chemical composition of the photo-catalyst examined by ICP-MS using a PerkinElmer NexION 300X. The contact angle was performed on an OCA 40 contact angle measuring instruments (Beijing Eastern-Dataphy Instruments Co., Ltd.).

Supplementary Figure

XRD patterns was determined to provide the phase structures information for p-g-C_3N_4 and photo-catalyst composites **(Figure S1a)**. Both p-g-C_3N_4 and FeO_x/C_3N_4-P3 had distinct diffraction peaks at 27.4° which can be indexed to graphitic materials as the (002) crystal plane of p-g-C_3N_4. By comparing p-g-C_3N_4 and FeO_x/C_3N_4-P, the diffraction peaks at 35.7° and 54° can be observed, which was corresponding to Fe_2O_3, respectively. There were some difference between the FeO_x/C_3N_4-H and FeO_x/C_3N_4-P3 samples, indicating that the important role of photo deposition. Besides, the peak at the position of 13.0° was disappeared, suggesting the changes of crystal structure should not be neglected, which was further revealed that FeO_x photo-oxidation deposition at the surface of p-g-C_3N_4. The optical properties **(Figure S1b)** and electronic band structures **(Figure S6)** of the prepared photocatalysts were investigated by UV–vis diffuse reflectance spectra (DRS). Obviously, the p-g-C_3N_4 had an absorption edge of 450 nm, with the calculated band gaps approximately about 2.80 eV. The CB and VB of p-g-C_3N_4 lie at -1.0 and 1.8 eV, respectively. Compared with pure p-g-C_3N_4, FeO_x-B displays a wide light absorption ranging up to 660 nm, resulting from its intrinsic narrow bandgap of 2.02 eV. In addition, the absorption edges of the FeO_x/C_3N_4-P3 were considerably red-shifted to longer wavelengths about at 600 nm, which will result in higher photocatalytic activities of FeO_x/C_3N_4-P3 hetero-structure.

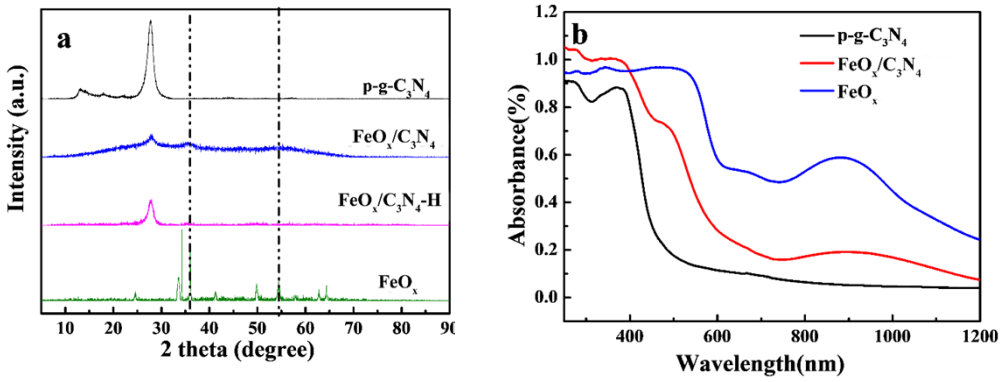

Supplementary Figure 1. (a) XRD patterns and (b) diffuse reflectance UV-vis spectra of p-g-C_3N_4, Fe_2O_3/C_3N_4-P, Fe_2O_3-H/p-g-C_3N_4 and Fe_2O_3-B composites.

X-ray photoelectron spectroscopy was employed to analyse the chemical composition of the FeO_x/C_3N_4-P3 photo-catalyst. The high-resolution XPS spectrum of Fe 2p (**Figure S2a**) can be presented two peaks at 711.4 and 724.0 eV which can be consistent with Fe $2p_{3/2}$ and Fe $2p_{1/2}$, respectively. The O 1s peaks at 532.0 and 529.8 eV which are respectively assigned to the lattice oxygen and surface hydroxyl groups (**Figure S2b**). The XPS spectrum of C 1S and N1s which can be ascribed to the p-g-C_3N_4. The peaks of C 1s (**Figure S2c**) at 285.0 eV and 288.2 eV were attributed to surface adventitious carbon and C–N–C coordination, respectively. The N 1s XPS spectrum of the p-g-C_3N_4 sample (**Figure S2d**) were located at 398.7 eV and 400.5 eV, which corresponding to the C–N–C groups and tertiary nitrogen N–C_3 groups.

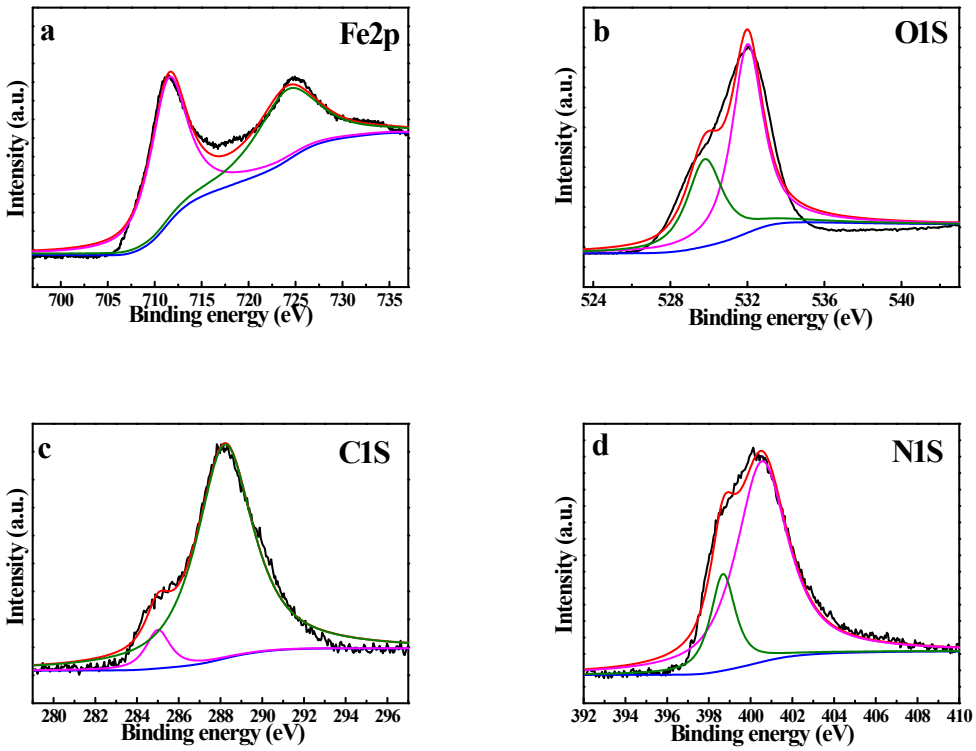

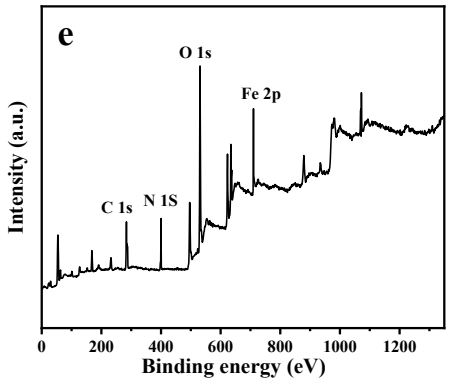

Supplementary Figure 2. XPS high-resolution spectrum of (a) Fe 2p, (b) O 1s, (c) C 1s, (d) N 1s of the FeO_x/p-g-C_3N_4 sample.

The transmission electron microscopy (TEM) images of the samples are shown in **Figure S3.** As shown in **Figure S3a and b**, the p-g-C_3N_4 sample was composed numerous mesopores of one hundred of nanometres in size, revealing the successful porousification in p-g-C_3N_4. The TEM images **(Figure S3c and S3d)** displayed that FeO_x nanoplates successfully deposited on the surface of p-g-C_3N_4 nanosheets. The HRTEM image showed crystalline with a lattice fringe spacing of 0.355 nm, which matched the spacing of the FeO_x lattice (101). And the content of FeO_x in the FeO_x/C_3N_4-P3 sample was calculated to be about 38.2 wt% (obtained by ICP-MS test). Through the result of TEM, the FeO_x are deposited on the surface of margin of p-g-C_3N_4, leading to the formation of a hetero-structure interface.

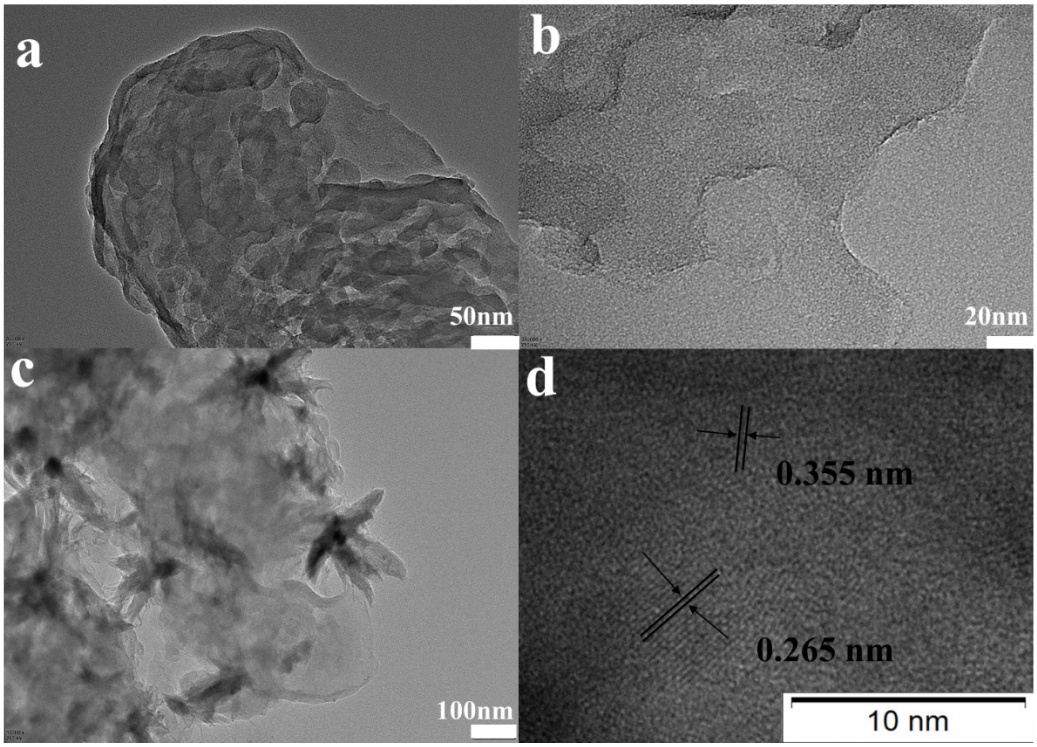

Supplementary Figure 3. (a and b) TEM of p-g-C_3N_4. (c and d) TEM and HRTEM images of FeO_x/C_3N_4-P3 sample.

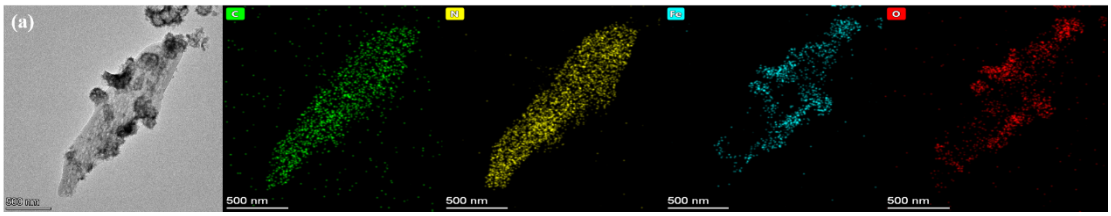

Supplementary Figure 4. The corresponding TEM elemental mapping images of elemental C, N, Fe, and O in the marked area.

The elemental mapping images (Figure S4) clearly demonstrate that elements C, N, Fe, and O are evenly distributed in FeO_x/C_3N_4-P3 sample.

The nitrogen (N_2) adsorption–desorption isotherms were measured and analyzed to characterize the textural properties of the samples (**Figure S5**). Both two samples showed type IV adsorption-desorption isotherms with H_3 hysteresis loop, indicating the formation of fissure-like pore. The Barret–Joyner–Halenda (BJH) pore size distribution curve was given in the inset of **Figure S5**. It was shown that the p-g-C_3N_4 sample displayed double peak size distribution, while the FeO_x/C_3N_4-P3 sample formed an aperture of around 20 nm.

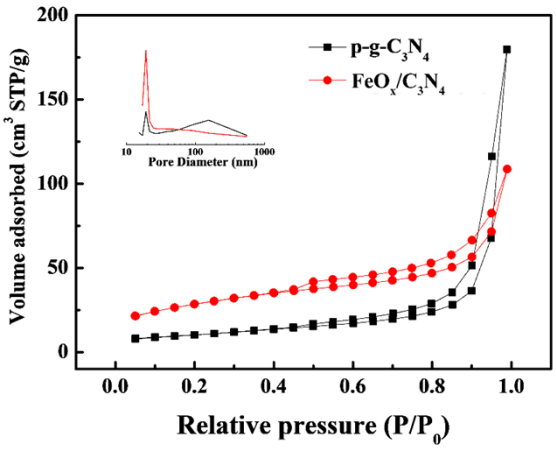

Supplementary Figure 5. Nitrogen adsorption–desorption isotherms and Barret-Joyner-Halenda (BJH) pore size distribution plots (inset) of p-g-C_3N_4 and FeO_x/C_3N_4-P3 composites.

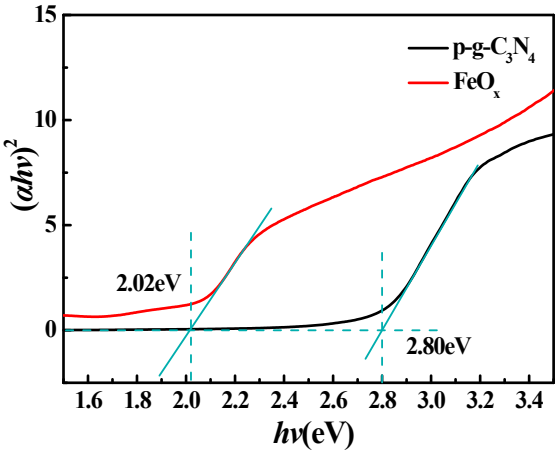

Supplementary Figure 6. Tauc-plot of the $(\alpha hv)^2$ versus hv for p-g-C_3N_4 and Fe_2O_3.

In general, the band edge positions of CB and VB of a semiconductor can be determined using Tauc-plot method. 2 The conduction band (CB) edge of a semiconductor at zero charge can be determined using the following equation:

$$E_{CB} = \chi - E^e - 1/2E_g \quad (1)$$

$$E_{VB} = E_g + E_{CB} \quad (2)$$

Where, E_{CB} is the CB edge potential, E_{VB} is the valance band (VB) edge potential, and χ is the electronegativity of the semiconductor, expressed as the geometric mean of the absolute electronegativity of the constituent atoms, which is defined as the arithmetic mean of the atomic electron affinity and the first ionization energy. E^e is the energy of free electrons on the hydrogen scale ≈4.5 eV and E_g is the band gap of the semiconductor. The CB and VB of Fe_2O_3 can be calculated from the empirical formula, which are 0.36 and 2.38 eV, respectively.

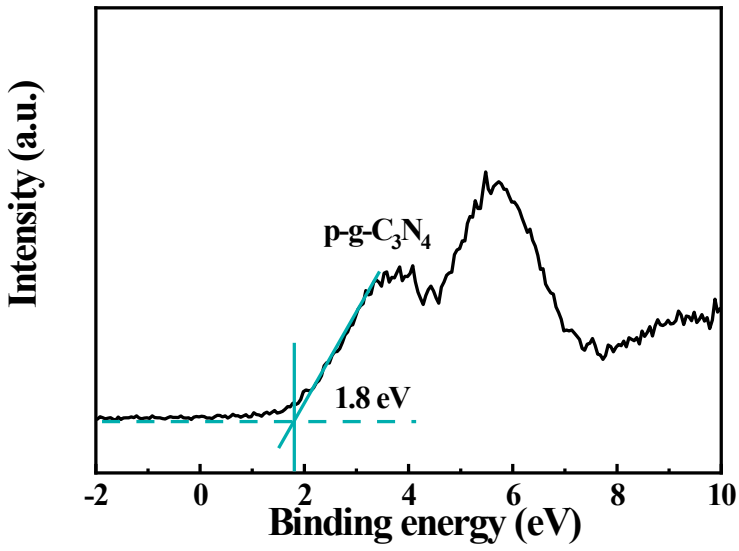

Supplementary Figure 7. Valence band spectra of p-g-C_3N_4.

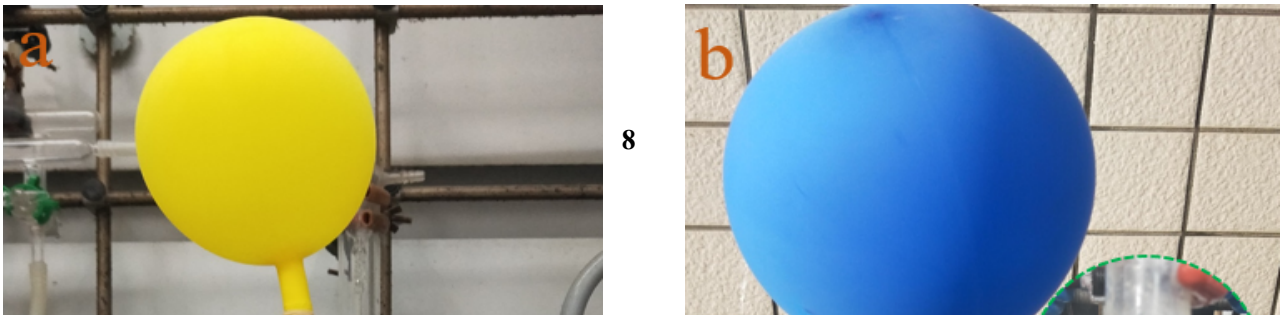

Supplementary Figure 8. Dispersion of p-g-C_3N_4 (a) and FeO_x/C_3N_4-P3 (b) composite in the reaction solution.

Details optimization reaction conditions

Supplementary Table 1. Optimization of reaction conditions[a]

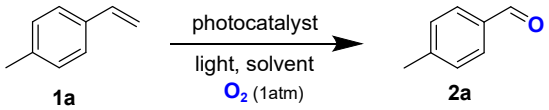

1a **2a**

Entry	Catalyst	Light	solvent	Yield(%)[b]
1	FeO_x/C_3N_4-P1 (20 mg)	Xe lamp (250 W)	H_2O	48
2	FeO_x/C_3N_4-P2 (20 mg)	Xe lamp (250 W)	H_2O	71
3	FeO_x/C_3N_4-P3 (20 mg)	Xe lamp (250 W)	H_2O	78
4	FeO_x/C_3N_4-P4 (20 mg)	Xe lamp (250 W)	H_2O	63
5	CoO_x/C_3N_4-P3 (20 mg)	Xe lamp (250 W)	H_2O	44
6	MnO_x/C_3N_4-P3 (20 mg)	Xe lamp (250 W)	H_2O	53

7	p-g-C_3N_4 (20 mg)	Xe lamp (250 W)	H_2O	40
8	Fe_2O_3/C_3N_4-H (20 mg)	Xe lamp (250 W)	H_2O	42
9	FeO_x/C_3N_4-C (20 mg)	Xe lamp (250 W)	H_2O	57
10	Fe_2O_3 (20 mg)	Xe lamp (250 W)	H_2O	No
11	$Ru(bpy)_3Cl_2$ (2 mol%)	Blue LED (5 W)	H_2O	trace
12	$Ir(ppy)_3$ (2 mol%)	Blue LED (5 W)	H_2O	trace
13	Eosin Y (2 mol%)	Blue LED (5W)	H_2O	trace
14	Rhodamine B (2 mol%)	Blue LED (5 W)	H_2O	trace
15	p-g-C_3N_4 (20 mg)	Xe lamp (250 W)	MeCN/H_2O (1:1)	51
16	FeO_x/C_3N_4-P3 (20 mg)	Xe lamp (250 W)	MeCN/H_2O (1:1)	78
17	FeO_x/C_3N_4-P3 (20 mg)	Xe lamp (250 W)	dry MeCN	trace
18	FeO_x/C_3N_4-P3 (30 mg)	Xe lamp (250 W)	H_2O	73
19	FeO_x/C_3N_4-P3 (10 mg)	Xe lamp (250 W)	H_2O	47
20	without catalyst	Xe lamp (250 W)	H_2O	No
21	FeO_x/C_3N_4-P3 (20 mg)	without light	H_2O	No
22	FeO_x/C_3N_4-P3 (20 mg)	sunlight	H_2O	75

[a] Reactionconditions:4-methylstyrene (1 mmol), solvent (2 mL), the reaction filled with oxygen (1 atm), at room temperature, irradiation for 6 h. [b] isolated yield.

As can be seen, 78% yield of desired oxidative cleavage product was obtained when FeO_x/C_3N_4-P3 was used as photocatalyst after 6 h irradiation (Table S1, entries 3). Other photo-oxidation-doped CoO_x/C_3N_4-P, MnO_x/C_3N_4-P and porous graphite phase carbon nitride (p-g-C_3N_4) were also tested and gave inferior results (Table S1, entries 5-7). Moreover, lower yields of **2a** were obtained when Fe_2O_3-doped C_3N_4 prepared by hydrothermal (Table S1, entry 8) or calcination (Table S1, entry 9). While no reaction was observed when Fe_2O_3 was used directly (Table S1, entry 10). These results highlighting the critical role of the interacting model between C_3N_4 and FeO_x in controlling the activity of the photocatalyst in the aerobic cleavage. Additionally, typical homogeneous photocatalyst such as $Ru(bpy)_3Cl_2$, $Ir(ppy)_3$, Eosin Y and Rhodamine B were also tested, however, not able to provide any significant transformation in water (Table S1, entries 11-14). Although, p-g-C_3N_4 could disperses well in MeCN/H_2O = 1：1, lower yield was obtained when compared the result of Fe_2O_3/C_3N_4-P3 in the same condition (Table S1, entries 15, 16). This observation strongly indicates that the deposited FeO_x significantly improved the dispersion and catalytic performance of the C_3N_4. Further study showed that water had a significant impact on the reaction, trace amount of cleavage product was observed when the reaction carried out in anhydrous MeCN (Table S1, entry 17). In addition, tuning the catalyst amount did not improve the performance (Table S1, entries 18, 19). Finally, the model reaction was carried out without light or photocatalyst. As expected, no desired product was observed respectively. (Table S1, entries 20, 21). It is worth noting that the reaction could work well under sunlight (Table S1, entry 22) which provided an opportunity for the use of inexhaustible solar energy synthesis for fine chemicals.

Supplementary Data

The H_2O^{18} isotope experiment.

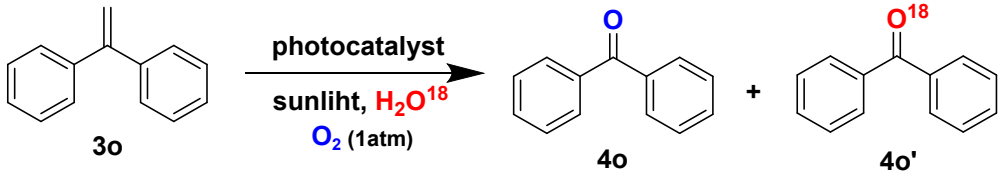

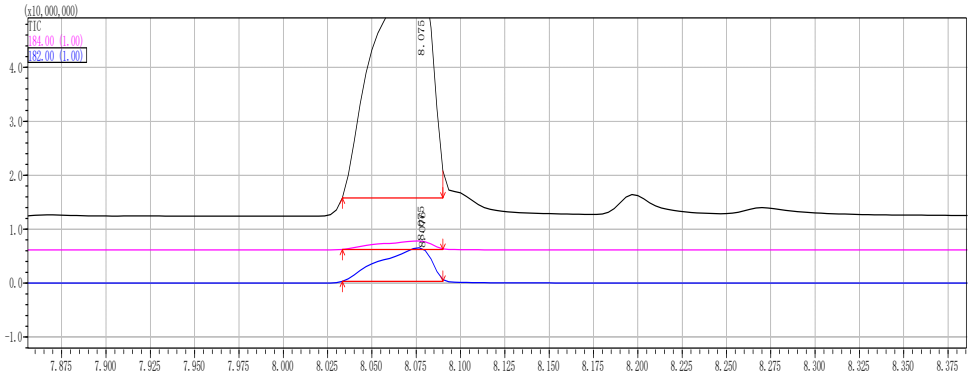

So':So=3221985: 12251171≈1:3.8

The $^{18}O_2$ isotope experiment.

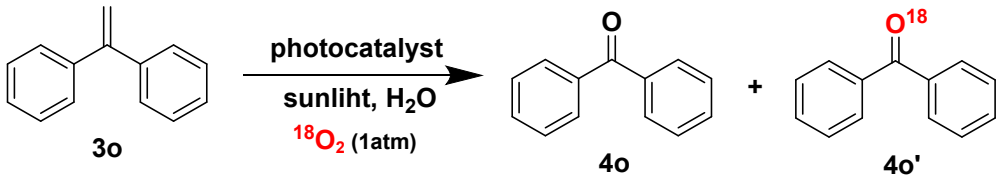

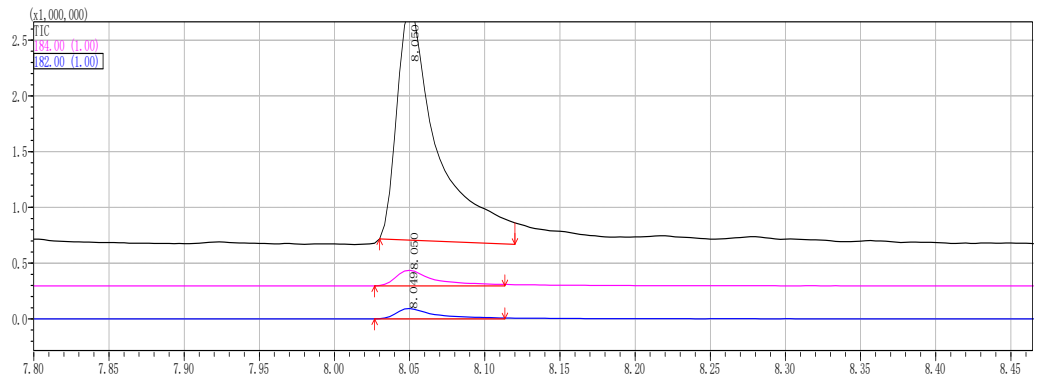

So':So=255877: 171440≈1:0.67

The plausible HO• and HOO• formation process

$$H_2O+O_2 \xrightarrow[\cancel{H_2O_2}]{h\nu,\ C_3N_4} \quad \text{(SR-1)}$$

$Fe^{2+} + H_2O_2 \rightarrow Fe^{3+} + OH^- + OH\cdot$ (SR-2)

$OH\cdot + Fe^{2+} \rightarrow OH^- + Fe^{3+}$ (SR-3)

$Fe^{3+} + H_2O_2 \rightarrow Fe\text{-}OOH_2^+ + H^+$ (SR-4)

$Fe\text{-}OOH_2^+ \rightarrow HO_2\cdot + Fe^{2+}$ (SR-5)

$Fe^{2+} + HO^{2\cdot} \rightarrow Fe^{3+} + HO_2^-$ (SR-6)

$Fe^{3+} + HO2\cdot \rightarrow Fe^{2+} + H^+ + O_2$ (SR-7)

$OH\cdot + H_2O_2 \rightarrow H_2O + HO_2\cdot$ (SR-8)

References

[1] Su, F. Z., Mathew, S. C., Lipner, G., Fu, X. Z., Antonietti, M., Blechert, S., Wang, X. C. *J. Am. Chem. Soc.,* **2010**, *132*, 16299.

[2] Babasaheb, B. S., Gavade, N. L., Shinde, H., Mahajan, P., Lee, K. H., Mane, N., Deshmukh, A., Garadkar, K., Bhuse, V. *ACS Appl. Nano Mater.,* **2018**, *1*, 4682.

NMR Spectra of Products

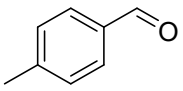

4-Methylbenzaldehyde (**2a**). Colorless liquid (90mg, 75%; 94mg, 78%[b]). ^{1}H NMR (400 MHz, $CDCl_3$) δ 9.96 (s, 1H), 7.78 (d, *J* = 8.1 Hz, 2H), 7.45 – 7.23 (m, 2H), 2.44 (s, 3H). ^{13}C NMR (101 MHz, $CDCl_3$) δ 192.0, 145.5, 134.2, 130.2, 129.8, 129.7, 129.2, 21.8. ESI-MS: m/z =121 $[M+1]^+$.

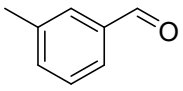

3-Methylbenzaldehyde (**2b**). Colorless liquid (101mg, 84%; 96mg, 80%[b]). ^{1}H NMR (400 MHz, $CDCl_3$) δ 10.01 (s, 1H), 7.70 (dd, *J* = 6.9, 1.1 Hz, 2H), 7.56 – 7.38 (m, 2H), 2.46 (s, 3H). ^{13}C NMR (101 MHz, $CDCl_3$) δ 192.6, 138.9, 136.5, 135.3, 130.0, 128.9, 127.2, 21.2. ESI-MS: m/z =121 $[M+1]^+$.

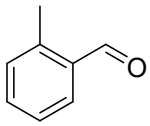

2-Methylbenzaldehyde (**2c**). Colorless liquid (68mg, 57%; 73mg, 61%[b]). ^{1}H NMR (400 MHz, $CDCl_3$) δ 10.27 (s, 1H), 7.80 (dd, *J* = 7.6, 1.2 Hz, 1H), 7.48 (td, *J* = 7.5, 1.4 Hz, 1H), 7.36 (t, *J* = 7.5 Hz, 1H), 7.26 (d, *J* = 7.6 Hz, 1H), 2.67 (s, 3H). ^{13}C NMR (101 MHz, $CDCl_3$) δ 192.8, 140.6, 134.1, 133.7, 132.1, 131.8, 126.3, 19.6. ESI-MS: m/z =121 $[M+1]^+$.

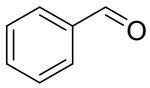

Benzaldehyde (**2d**). Colorless liquid (82mg, 77%; 78mg, 74%[b]). ^{1}H NMR (400 MHz, $CDCl_3$) δ 10.02 (s, 1H), 7.88 (dd, *J* = 8.3, 1.4 Hz, 2H), 7.68 – 7.59 (m, 1H), 7.53 (dd, *J* = 10.4, 4.6 Hz, 2H). ^{13}C NMR (101 MHz, $CDCl_3$) δ 192.4, 136.4, 134.5, 129.7, 129.0. ESI-MS: m/z =107 $[M+1]^+$.

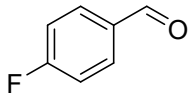

4-Fluorobenzaldehyde (**2e**). Colorless liquid (88mg, 71%; 97mg, 78%[b]). ^{1}H NMR (400 MHz, $CDCl_3$) δ 9.98 (s, 1H), 7.99 – 7.85 (m, 2H), 7.22 (dd, *J* = 11.9, 5.2 Hz, 2H). ^{13}C NMR (101 MHz, $CDCl_3$) δ 190.5, 167.8, 133.0, 133.0, 132.3, 132.2, 116.5, 116.2. ESI-MS: m/z =125 $[M+1]^+$.

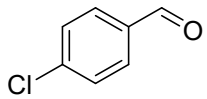

4-Chlorobenzaldehyde (**2f**). Colorless solid (112mg, 80%; 101mg, 72%[b]); m.p. 48℃. ^{1}H NMR (400 MHz, $CDCl_3$) δ 10.00 (s, 1H), 7.91 – 7.79 (m, 2H), 7.58 – 7.48 (m, 2H). ^{13}C NMR (101 MHz, CD_3OD) δ 197.3, 144.6, 140.1, 136.4, 134.5. ESI-MS: m/z =141 $[M+1]^+$.

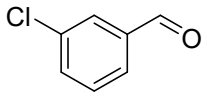

3-Chlorobenzaldehyde (**2g**). Colorless liquid (99mg, 71%; 102mg, 73%[b]). ^{1}H NMR (400 MHz, $CDCl_3$) δ 9.98 (s, 1H), 7.85 (t, *J* = 1.8 Hz, 1H), 7.77 (dt, *J* = 7.6, 1.3 Hz, 1H), 7.60 (ddd, *J* = 8.0, 2.2, 1.2 Hz, 1H), 7.49 (t, *J* = 7.8 Hz, 1H). ^{13}C NMR (101 MHz, $CDCl_3$) δ 190.8, 137.8, 135.4, 134.4, 130.4, 129.3, 128.0. ESI-MS: m/z =141 $[M+1]^+$.

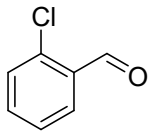

2-Chlorobenzaldehyde (**2h**). Colorless liquid (64mg, 46%; 76mg, 54%[b]). ^{1}H NMR (400 MHz, $CDCl_3$) δ 10.48 (d, *J* = 0.8 Hz, 1H), 7.92 (dd, *J* = 7.7, 1.8 Hz, 1H), 7.53 (ddd, *J* = 8.1, 7.2, 1.8 Hz, 1H), 7.48 – 7.43 (m, 1H), 7.41 – 7.36 (m, 1H). ^{13}C NMR (101 MHz, $CDCl_3$) δ 189.7, 137.9, 135.1, 132.5, 130.6, 129.4, 127.3. ESI-MS: m/z =141 $[M+1]^+$.

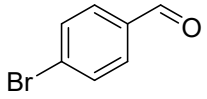

4-Bromobenzaldehyde (**2i**). Colorless solid (142mg, 77%; 125mg, 68%[b]); m.p. 55-58℃. ^{1}H NMR (400 MHz, $CDCl_3$) δ 10.00 (s, 1H), 7.83 – 7.74 (m, 2H), 7.73 – 7.66 (m, 2H). ^{13}C NMR (101 MHz, $CDCl_3$) δ 191.0, 135.1, 132.4, 131.0, 129.7. ESI-MS: m/z =185 $[M+1]^+$.

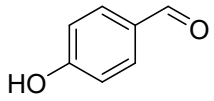

4-Hydroxybenzaldehyde (**2j**). Yellow solid (81mg, 66%; 84mg, 69%[b]); m.p. 112-116℃. ^{1}H NMR (400 MHz, $CDCl_3$) δ 9.89 (s, 1H), 7.91 – 7.79 (m, 2H), 7.08 – 6.94 (m, 2H). ^{13}C NMR (101 MHz, $CDCl_3$) δ 191.18, 161.54, 132.51, 129.92, 116.01. ESI-MS: m/z =123$[M+1]^+$.

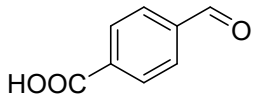

4-Formylbenzoic acid (**2k**). White solid (113mg, 75%; 105mg, 70%[b]); m.p. 247℃. ^{1}H NMR (400 MHz, DMSO) δ 13.39 (s, 1H), 10.09 (s, 1H), 8.19 – 8.08 (m, 2H), 8.06 – 7.95 (m, 2H). ^{13}C NMR (101 MHz, DMSO) δ 193.4, 167.0, 139.3, 136.1, 130.4, 130.0. ESI-MS: m/z =151 $[M+1]^+$.

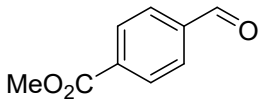

Methyl 4-formylbenzoate (**2l**). White solid (115mg, 70%; 126mg, 77%[b]); m.p. 59-63℃. ^{1}H NMR (400 MHz, $CDCl_3$) δ 10.10 (s, 1H), 8.26 – 8.14 (m, 2H), 8.02 – 7.88 (m, 2H), 3.96 (s, 3H). ^{13}C NMR (101 MHz, $CDCl_3$) δ 191.6, 166.0, 139.2, 135.1, 130.2, 129.5, 52.5. ESI-MS: m/z =165 $[M+1]^+$.

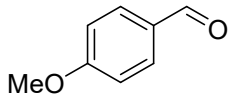

4-Methoxybenzaldehyde (**2m**). Colorless liquid (84mg, 62%; 90mg, 66%[b]). ^{1}H NMR (400 MHz, $CDCl_3$) δ 9.89 (s, 1H), 7.96 – 7.76 (m, 2H), 7.12 – 6.92 (m, 2H), 3.89 (s, 3H). ^{13}C NMR (101 MHz, $CDCl_3$) δ 190.8, 164.6, 132.0, 130.0, 114.3, 55.6. ESI-MS: m/z =137 $[M+1]^+$.

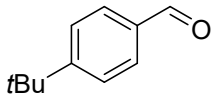

4-(Tert-butyl)benzaldehyde (**2n**). Faint yellow liquid (115mg, 71%; 109mg, 67%[b]). ^{1}H NMR (400 MHz, $CDCl_3$) δ 10.01 (s, 1H), 7.84 (d, *J* = 8.4 Hz, 2H), 7.58 (d, *J* = 8.3 Hz, 2H), 1.38 (s, 9H). ^{13}C NMR (101 MHz, $CDCl_3$) δ 192.0, 158.4, 134.1, 129.7, 126.0, 35.4, 31.1. ESI-MS: m/z =163 $[M+1]^+$.

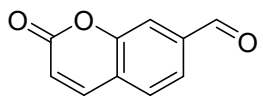

2-Oxo-2H-chromene-7-carbaldehyde (**2o**). White solid (101mg, 58%; 110mg, 63%[b]); m.p. 90-92℃. ^{1}H NMR (400 MHz, $CDCl_3$) δ 10.11 (s, 1H), 7.86 – 7.73 (m, 3H), 7.68 (d, *J* = 8.3 Hz, 1H), 6.60 (d, *J* = 9.6 Hz, 1H). ^{13}C NMR (101 MHz, $CDCl_3$) δ 190.5, 159.8, 154.2, 142.3, 138.4, 128.7, 124.5, 123.3, 119.5, 118.2. ESI-MS: m/z =175 $[M+1]^+$.

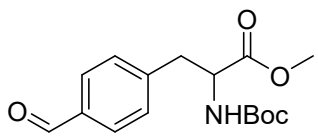

Methyl 2-((tert-butoxycarbonyl)amino)-3-(4-formylphenyl)propanoate (**2p**). White solid (212mg, 69%; 224mg, 73%[b]); m.p. 201-203℃. ^{1}H NMR (400 MHz, MeOD) δ 9.97 (s, 1H), 7.86 (d, *J* = 8.0 Hz, 2H), 7.46 (d, *J* = 8.0 Hz, 2H), 7.22 (d, *J* = 7.9 Hz, 1H), 4.44 (dd, *J* = 9.4, 5.4 Hz, 1H), 3.73 (s, 3H), 3.25 (dd, *J* = 13.8, 5.3 Hz, 1H), 3.02 (dd, *J* = 13.7, 9.5 Hz, 1H), 1.38 (s, 9H). ^{13}C NMR (101 MHz, MeOD) δ 192.4, 172.4, 156.4, 144.7, 135.3, 129.8, 129.4, 79.3, 54.7, 51.3, 37.4, 27.2. ESI-MS: m/z =308 $[M+1]^+$.

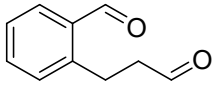

2-(3-Oxopropyl)benzaldehyde (**2q**). Yellow liquid (79mg, 49%). ^{1}H NMR (400 MHz, $CDCl_3$) δ 10.19 (s, 1H), 9.85 (s, 1H), 7.83 (dd, *J* = 7.6, 1.3 Hz, 1H), 7.55 (td, *J* = 7.4, 1.4 Hz, 1H), 7.50 – 7.43 (m, 1H), 7.35 (d, *J* = 7.4 Hz, 1H), 3.38 (t, *J* = 7.5 Hz, 2H), 2.82 (td, *J* = 7.5, 1.2 Hz, 2H). ^{13}C NMR (101 MHz, $CDCl_3$) δ 195.7, 189.1, 140.4, 130.6, 130.2, 129.9, 127.4, 126.5, 125.0, 123.6, 123.0, 41.1, 27.9, 23.8. ESI-MS: m/z =163 $[M+1]^+$.

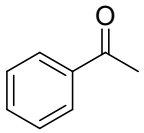

Acetophenone (**4a**). Colorless liquid (101mg, 84%). ^{1}H NMR (400 MHz, $CDCl_3$) δ 8.07 – 7.88 (m, 2H), 7.62 – 7.54 (m, 1H), 7.52 – 7.45 (m, 2H), 2.62 (s, 3H). ^{13}C NMR (126 MHz, $CDCl_3$) δ 197.1, 136.0, 132.0, 130.0, 128.4, 26.6. ESI-MS: m/z =121 $[M+1]^+$.

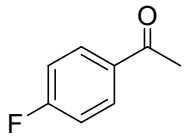

1-(4-Fluorophenyl)ethan-1-one (**4b**). Colorless liquid (115mg, 83%). ^{1}H NMR (400 MHz, $CDCl_3$) δ 8.10 – 7.83 (m, 2H), 7.09 (t, *J* = 8.6 Hz, 2H), 2.55 (s, 3H). ^{13}C NMR (101 MHz, $CDCl_3$) δ 196.4, 167.0, 164.5, 133.6, 133.6, 131.0, 130.9, 115.7, 115.5, 26.5. ESI-MS: m/z =139 $[M+1]^+$.

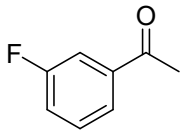

1-(3-Fluorophenyl)ethan-1-one (**4c**). Colorless liquid (112mg, 81%). ^{1}H NMR (400 MHz, $CDCl_3$) δ 7.76 – 7.68 (m, 1H), 7.62 (ddd, *J* = 9.5, 2.4, 1.6 Hz, 1H), 7.43 (td, *J* = 8.0, 5.5 Hz, 1H), 7.30 – 7.20 (m, 1H), 2.59 (s, 3H). ^{13}C NMR (101 MHz, $CDCl_3$) δ 196.7, 196.6, 164.1, 161.6, 139.2, 139.2, 130.3, 130.2, 124.1, 124.1, 120.2, 119.9, 115.0, 114.8, 26.6. ESI-MS: m/z =139 $[M+1]^+$.

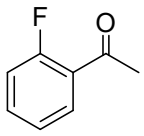

1-(2-Fluorophenyl)ethan-1-one (**4d**). Colorless liquid (55mg, 40%). ^{1}H NMR (400 MHz, $CDCl_3$) δ 7.86 (td, *J* = 7.7, 1.9 Hz, 1H), 7.51 (dddd, *J* = 8.3, 7.1, 5.0, 1.9 Hz, 1H), 7.24 – 7.17 (m, 1H), 7.12 (ddd, *J* = 11.2, 8.3, 0.8 Hz, 1H), 2.63 (d, *J* = 4.9 Hz, 3H). ^{13}C NMR (101 MHz, $CDCl_3$) δ 195.8, 195.8, 163.5, 160.9, 134.7, 134.6, 130.6, 130.5, 125.8, 125.7, 124.4, 124.3, 116.7, 116.5, 31.4, 31.3. ESI-MS: m/z =139 $[M+1]^+$.

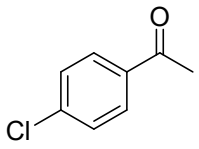

1-(4-Chlorophenyl)ethan-1-one (**4e**). Colorless liquid (126mg, 82%). ^{1}H NMR (400 MHz, $CDCl_3$) δ 8.04 – 7.82 (m, 2H), 7.58 – 7.36 (m, 2H), 2.62 (s, 3H). ^{13}C NMR (101 MHz, $CDCl_3$) δ 196.8, 139.6, 135.5, 129.7, 128.9, 26.5. ESI-MS: m/z =155 $[M+1]^+$.

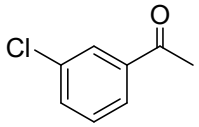

1-(3-Chlorophenyl)ethan-1-one (**4f**). Faint yellow liquid (120mg, 78%). ^{1}H NMR (400 MHz, $CDCl_3$) δ 7.92 (t, *J* = 1.8 Hz, 1H), 7.86 – 7.78 (m, 1H), 7.53 (ddd, *J* = 8.0, 2.1, 1.1 Hz, 1H), 7.40 (t, *J* = 7.9 Hz, 1H), 2.59 (s, 3H). ^{13}C NMR (101 MHz, $CDCl_3$) δ 196.6, 138.6, 134.9, 133.0, 129.9, 128.4, 126.4, 26.6. ESI-MS: m/z =155 $[M+1]^+$.

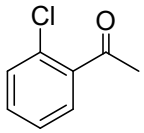

1-(2-Chlorophenyl)ethan-1-one (**4g**). Colorless liquid (71mg, 46%). ^{1}H NMR (400 MHz, $CDCl_3$) δ 7.58 – 7.51 (m, 1H), 7.46 – 7.35 (m, 2H), 7.32 (ddd, *J* = 7.5, 6.9, 1.8 Hz, 1H), 2.65 (s, 3H). ^{13}C NMR (101 MHz, $CDCl_3$) δ 200.4, 139.2, 132.0, 131.3, 130.6, 129.4, 126.9, 30.7. ESI-MS: m/z =155 $[M+1]^+$.

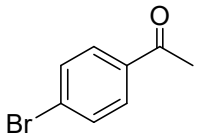

1-(4-Bromophenyl)ethan-1-one (**4h**). Colorless solid (135mg, 68%); m.p. 108-110℃. ^{1}H NMR (400 MHz, $CDCl_3$) δ 7.95 – 7.72 (m, 2H), 7.70 – 7.51 (m, 2H), 2.59 (s, 3H). ^{13}C NMR (101 MHz, $CDCl_3$) δ 197.0, 135.8, 131.9, 129.8, 128.3, 26.5. ESI-MS: m/z =199 $[M+1]^+$.

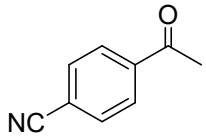

4-Acetylbenzonitrile (**4i**). Faint yellow crystalline powder (119mg, 82%); m.p. 56-59℃. ^{1}H NMR (400 MHz, $CDCl_3$) δ 8.14 – 7.89 (m, 2H), 7.76 (d, *J* = 8.5 Hz, 2H), 2.63 (s, 3H). ^{13}C NMR (101 MHz, $CDCl_3$) δ 196.5, 139.9, 132.5, 128.7, 117.9, 116.4, 26.7. ESI-MS: m/z =146 $[M+1]^+$.

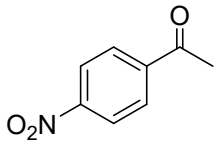

1-(4-Nitrophenyl)ethan-1-on (**4j**). Light yellow crystal (142mg, 86%); m.p. 75-78℃. ^{1}H NMR (400 MHz, $CDCl_3$) δ 8.30 (d, *J* = 8.9 Hz, 2H), 8.19 – 8.01 (m, 2H), 2.68 (s, 3H). ^{13}C NMR (101 MHz, $CDCl_3$) δ 196.3, 150.4, 141.4, 129.3, 123.8, 26.9. ESI-MS: m/z =166 $[M+1]^+$.

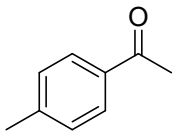

1-(*P*-tolyl)ethan-1-one (**4k**). Colorless liquid (115g, 86%). ^{1}H NMR (400 MHz, $CDCl_3$) δ 7.88 (d, *J* = 8.2 Hz, 2H), 7.36 – 7.22 (m, 2H), 2.61 (s, 3H), 2.44 (s, 3H). ^{13}C NMR (101 MHz, $CDCl_3$) δ 197.8, 143.9, 134.8, 129.2, 128.4, 26.5, 21.6. ESI-MS: m/z =135 $[M+1]^+$.

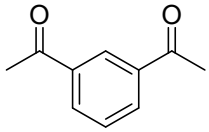

1,1'-(1,3-Phenylene)bis(ethan-1-one) (**4l**). Yellow liquid (115mg, 71%). ^{1}H NMR (400 MHz, $CDCl_3$) δ 8.53 (t, *J* = 1.6 Hz, 1H), 8.16 (dd, *J* = 7.8, 1.7 Hz, 2H), 7.59 (t, *J* = 7.7 Hz, 1H), 2.67 (s, 6H). ^{13}C NMR (101 MHz, $CDCl_3$) δ 197.3, 137.4, 132.5, 129.0, 128.0, 26.7. ESI-MS: m/z =163 $[M+1]^+$.

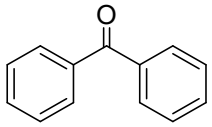

Benzophenone (**4m**). White solid (166mg, 91%); m.p. 47-51℃. ^{1}H NMR (400 MHz, $CDCl_3$) δ 7.84 (ddd, *J* = 7.3, 2.9, 1.6 Hz, 4H), 7.67 – 7.58 (m, 2H), 7.51 (tt, *J* = 6.7, 1.2 Hz, 4H). ^{13}C NMR (101 MHz, $CDCl_3$) δ 196.8, 137.6, 132.4, 130.1, 128.3. ESI-MS: m/z =183 $[M+1]^+$.

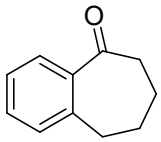

6,7,8,9-Tetrahydro-5H-benzo[7]annulen-5-one (**4n**). Colorless liquid (61mg, 39%). ^{1}H NMR (400 MHz, $CDCl_3$) δ 7.72 (dd, *J* = 7.7, 1.2 Hz, 1H), 7.40 (td, *J* = 7.5, 1.4 Hz, 1H), 7.33 – 7.24 (m, 1H), 7.19 (d, *J* = 7.5 Hz, 1H), 3.00 – 2.82 (m, 2H), 2.81 – 2.63 (m, 2H), 1.98 – 1.67 (m, 4H). ^{13}C NMR (101 MHz, $CDCl_3$) δ 206.1, 141.3, 138.8, 132.2, 129.7, 128.5, 126.6, 40.8, 32.5, 25.2, 20.9. ESI-MS: m/z =161 $[M+1]^+$.

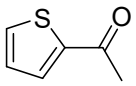

1-(Thiophen-2-yl)ethan-1-one (**4o**). Yellow liquid (111mg, 88%). ^{1}H NMR (400 MHz, $CDCl_3$) δ 7.65 (ddd, *J* = 6.0, 4.4, 1.0 Hz, 2H), 7.11 (dd, *J* = 4.9, 3.8 Hz, 1H), 2.54 (s, 3H). ^{13}C NMR (101 MHz, $CDCl_3$) δ 190.7, 144.5, 133.8, 132.5, 128.2, 26.9. ESI-MS: m/z =127 $[M+1]^+$.

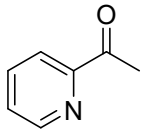

1-(Pyridin-2-yl)ethan-1-one (**4p**). Colorless liquid (68mg, 56%). ^{1}H NMR (400 MHz, $CDCl_3$) δ 8.61 (ddd, *J* = 4.7, 1.5, 0.8 Hz, 1H), 8.02 – 7.90 (m, 1H), 7.76 (td, *J* = 7.7, 1.7 Hz, 1H), 7.40 (ddd, *J* = 7.5, 4.8, 1.2 Hz, 1H), 2.65 (s, 3H). ^{13}C NMR (101 MHz, $CDCl_3$) δ 196.7, 196.6, 164.1, 161.6, 139.2, 139.2, 130.3, 130.2, 124.1, 124.1, 120.2, 119.9, 115.0, 114.8, 26.6. ESI-MS: m/z =122 $[M+1]^+$.

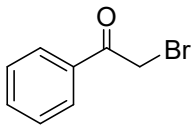

2-Bromo-1-phenylethan-1-one (**4q**). Colorless solid (127mg, 64%[c]); m.p. 48-51℃. ^{1}H NMR (400 MHz, $CDCl_3$) δ 8.06 – 7.97 (m, 2H), 7.68 – 7.57 (m, 1H), 7.51 (td, *J* = 7.9, 3.9 Hz, 2H), 4.48 (s, 2H). ^{13}C NMR (101 MHz, $CDCl_3$) δ 191.3, 134.0, 130.4, 129.2, 128.9, 128.9, 31.0. ESI-MS: m/z =199 $[M+1]^+$.

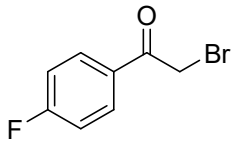

2-Bromo-1-(4-fluorophenyl)ethan-1-one (**4r**). White powder (177mg, 82%); m.p. 47-49℃. ^{1}H NMR (400 MHz, $CDCl_3$) δ 8.14 – 7.92 (m, 2H), 7.23 – 7.10 (m, 2H), 4.43 (s, 2H). ^{13}C NMR (101 MHz, $CDCl_3$) δ 189.9, 167.4, 164.9, 131.8, 131.7, 130.4, 130.3, 116.2, 116.0, 30.5. ESI-MS: m/z =217 $[M+1]^+$.

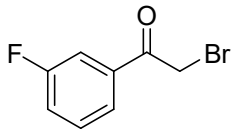

2-Bromo-1-(3-fluorophenyl)ethan-1-one (**4s**). White solid (166mg, 77%); m.p. 34-35℃. ^{1}H NMR (400 MHz, $CDCl_3$) δ 7.79 (ddd, *J* = 7.8, 1.5, 1.0 Hz, 1H), 7.69 (ddd, *J* = 9.3, 2.5, 1.7 Hz, 1H), 7.51 (td, *J* = 8.0, 5.5 Hz, 1H), 7.33 (tdd, *J* = 8.2, 2.6, 0.9 Hz, 1H), 4.44 (s, 2H). ^{13}C NMR (101 MHz, $CDCl_3$) δ 190.2, 190.1, 164.1, 161.6, 136.0, 135.9, 130.6, 130.6, 124.8, 124.7, 115.8, 115.6, 30.5. ESI-MS: m/z =217 $[M+1]^+$.

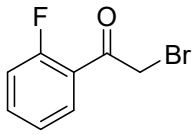

2-Bromo-1-(2-fluorophenyl)ethan-1-one (**4t**). Yellow liquid (153mg, 71%). ^{1}H NMR (400 MHz, $CDCl_3$) δ 7.93 (td, *J* = 7.6, 1.9 Hz, 1H), 7.59 (dddd, *J* = 8.3, 7.2, 5.1, 1.9 Hz, 1H), 7.28 (ddd, *J* = 8.4, 7.0, 1.1 Hz, 1H), 7.18 (ddd, *J* = 11.3, 8.3, 0.9 Hz, 1H), 4.53 (d, *J* = 2.4 Hz, 2H). ^{13}C NMR (101 MHz, $CDCl_3$) δ 189.1, 189.1, 163.0, 160.4, 135.7, 135.6, 131.5, 131.5, 124.9, 124.9, 116.8, 116.6, 36.1, 36.0. ESI-MS: m/z =217 $[M+1]^+$.

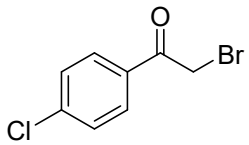

2-Bromo-1-(4-chlorophenyl)ethan-1-one (**4u**). White solid (195mg, 84%); m.p. 93-96℃. ^{1}H NMR (400 MHz, $CDCl_3$) δ 8.03 – 7.88 (m, 2H), 7.57 – 7.42 (m, 2H), 4.43 (s, 2H). ^{13}C NMR (101 MHz, $CDCl_3$) δ 190.2, 140.5, 132.3, 130.4, 129.2, 30.4. ESI-MS: m/z =233 $[M+1]^+$.

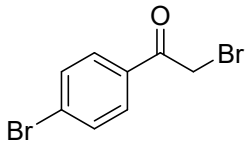

2-Bromo-1-(4-bromophenyl)ethan-1-one (**4v**). Colorless solid (226mg, 82%); m.p. 108-110℃. ^{1}H NMR (400 MHz, $CDCl_3$) δ 7.90 – 7.78 (m, 2H), 7.69 – 7.55 (m, 2H), 4.42 (s, 2H). ^{13}C NMR (101 MHz, $CDCl_3$) δ 190.4, 132.7, 132.2, 130.4, 129.3, 30.5. ESI-MS: m/z =277 $[M+1]^+$.

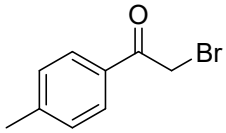

2-Bromo-1-(p-tolyl)ethan-1-one (**4w**). White solid (182mg, 86%); m.p. 46-48℃. ^{1}H NMR (400 MHz, $CDCl_3$) δ 7.90 (d, *J* = 8.3 Hz, 2H), 7.30 (dd, *J* = 11.0, 3.0 Hz,2H), 4.45 (s, 2H), 2.45 (s, 3H). ^{13}C NMR (101 MHz, $CDCl_3$) δ 191.0, 145.1, 131.5, 129.6, 129.1, 31.0, 21.8. ESI-MS: m/z =213 $[M+1]^+$.

[b] irradiated under 250W Xe lamp.

NMR Spectra

Compound 2a

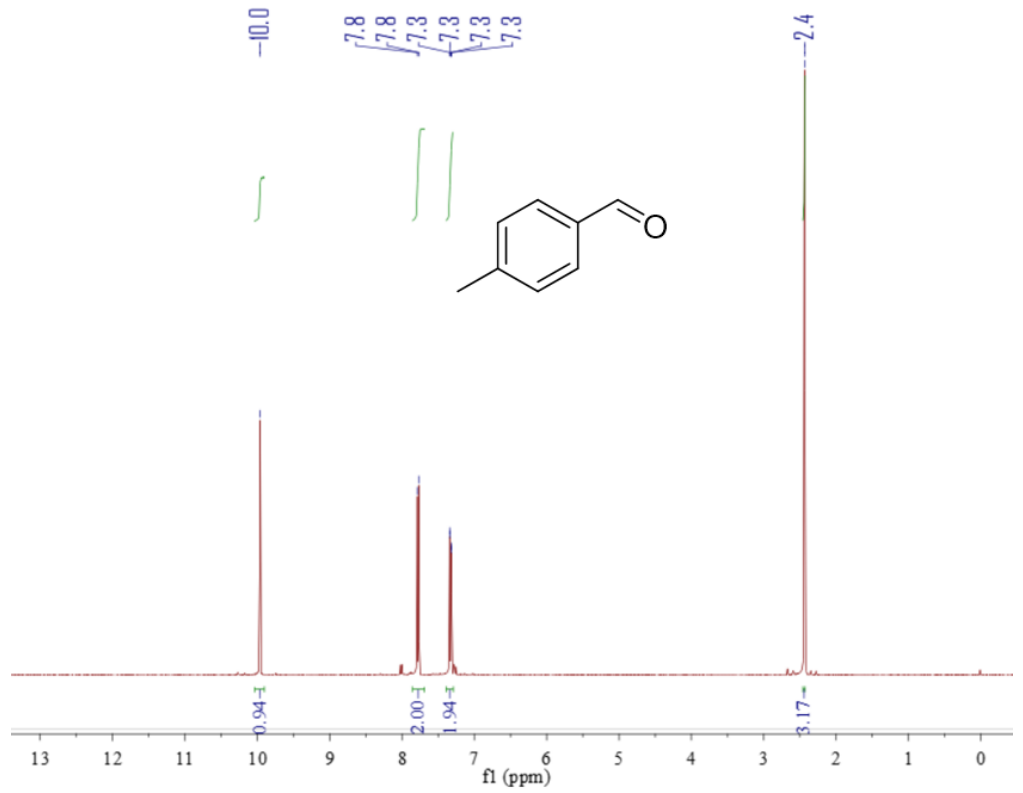
10.0
7.8
7.8
7.3
7.3
7.3
7.3
2.4
O
0.94
2.00
1.94
3.17
13 12 11 10 9 8 7 6 5 4 3 2 1 0
f1 (ppm)

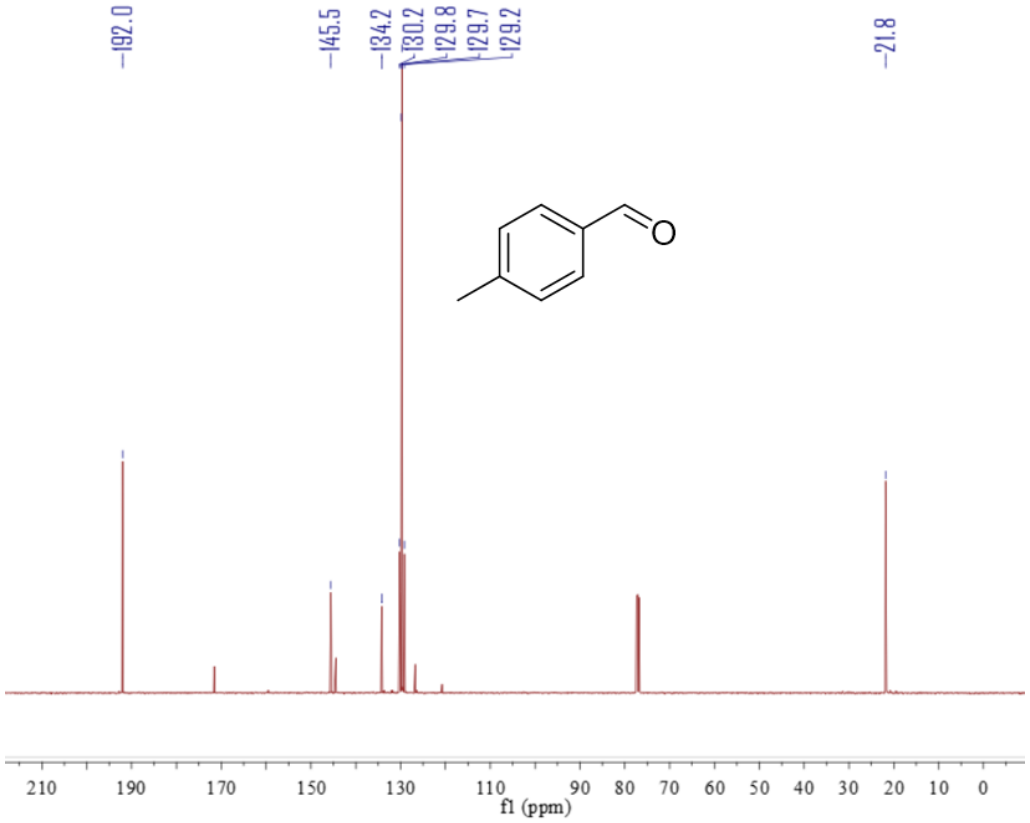
192.0
145.5
134.2
130.2
129.8
129.7
129.2
21.8
O
210 190 170 150 130 110 90 80 70 60 50 40 30 20 10 0
f1 (ppm)

Compound 2b

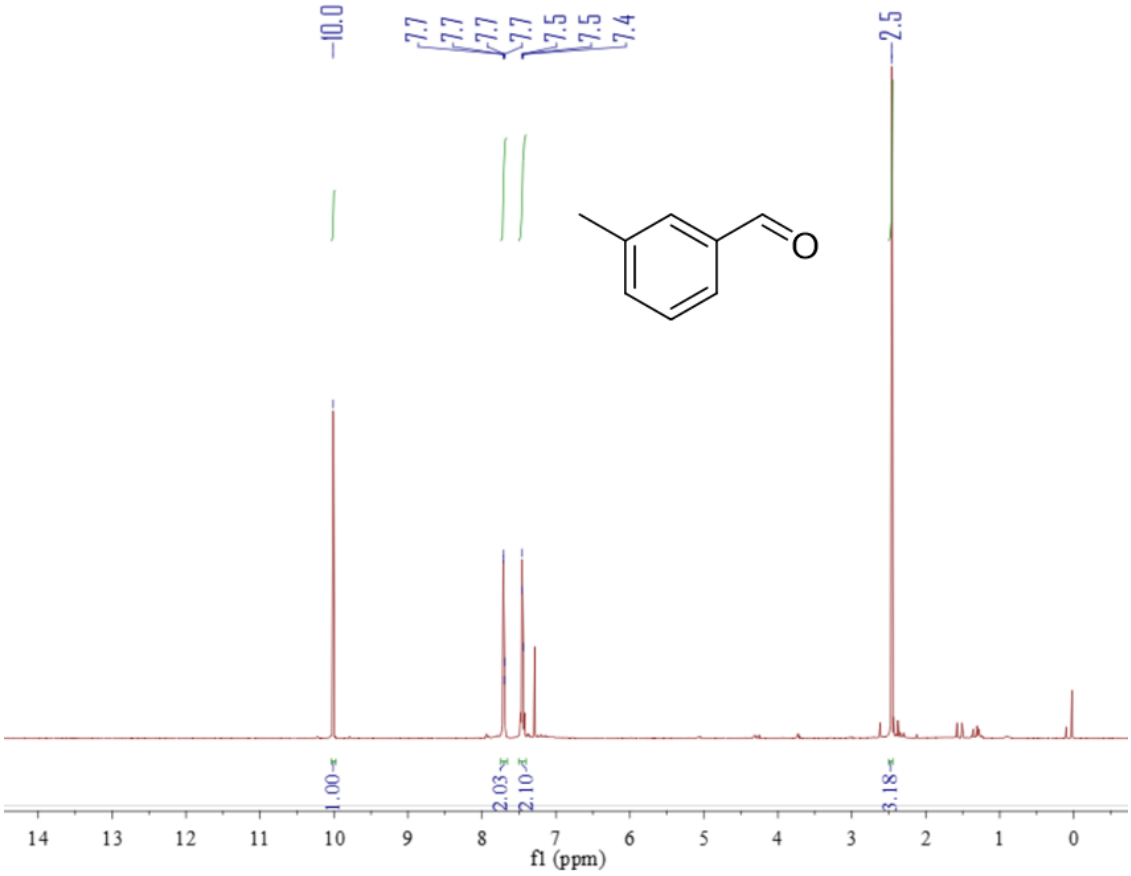
10.0
7.7
7.7
7.7
7.7
7.5
7.5
7.4
2.5
O
1.00
2.03
2.10
3.18
14 13 12 11 10 9 8 7 6 5 4 3 2 1 0
f1 (ppm)

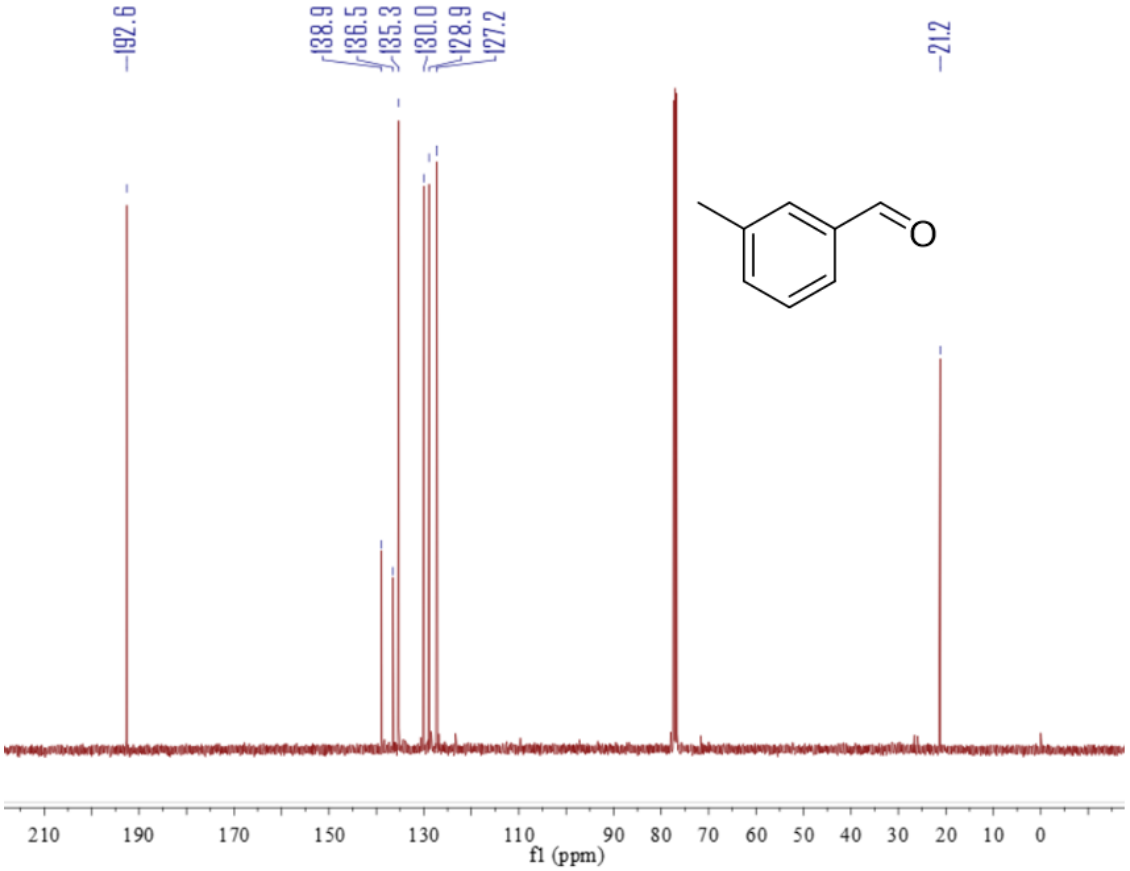
192.6
138.9
136.5
135.3
130.0
128.9
127.2
21.2
O
210 190 170 150 130 110 90 80 70 60 50 40 30 20 10 0
f1 (ppm)

Compound 2c

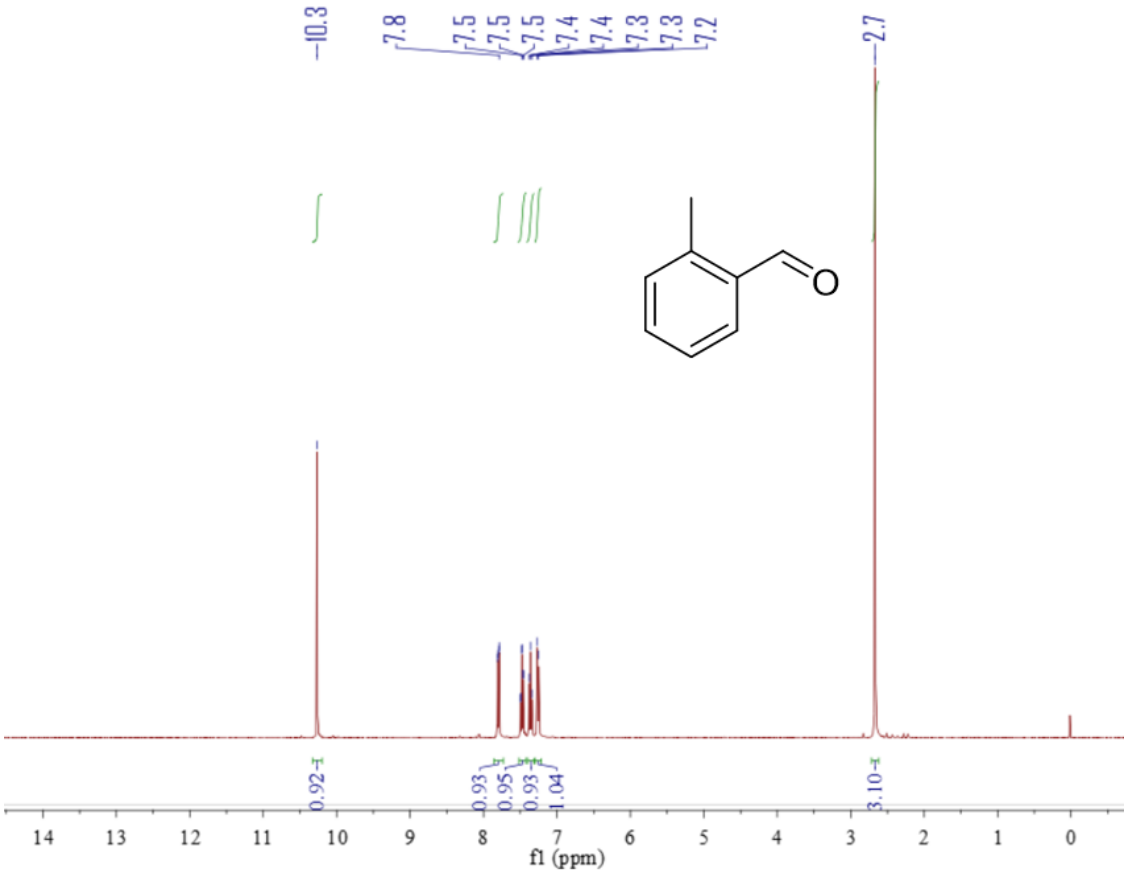
10.3
7.8
7.5
7.5
7.5
7.4
7.4
7.3
7.3
7.2
2.7
O
0.92
0.93
0.95
0.93
1.04
3.10
14 13 12 11 10 9 8 7 6 5 4 3 2 1 0
f1 (ppm)

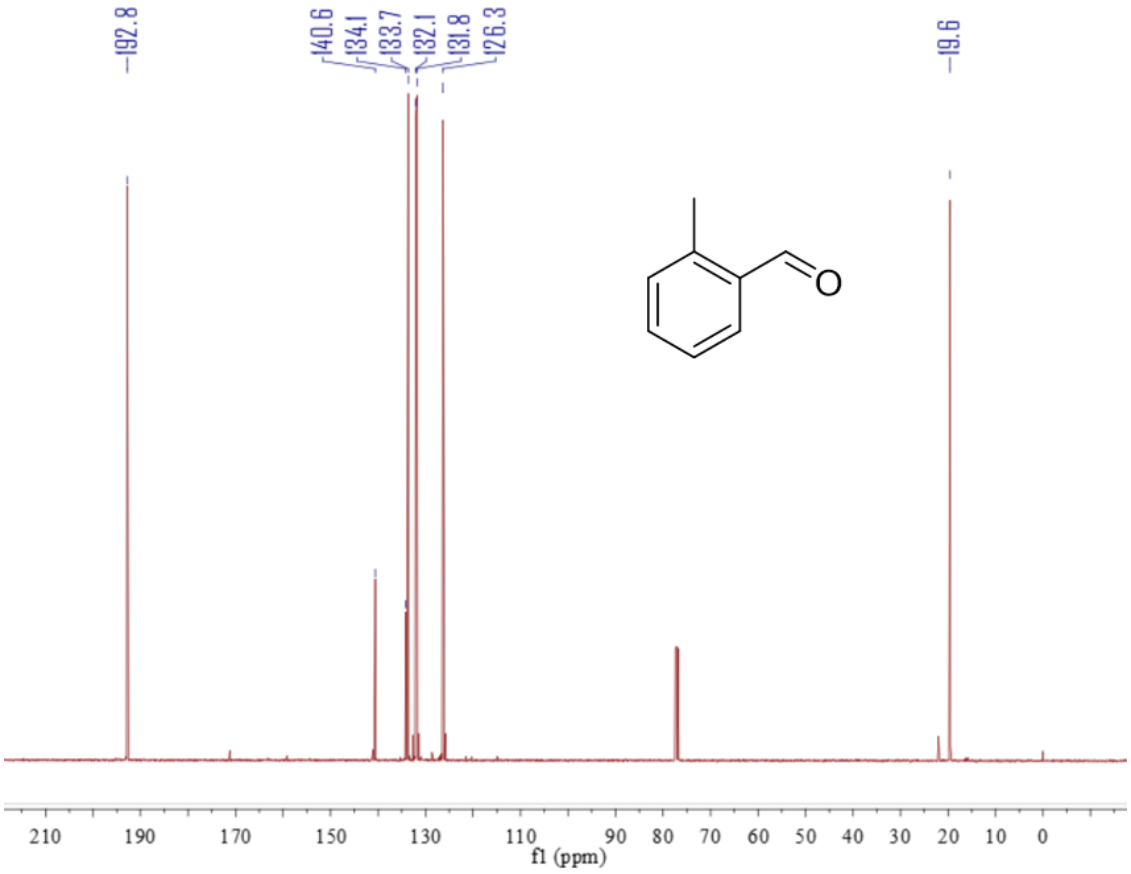
192.8
140.6
134.1
133.7
132.1
131.8
126.3
19.6
O
210 190 170 150 130 110 90 80 70 60 50 40 30 20 10 0
f1 (ppm)

Compound 2d

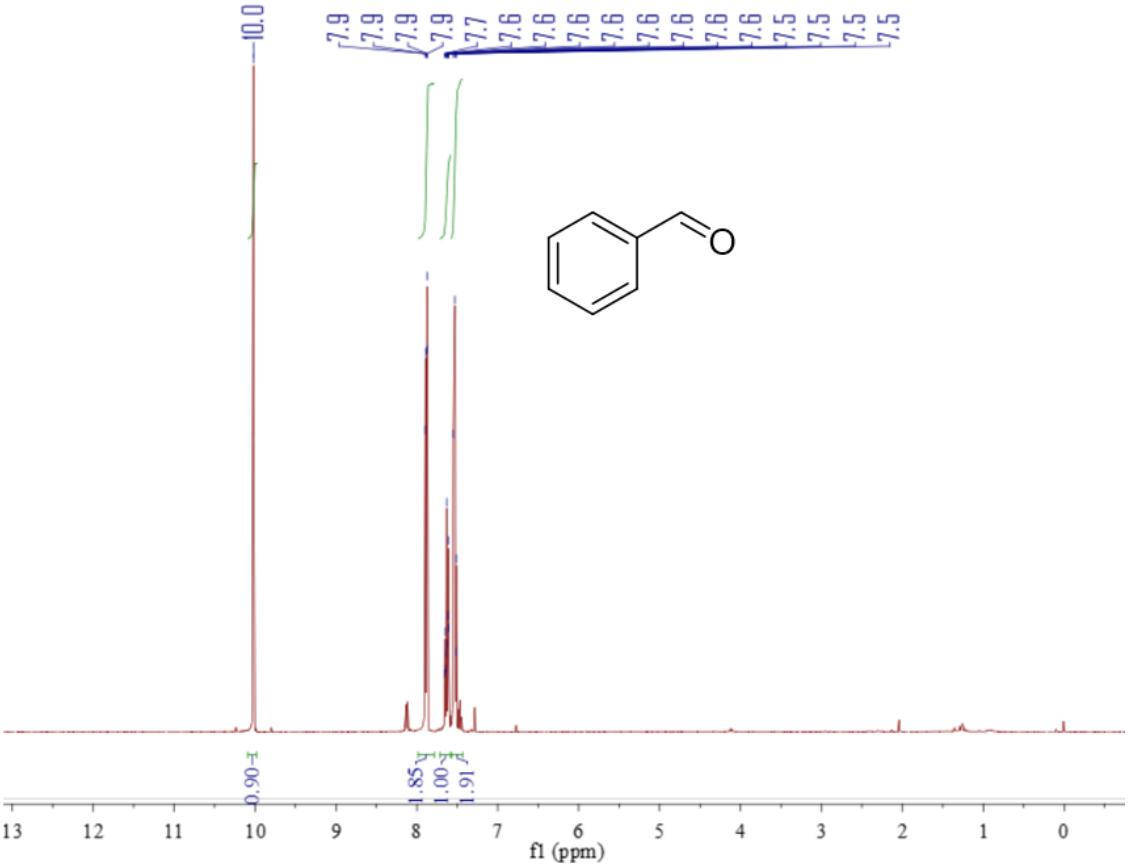
10.0
7.9
7.9
7.9
7.9
7.7
7.6
7.6
7.6
7.6
7.6
7.6
7.6
7.5
7.5
7.5
7.5
O
0.90
1.85
1.00
1.91
13 12 11 10 9 8 7 6 5 4 3 2 1 0
f1 (ppm)

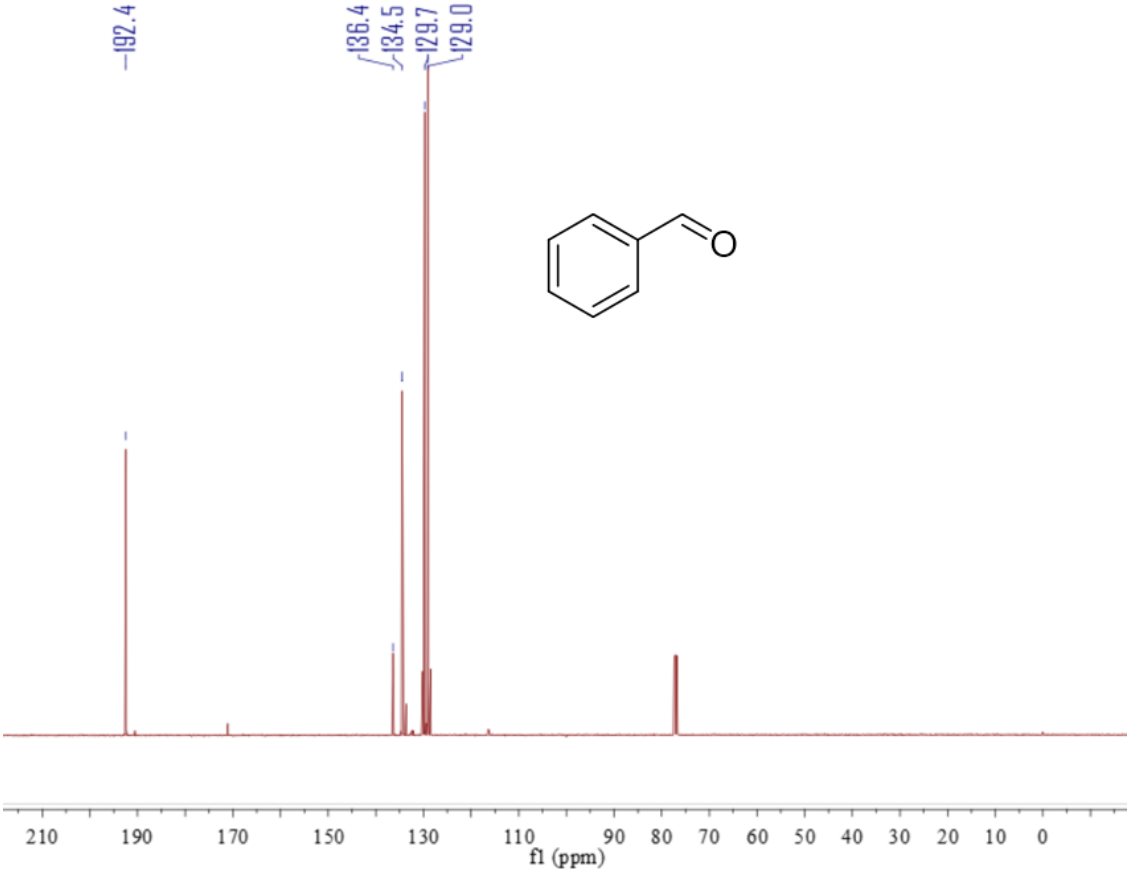
192.4
136.4
134.5
129.7
129.0
O
210 190 170 150 130 110 90 80 70 60 50 40 30 20 10 0
f1 (ppm)

Compound 2e

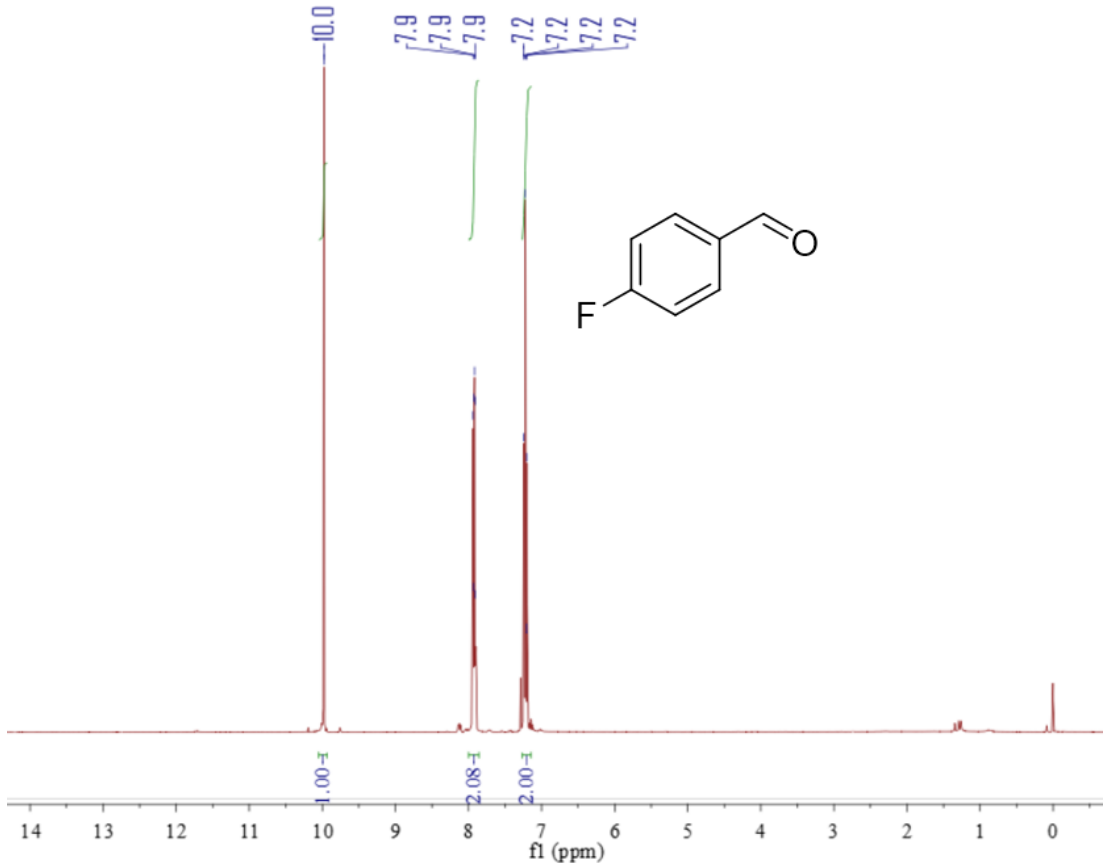
10.0
7.9
7.9
7.9
7.2
7.2
7.2
7.2
O
F
1.00
2.08
2.00
14 13 12 11 10 9 8 7 6 5 4 3 2 1 0
f1 (ppm)

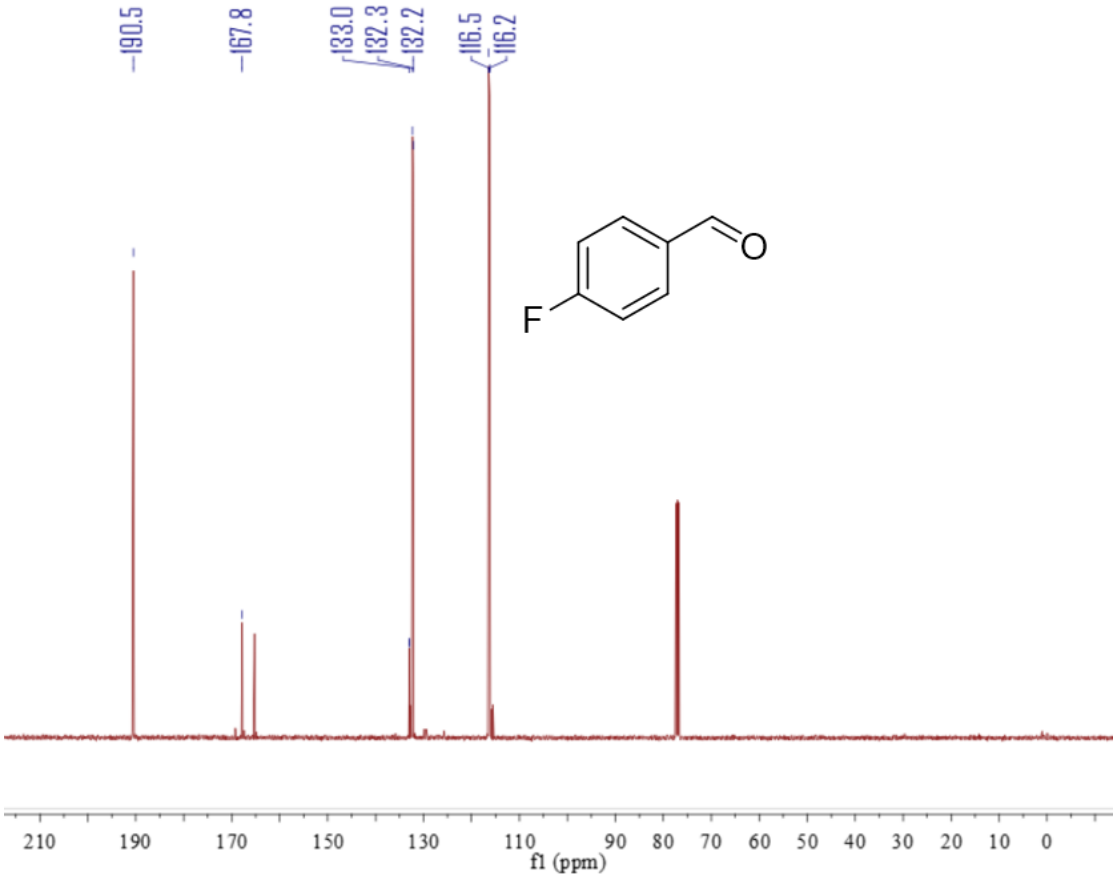
190.5
167.8
133.0
132.3
132.2
116.5
116.2
O
F
210 190 170 150 130 110 90 80 70 60 50 40 30 20 10 0
f1 (ppm)

Compound 2f

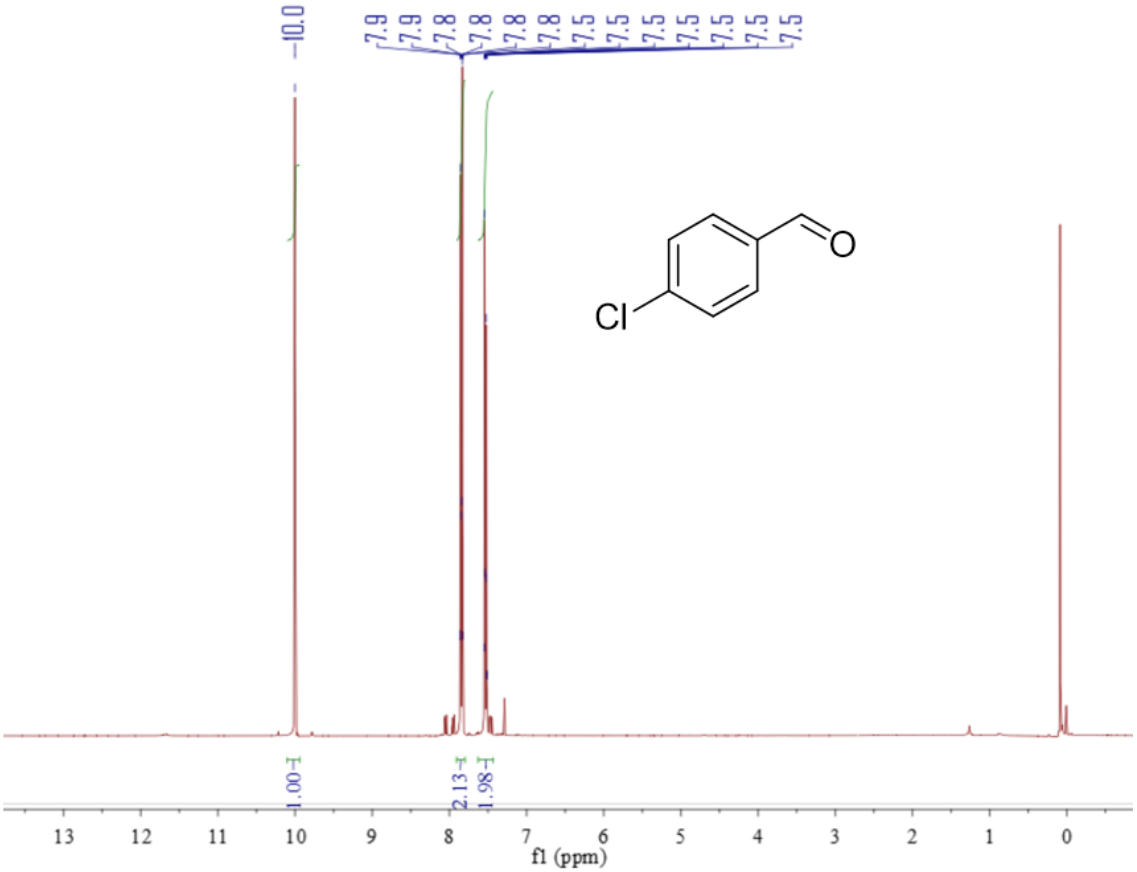
10.0
7.9
7.9
7.8
7.8
7.8
7.8
7.5
7.5
7.5
7.5
7.5
7.5
7.5
Cl
O
1.00
2.13
1.98
13 12 11 10 9 8 7 6 5 4 3 2 1 0
f1 (ppm)

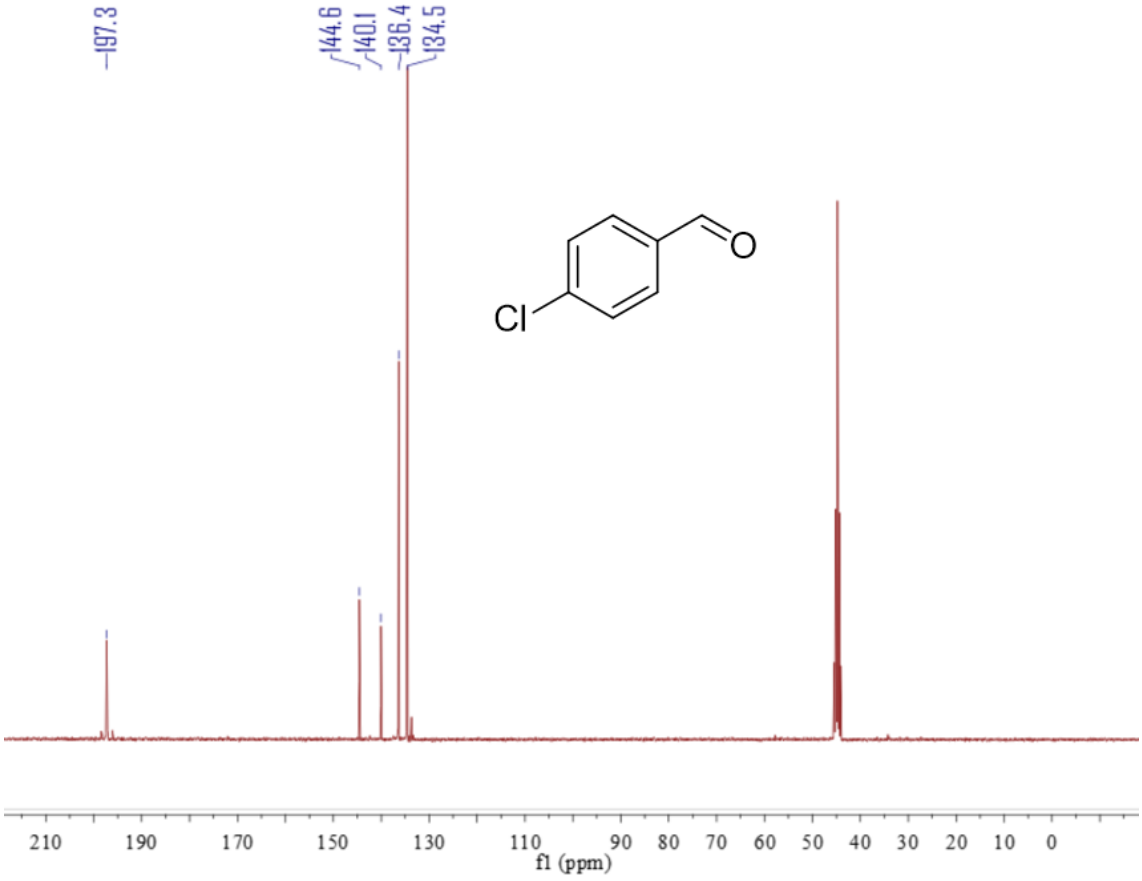
197.3
144.6
140.1
136.4
134.5
Cl
O
210 190 170 150 130 110 90 80 70 60 50 40 30 20 10 0
f1 (ppm)

Compound 2g

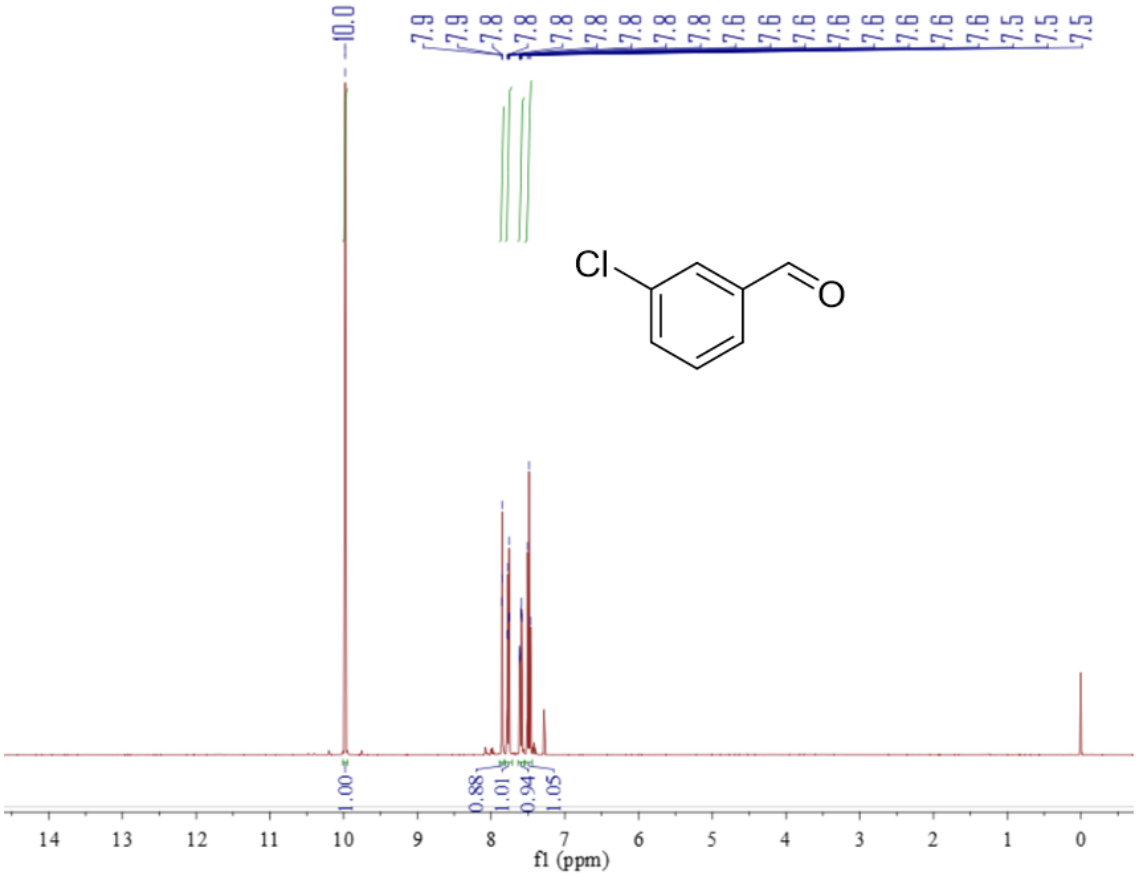
10.0
7.9
7.9
7.8
7.8
7.8
7.8
7.8
7.8
7.6
7.6
7.6
7.6
7.6
7.6
7.6
7.5
7.5
7.5
Cl
O
1.00
0.88
1.01
0.94
1.05
14 13 12 11 10 9 8 7 6 5 4 3 2 1 0
f1 (ppm)

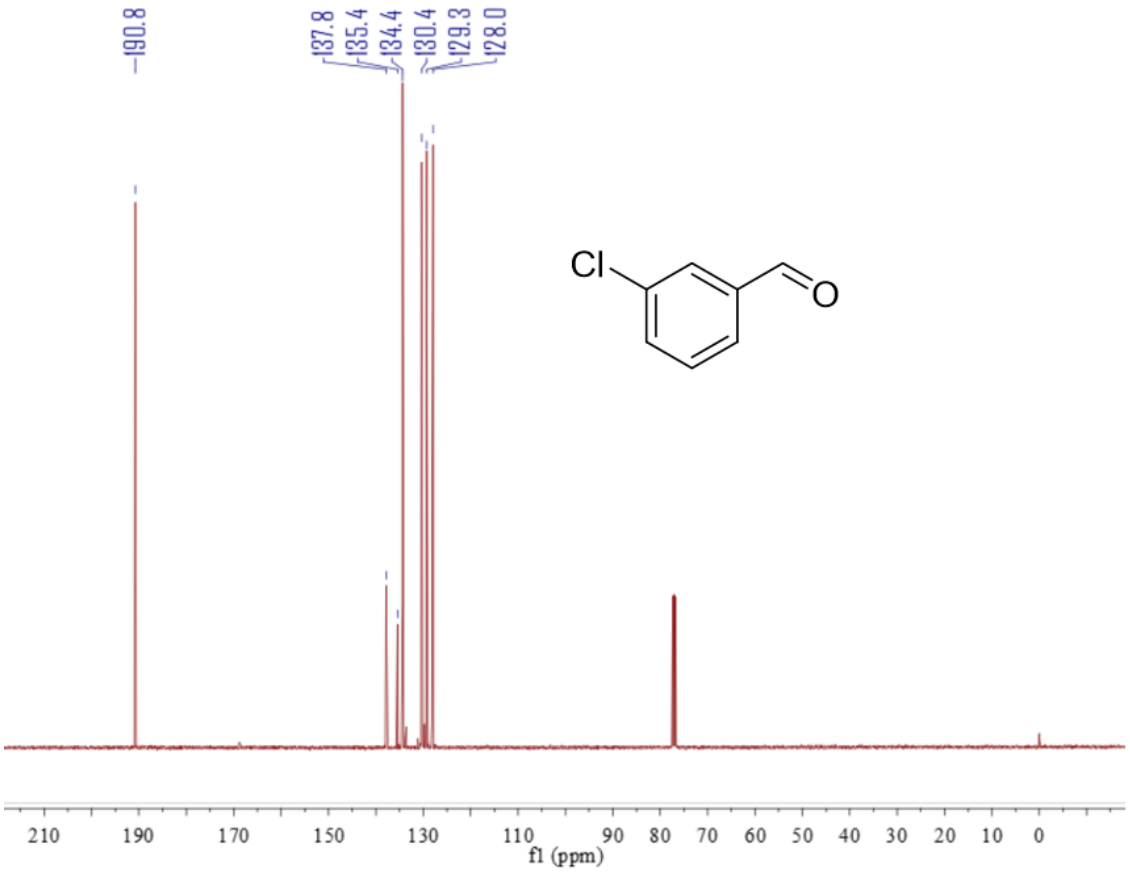
190.8
137.8
135.4
134.4
130.4
129.3
128.0
Cl
O
210 190 170 150 130 110 90 80 70 60 50 40 30 20 10 0
f1 (ppm)

Compound 2h

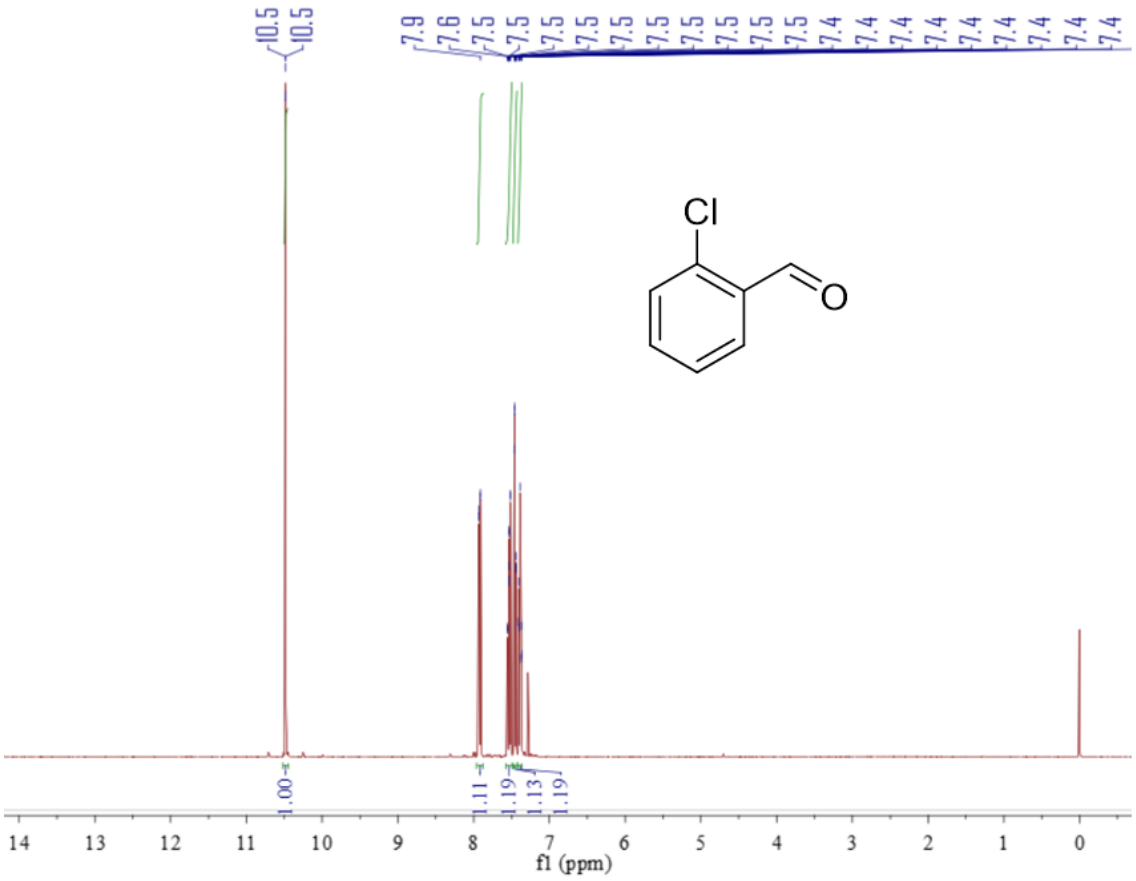
10.5
10.5
7.9
7.6
7.5
7.5
7.5
7.5
7.5
7.5
7.5
7.5
7.5
7.5
7.4
7.4
7.4
7.4
7.4
7.4
7.4
7.4
Cl
O
1.00
1.11
1.19
1.13
1.19
14 13 12 11 10 9 8 7 6 5 4 3 2 1 0
f1 (ppm)

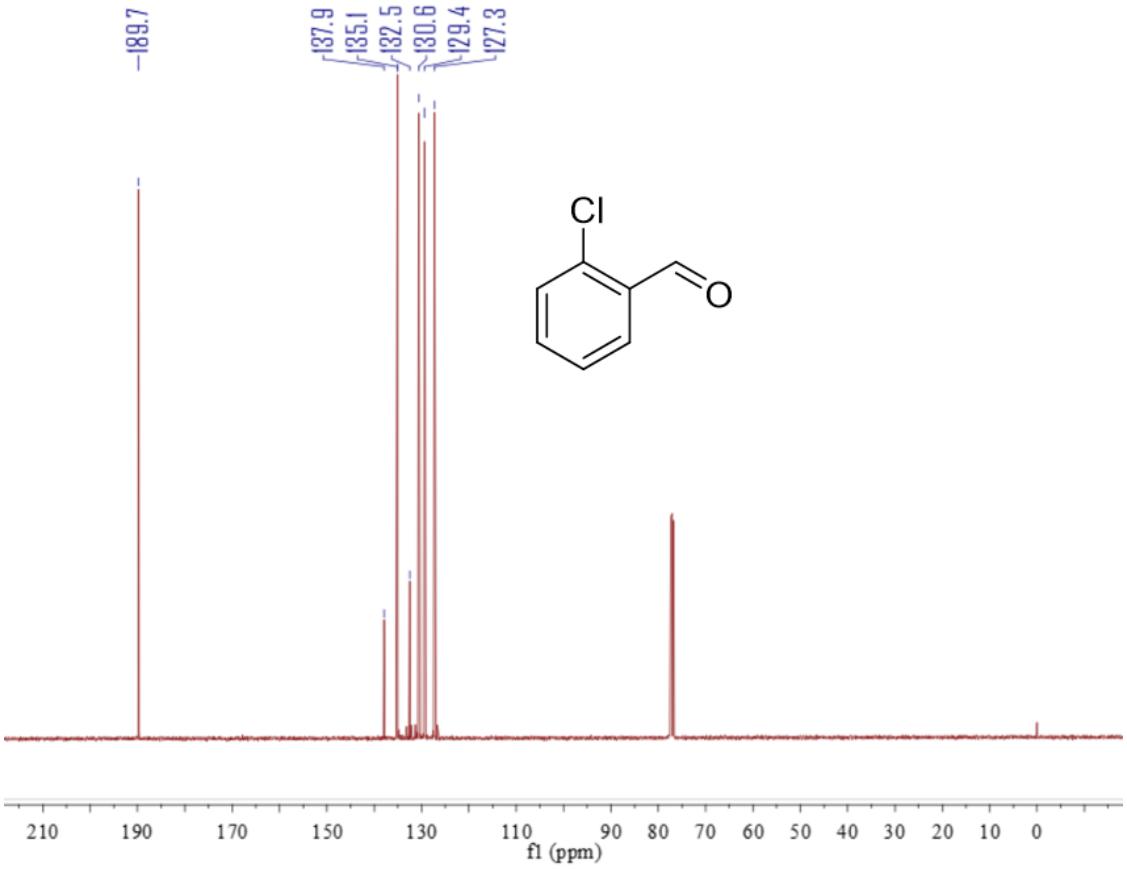
189.7
137.9
135.1
132.5
130.6
129.4
127.3
Cl
O
210 190 170 150 130 110 90 80 70 60 50 40 30 20 10 0
f1 (ppm)

Compound 2i

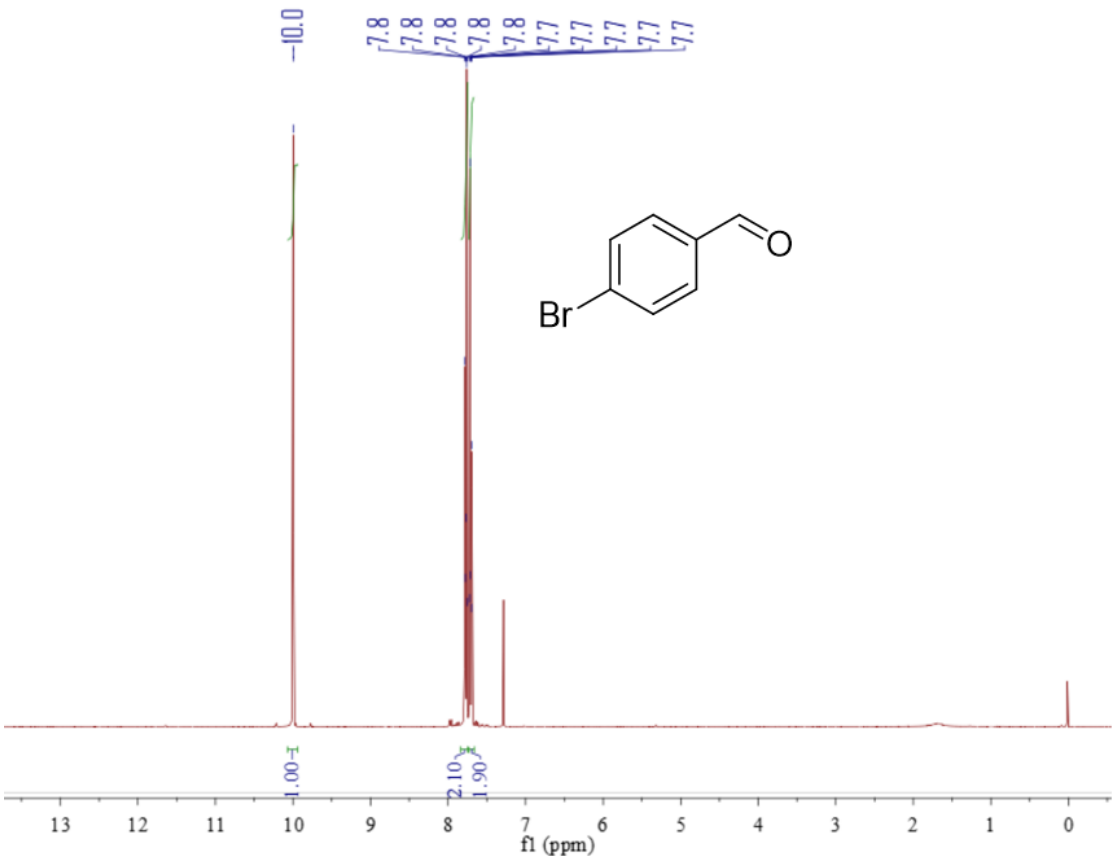
10.0
7.8
7.8
7.8
7.8
7.8
7.7
7.7
7.7
7.7
7.7
Br
O
1.00
2.10
1.90
13
12
11
10
9
8
7
6
5
4
3
2
1
0
f1 (ppm)

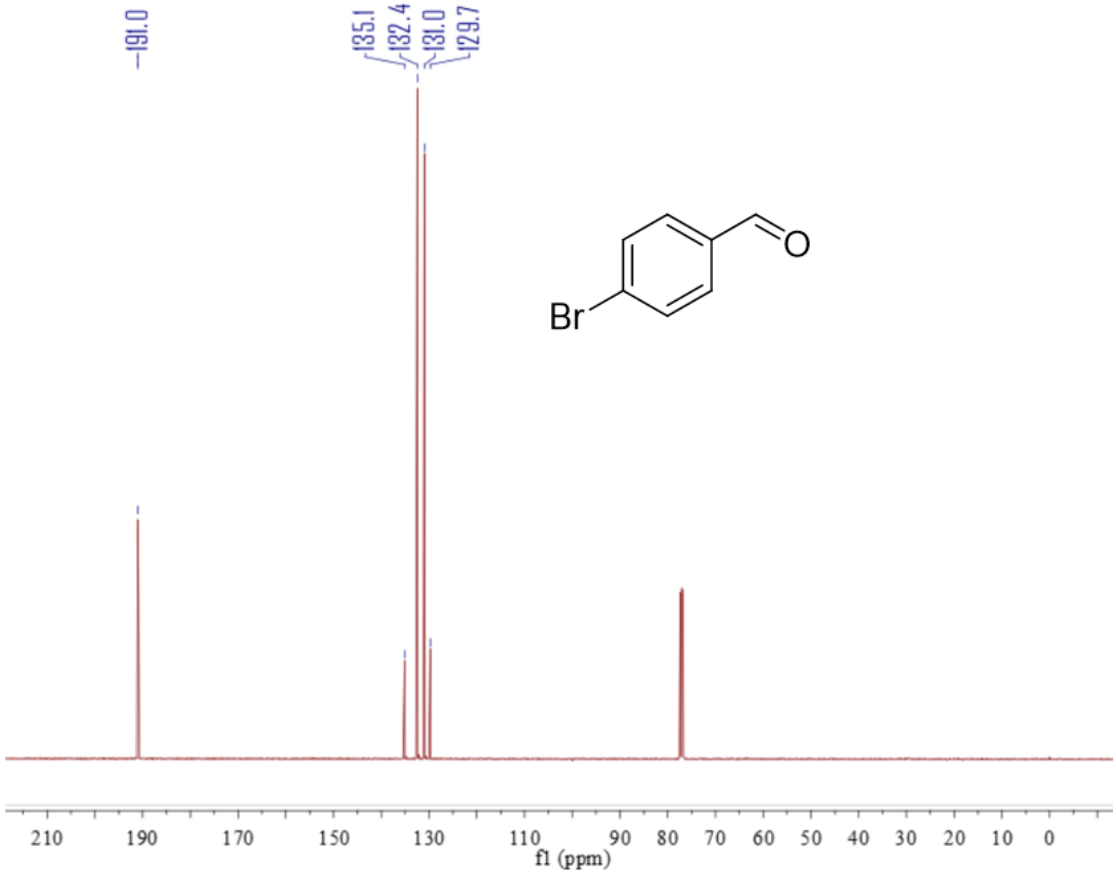
191.0
135.1
132.4
131.0
129.7
Br
O
210
190
170
150
130
110
90
80
70
60
50
40
30
20
10
0
f1 (ppm)

Compound 2j

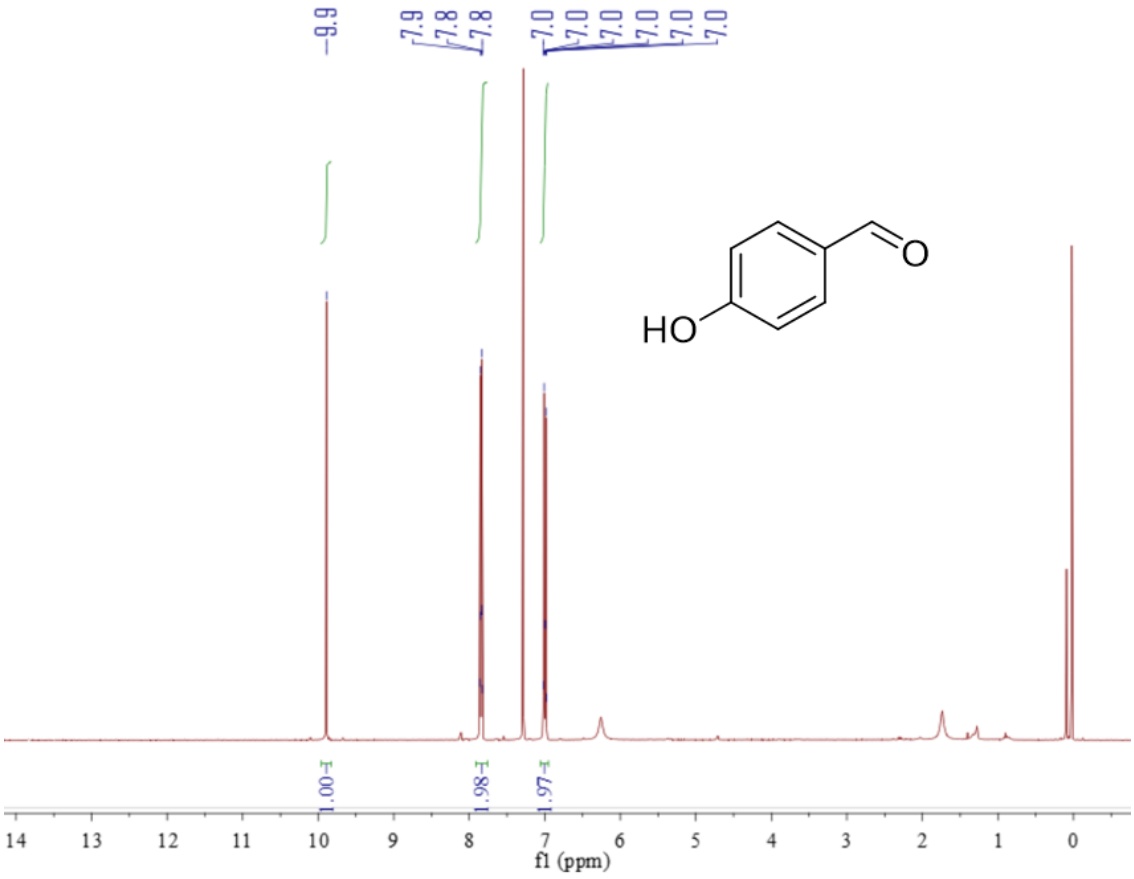
9.9
7.9
7.8
7.8
7.0
7.0
7.0
7.0
7.0
7.0
HO
O
1.00
1.98
1.97
14 13 12 11 10 9 8 7 6 5 4 3 2 1 0
f1 (ppm)

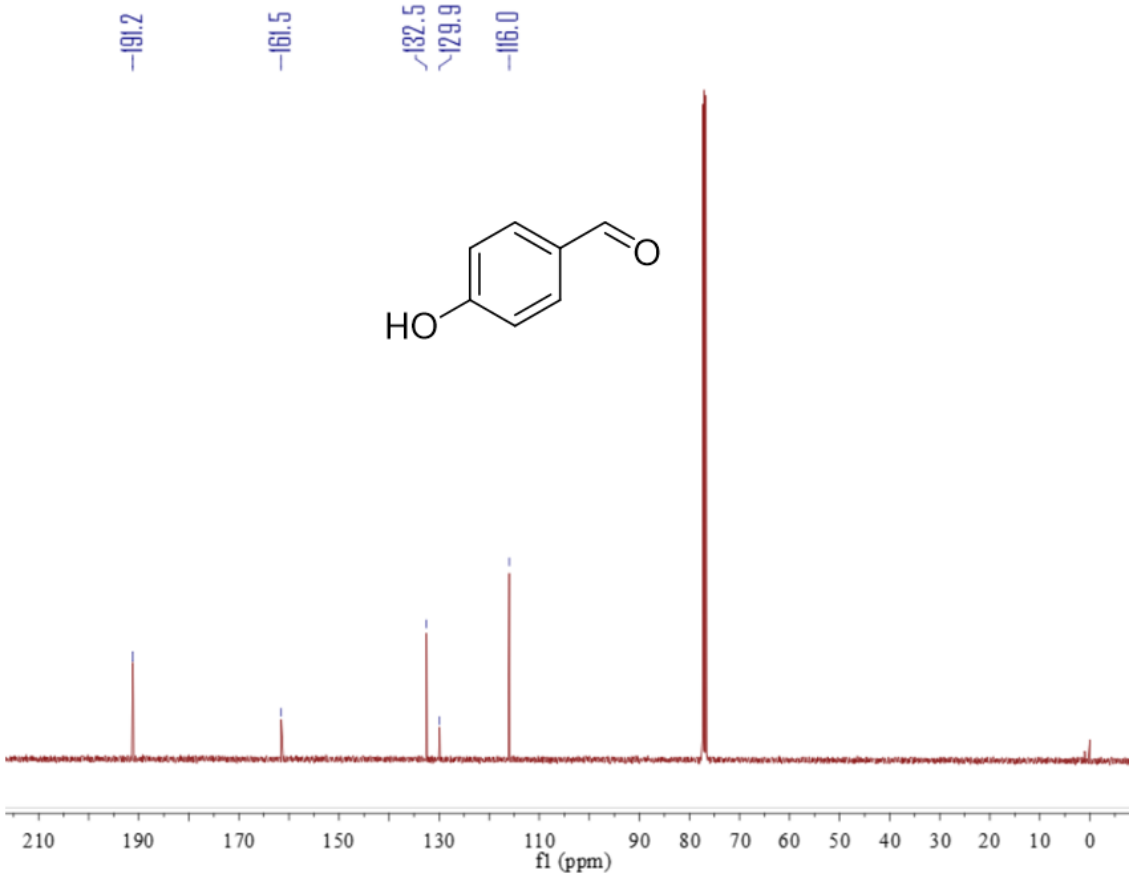
191.2
161.5
132.5
129.9
116.0
HO
O
210 190 170 150 130 110 90 80 70 60 50 40 30 20 10 0
f1 (ppm)

Compound 2k

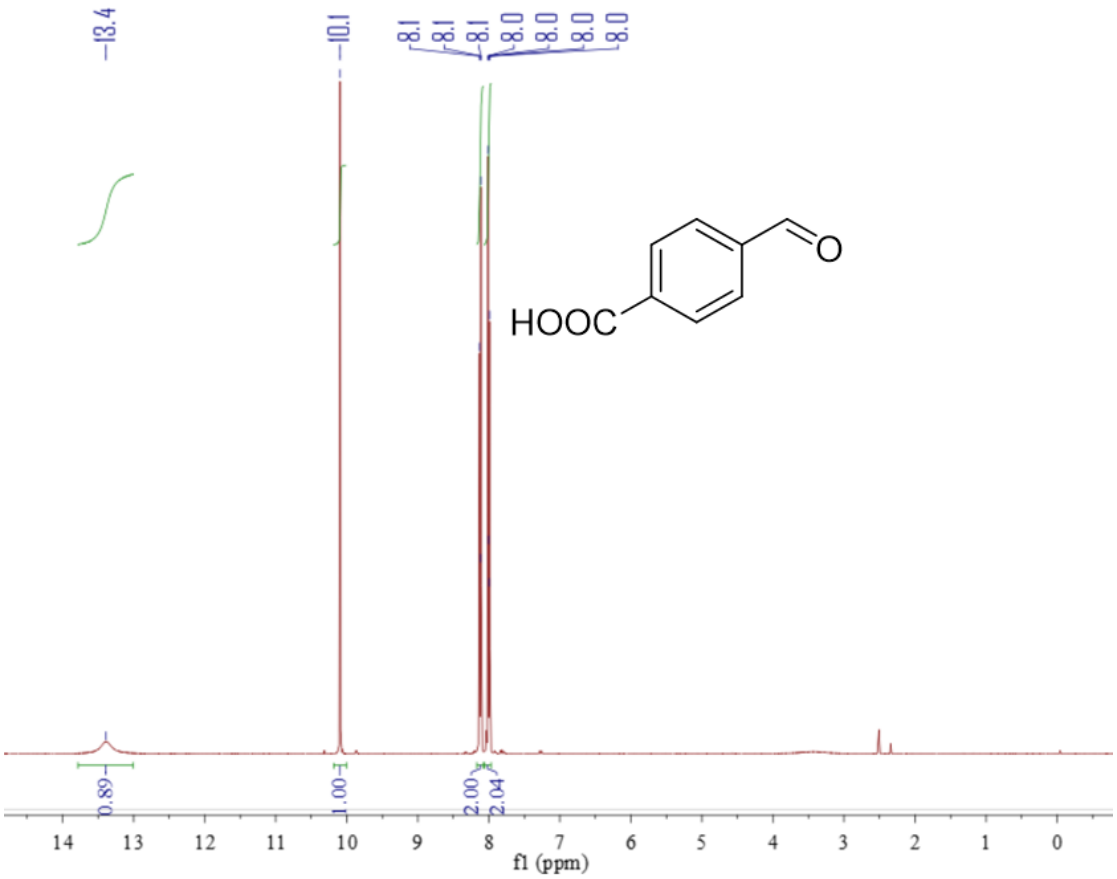
13.4
10.1
8.1
8.1
8.1
8.0
8.0
8.0
8.0
HOOC
O
0.89
1.00
2.00
2.04
14 13 12 11 10 9 8 7 6 5 4 3 2 1 0
f1 (ppm)


193.4
167.0
139.3
136.1
130.4
130.0
HOOC
O
210 190 170 150 130 110 90 80 70 60 50 40 30 20 10 0
f1 (ppm)

Compound 2l

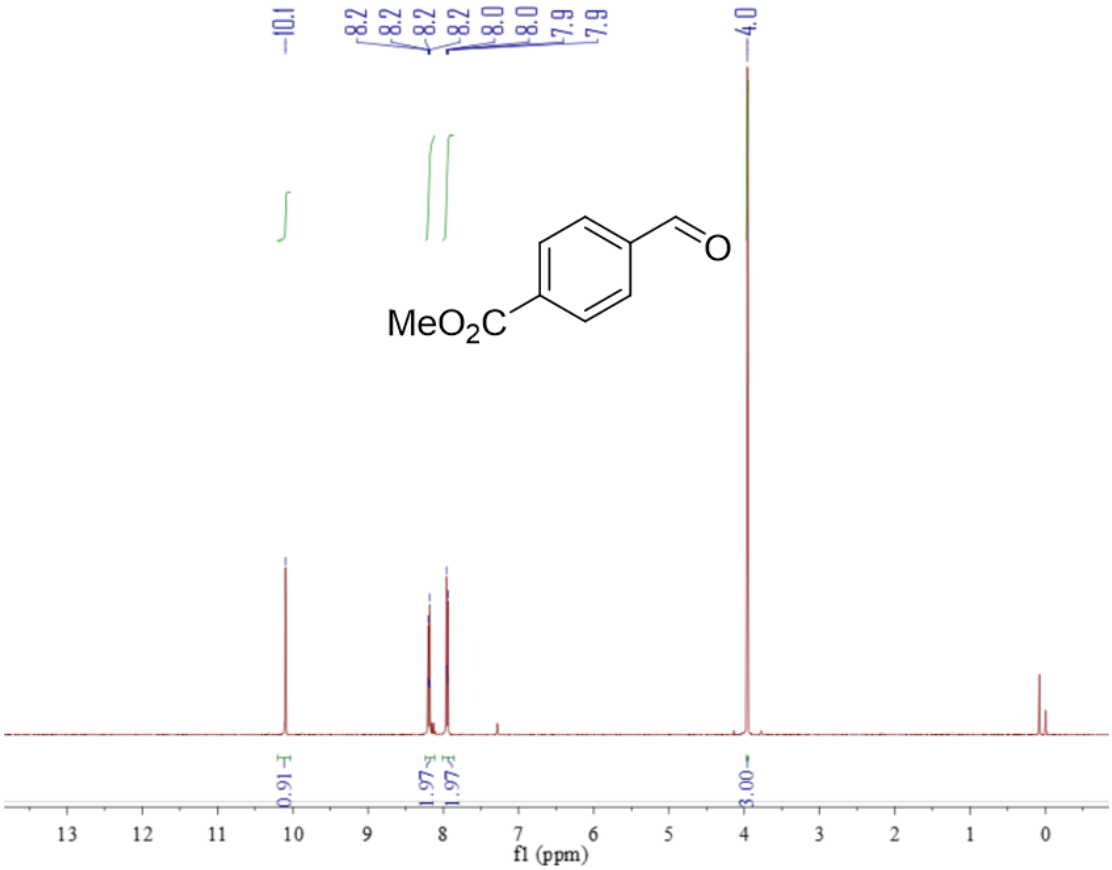
10.1
8.2
8.2
8.2
8.2
8.0
8.0
7.9
7.9
4.0
O
MeO2C
0.91
1.97
1.97
3.00
13 12 11 10 9 8 7 6 5 4 3 2 1 0
f1 (ppm)

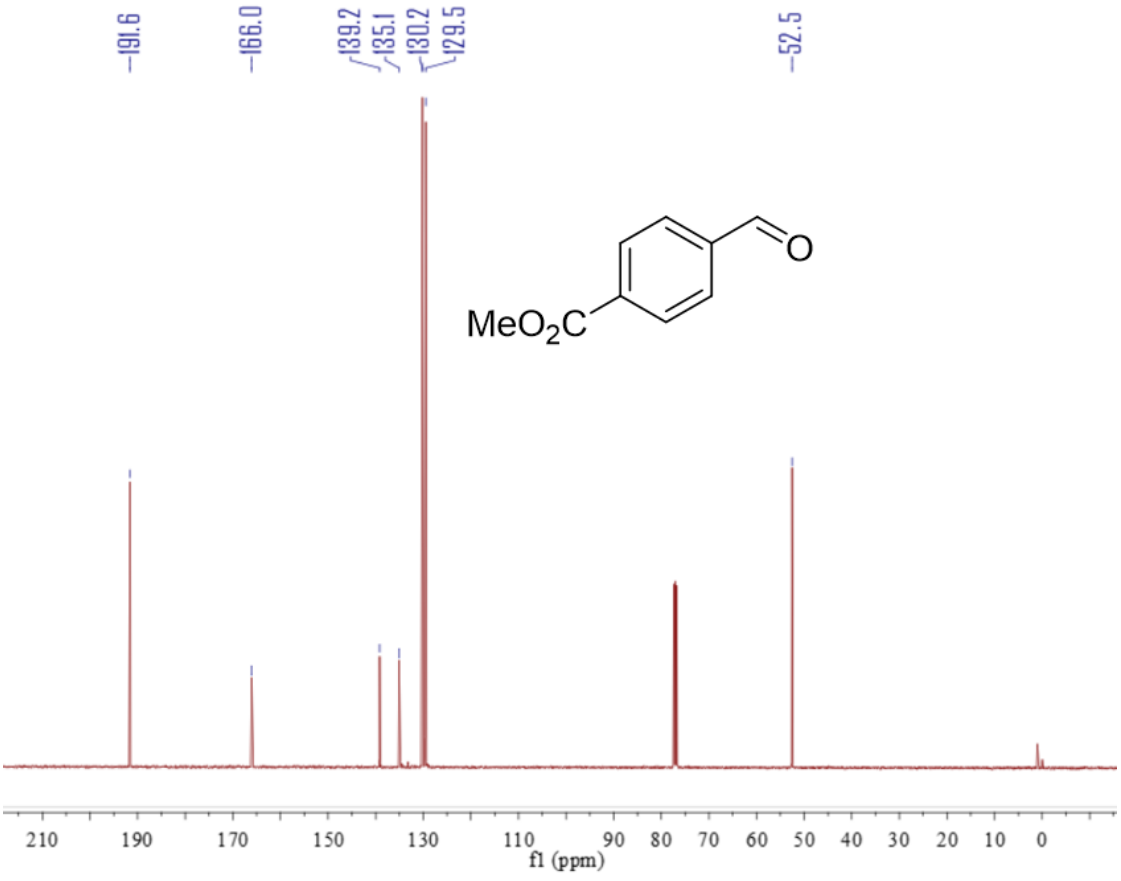
191.6
166.0
139.2
135.1
130.2
129.5
52.5
O
MeO2C
210 190 170 150 130 110 90 80 70 60 50 40 30 20 10 0
f1 (ppm)

Compound 2m

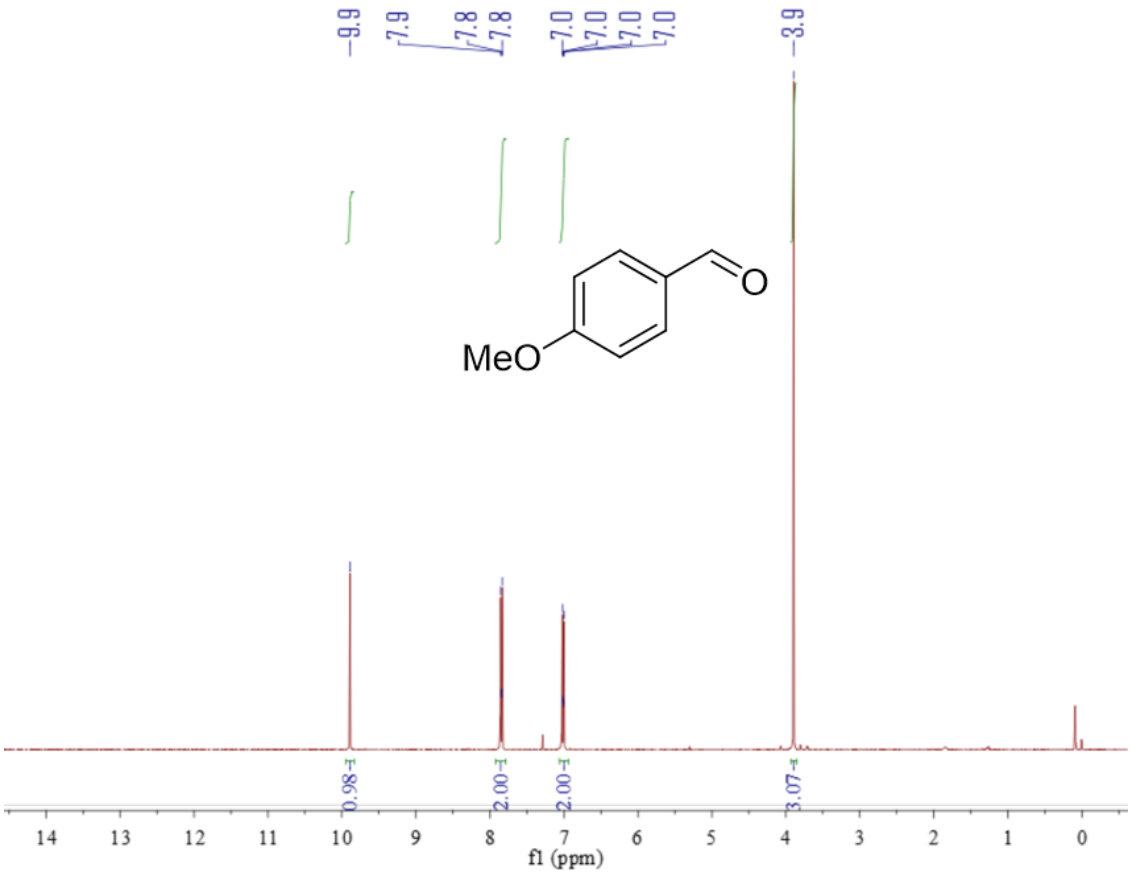
9.9
7.9
7.8
7.8
7.0
7.0
7.0
7.0
3.9
O
MeO
0.98
2.00
2.00
3.07
14 13 12 11 10 9 8 7 6 5 4 3 2 1 0
f1 (ppm)

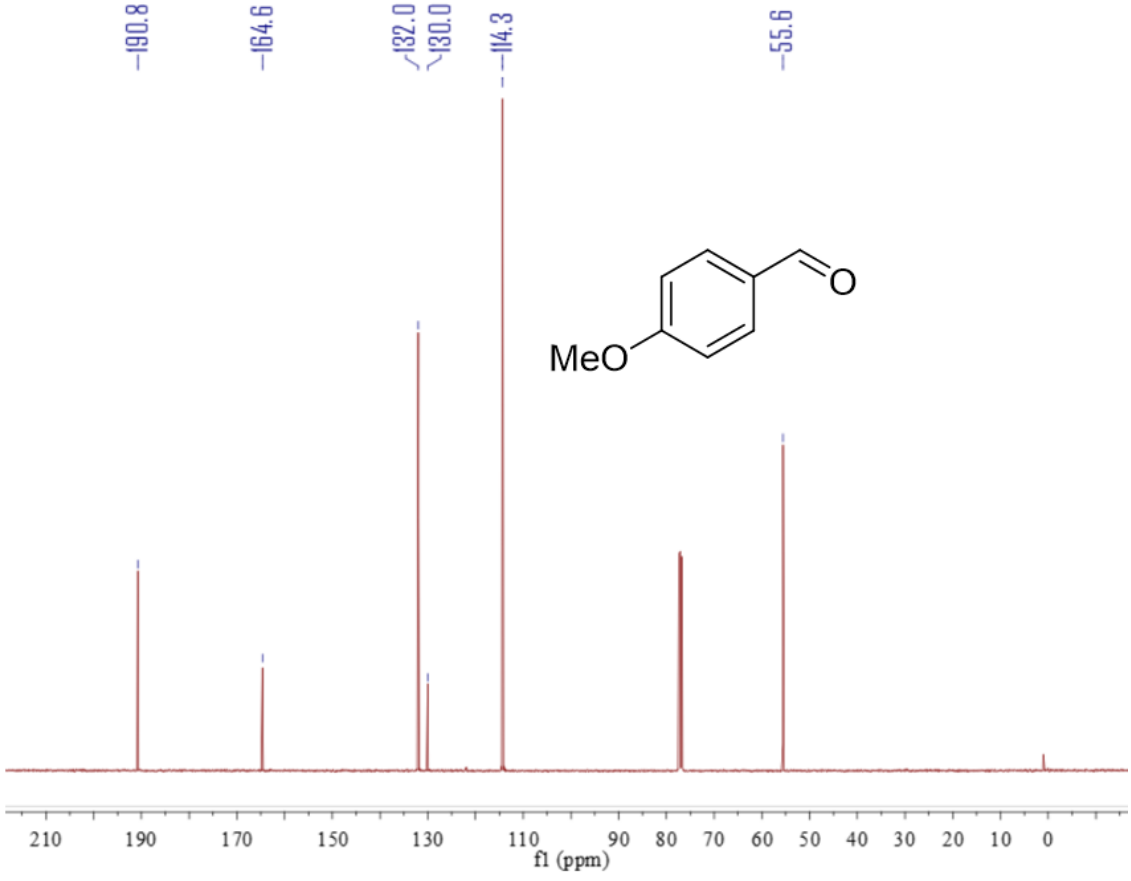
190.8
164.6
132.0
130.0
114.3
55.6
O
MeO
210 190 170 150 130 110 90 80 70 60 50 40 30 20 10 0
f1 (ppm)

Compound 2n

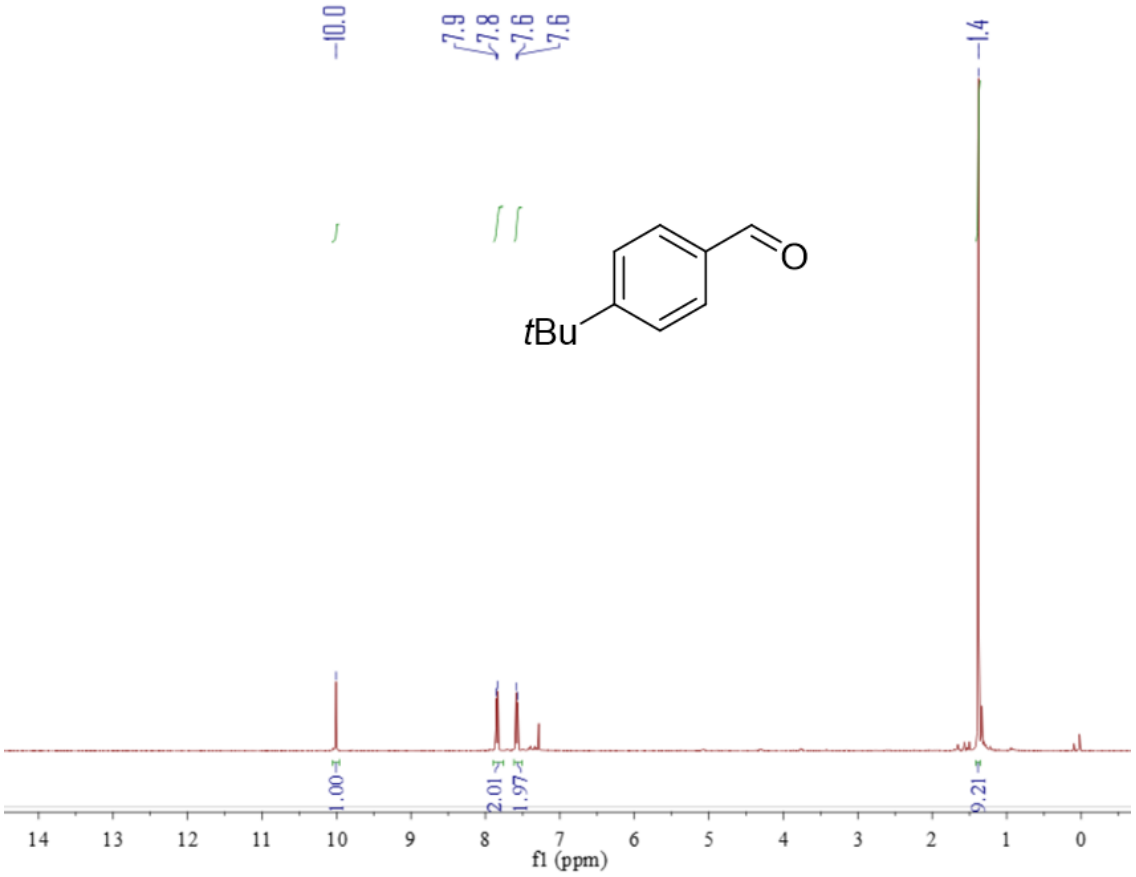
10.0
7.9
7.8
7.6
7.6
1.4
O
tBu
1.00
2.01
1.97
9.21
14 13 12 11 10 9 8 7 6 5 4 3 2 1 0
f1 (ppm)

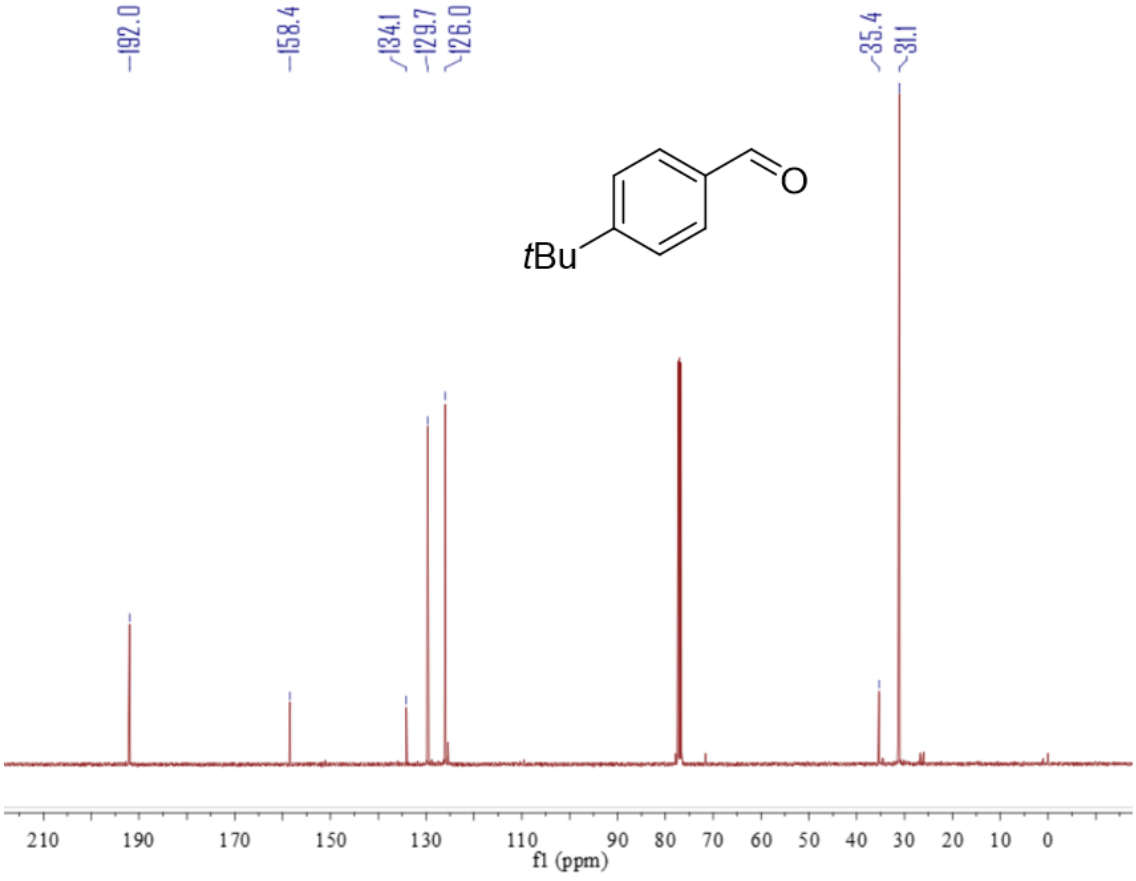
192.0
158.4
134.1
129.7
126.0
35.4
31.1
O
tBu
210 190 170 150 130 110 90 80 70 60 50 40 30 20 10 0
f1 (ppm)

Compound 2o

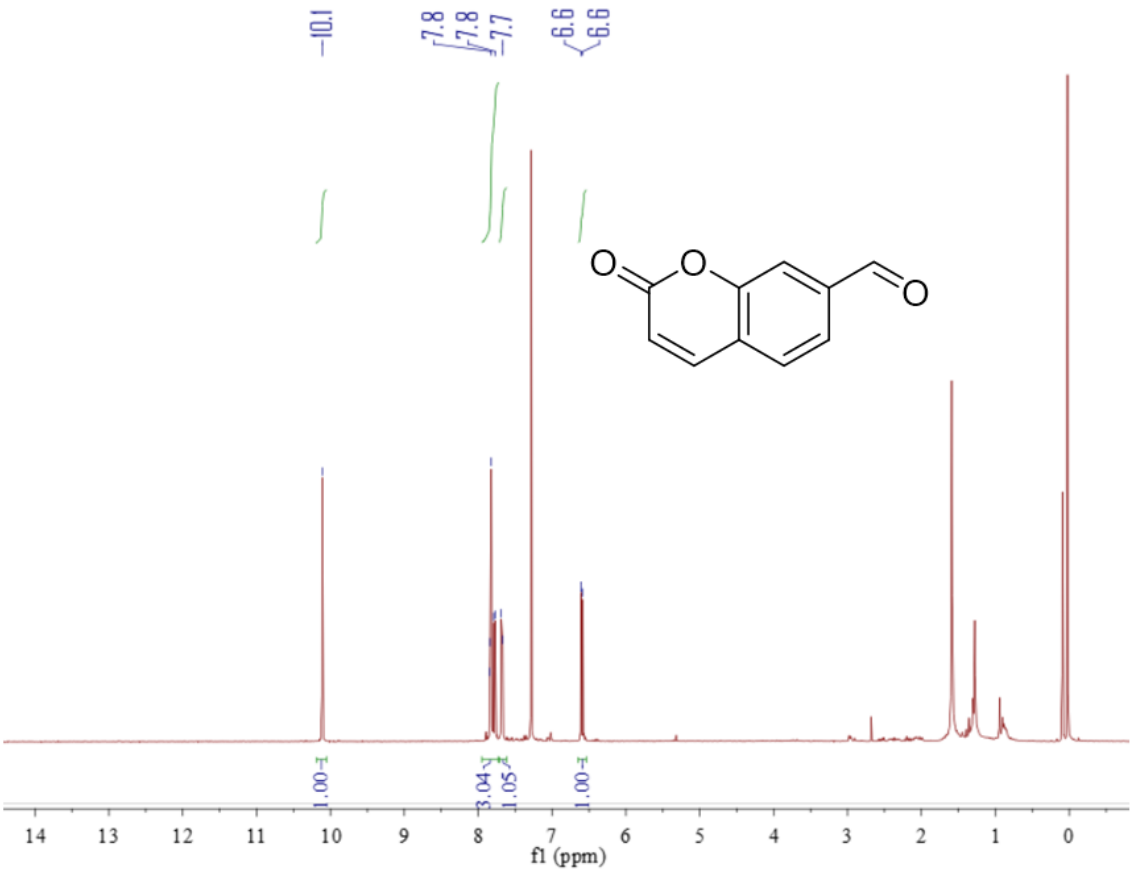
10.1
7.8
7.8
7.7
6.6
6.6
1.00
3.04
1.05
1.00
f1 (ppm)

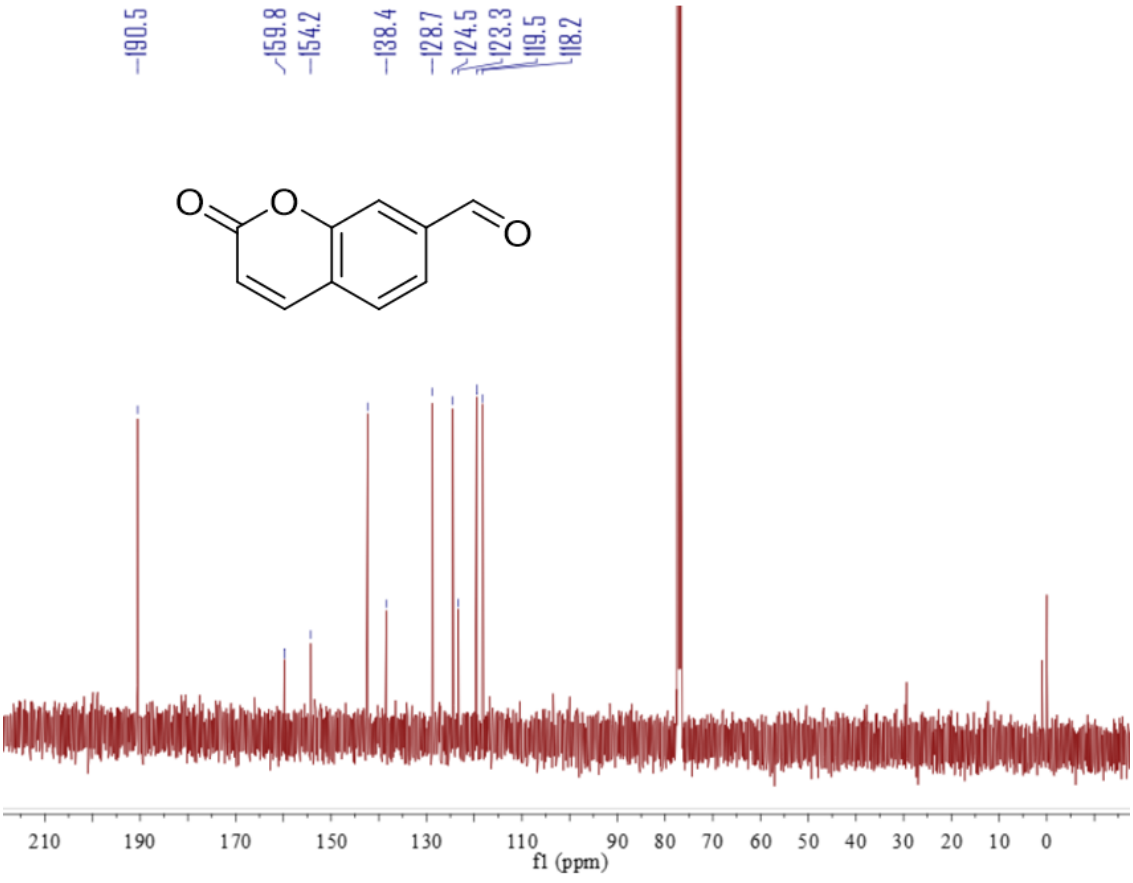
190.5
159.8
154.2
138.4
128.7
124.5
123.3
119.5
118.2
f1 (ppm)

Compound 2p

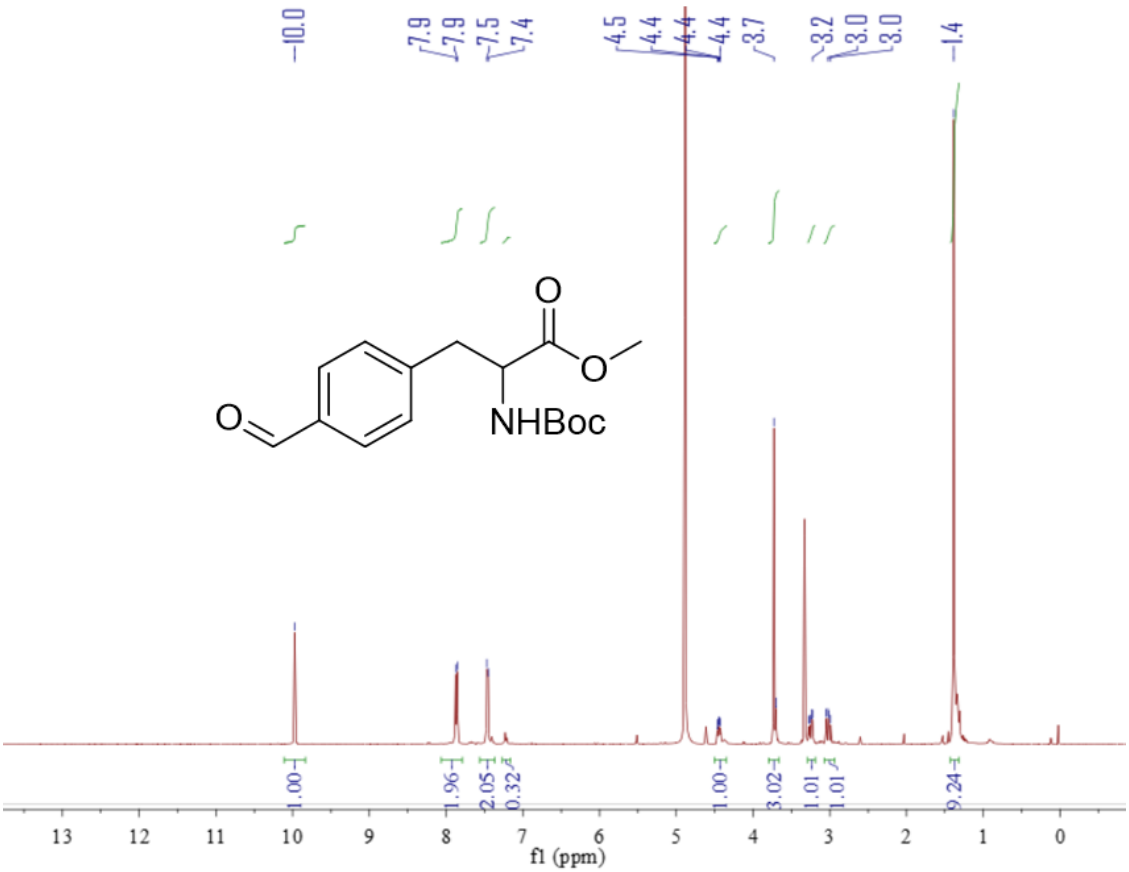
10.0
7.9
7.9
7.5
7.4
4.5
4.4
4.4
4.4
3.7
3.2
3.0
3.0
1.4
O
O
O
NHBoc
1.00
1.96
2.05
0.32
1.00
3.02
1.01
1.01
9.24
13 12 11 10 9 8 7 6 5 4 3 2 1 0
f1 (ppm)

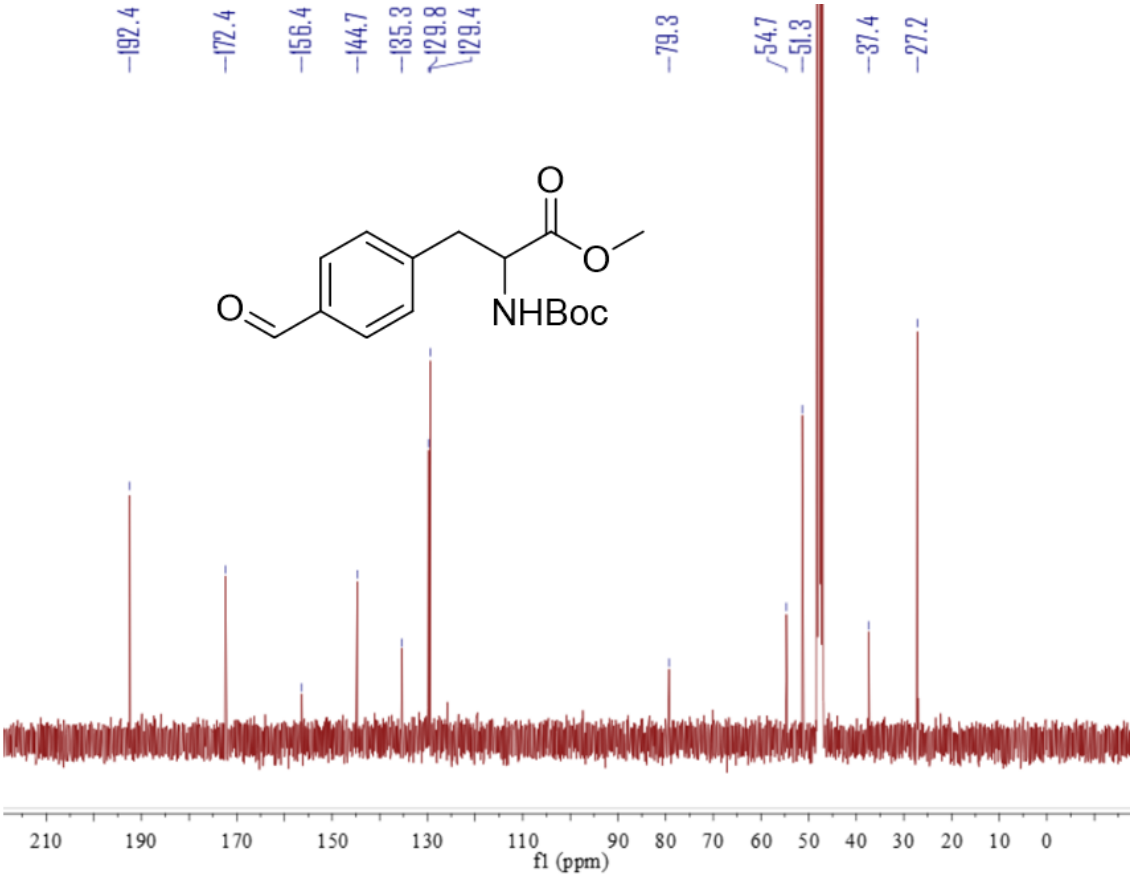
192.4
172.4
156.4
144.7
135.3
129.8
129.4
79.3
54.7
51.3
37.4
27.2
O
O
O
NHBoc
210 190 170 150 130 110 90 80 70 60 50 40 30 20 10 0
f1 (ppm)

Compound 2q

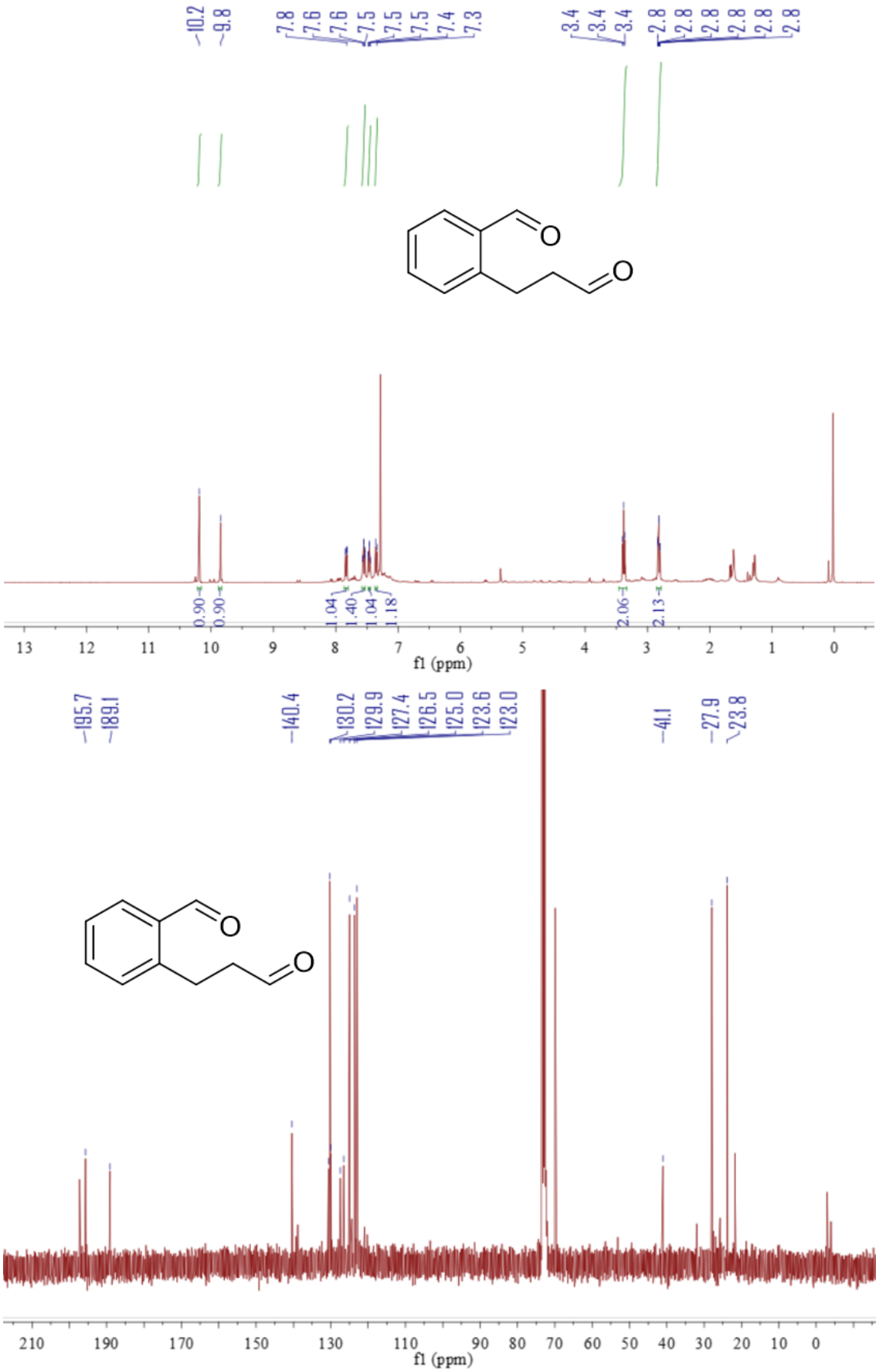
10.2
9.8
7.8
7.6
7.6
7.5
7.5
7.5
7.4
7.3
3.4
3.4
3.4
2.8
2.8
2.8
2.8
2.8
2.8
O
O
0.90
0.90
1.04
1.40
1.04
1.18
2.06
2.13
13 12 11 10 9 8 7 6 5 4 3 2 1 0
f1 (ppm)
195.7
189.1
140.4
130.2
129.9
127.4
126.5
125.0
123.6
123.0
41.1
27.9
23.8
O
O
210 190 170 150 130 110 90 80 70 60 50 40 30 20 10 0
f1 (ppm)

Compound 4a

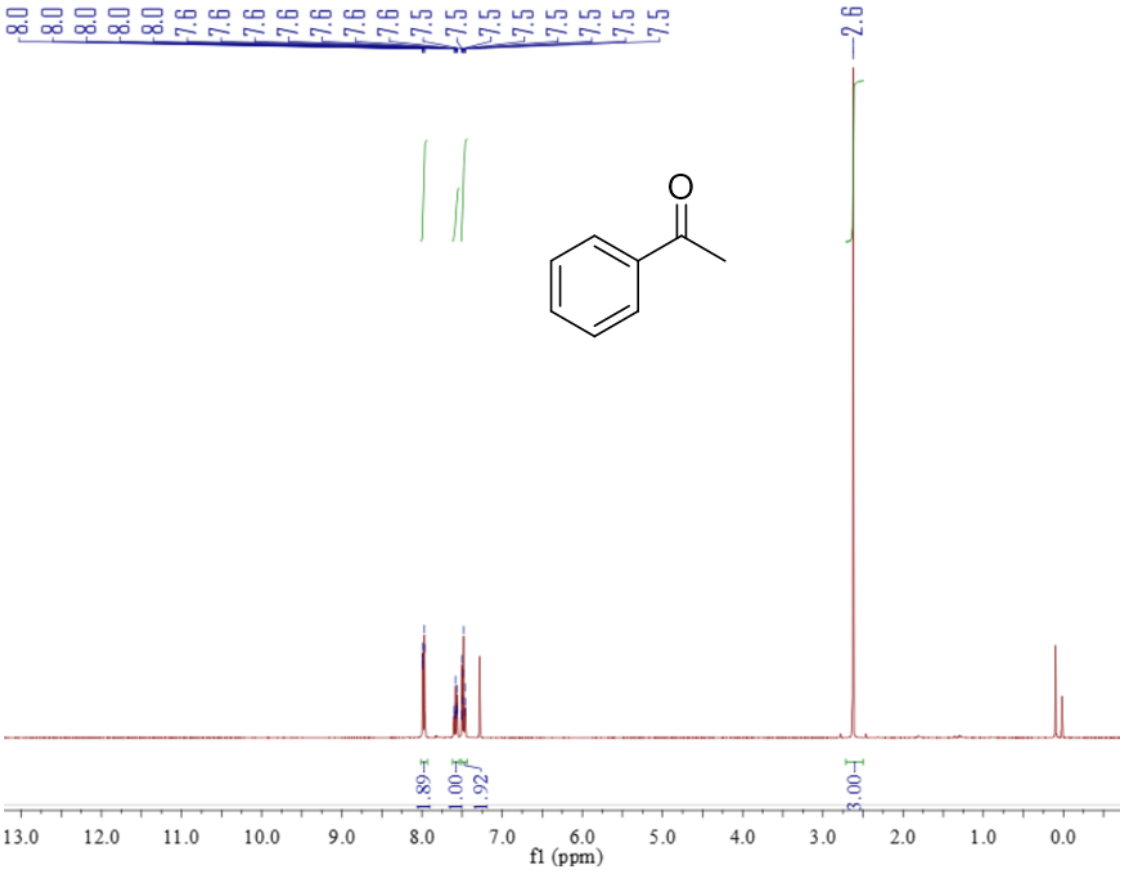
8.0
7.6
7.5
2.6
O
1.89
1.00
1.92
3.00
13.0
12.0
11.0
10.0
9.0
8.0
7.0
6.0
5.0
4.0
3.0
2.0
1.0
0.0
f1 (ppm)

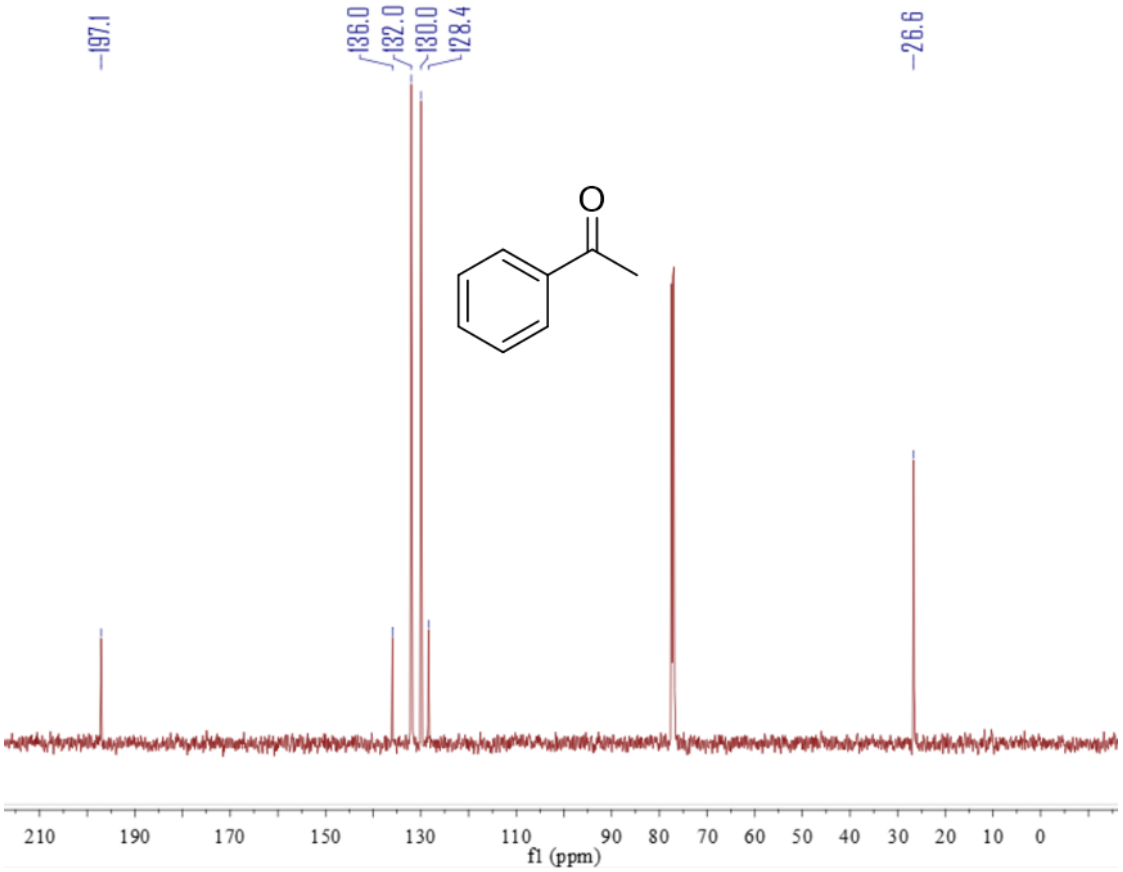
197.1
136.0
132.0
130.0
128.4
26.6
O
210
190
170
150
130
110
90
80
70
60
50
40
30
20
10
0
f1 (ppm)

Compound 4b

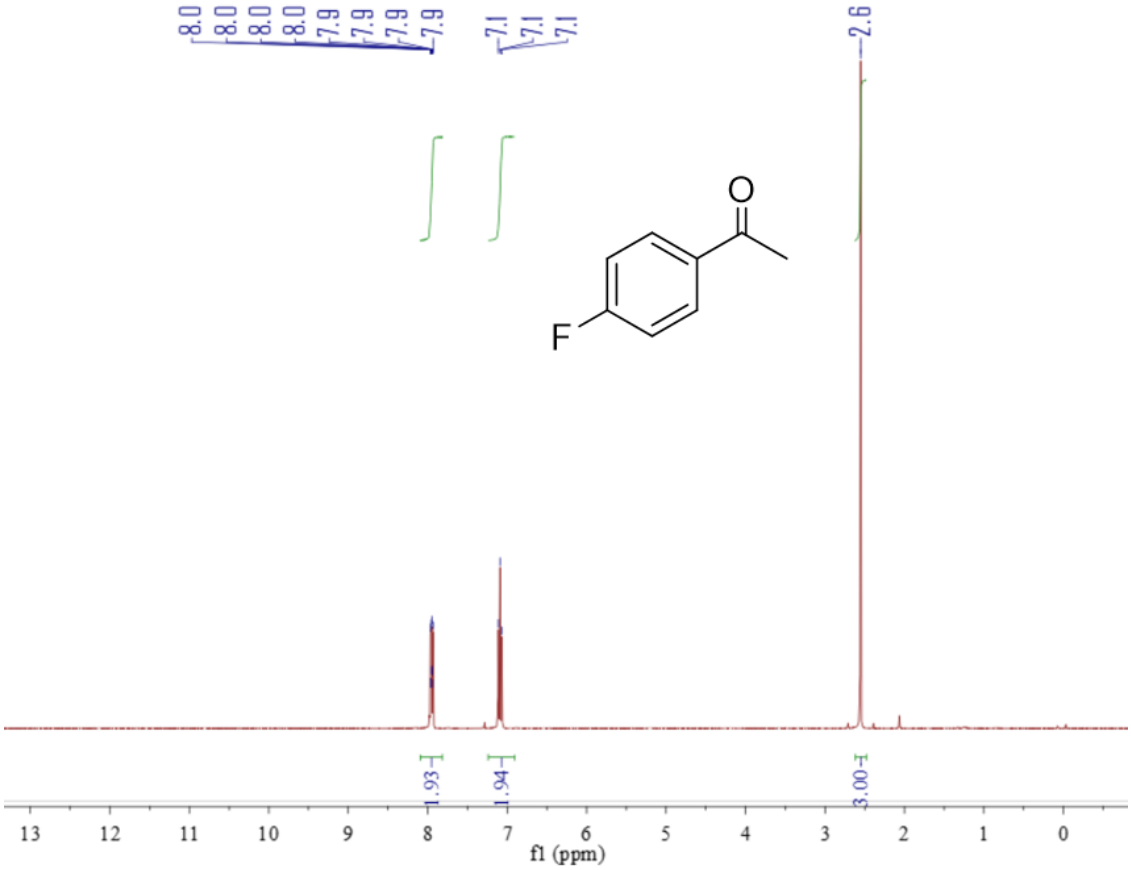
8.0
8.0
8.0
8.0
7.9
7.9
7.9
7.9
7.1
7.1
7.1
2.6
O
F
1.93
1.94
3.00
13 12 11 10 9 8 7 6 5 4 3 2 1 0
f1 (ppm)

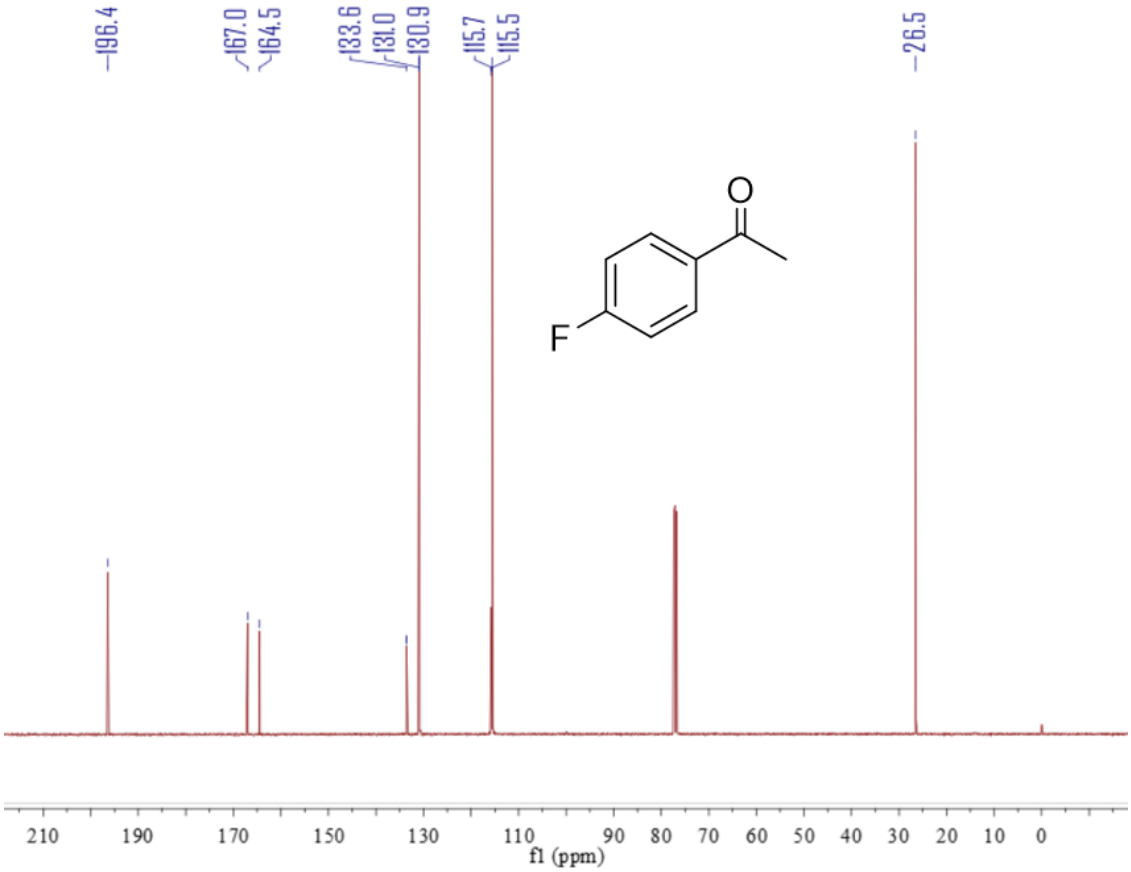
196.4
167.0
164.5
133.6
131.0
130.9
115.7
115.5
26.5
O
F
210 190 170 150 130 110 90 80 70 60 50 40 30 20 10 0
f1 (ppm)

Compound 4c

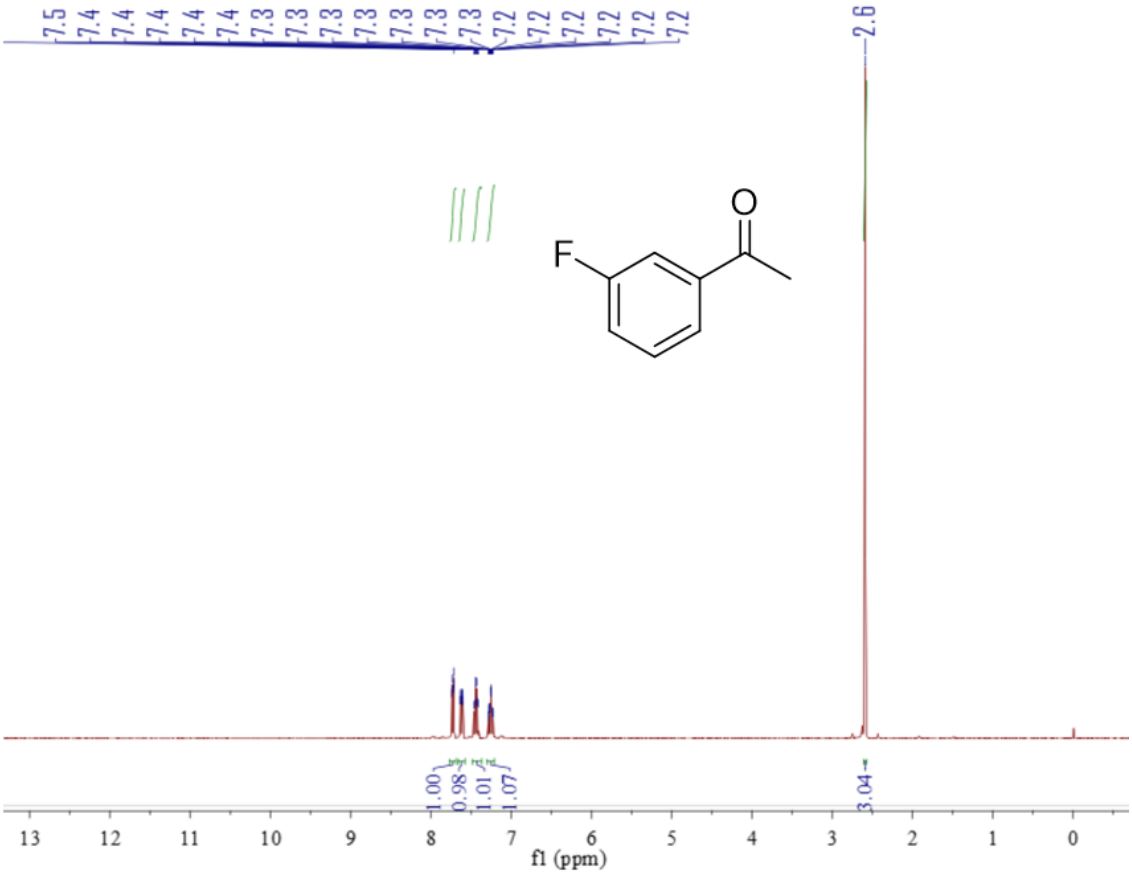
7.5
7.4
7.4
7.4
7.4
7.4
7.3
7.3
7.3
7.3
7.3
7.3
7.2
7.2
7.2
7.2
7.2
7.2
2.6
F
O
1.00
0.98
1.01
1.07
3.04
13
12
11
10
9
8
7
6
5
4
3
2
1
0
f1 (ppm)

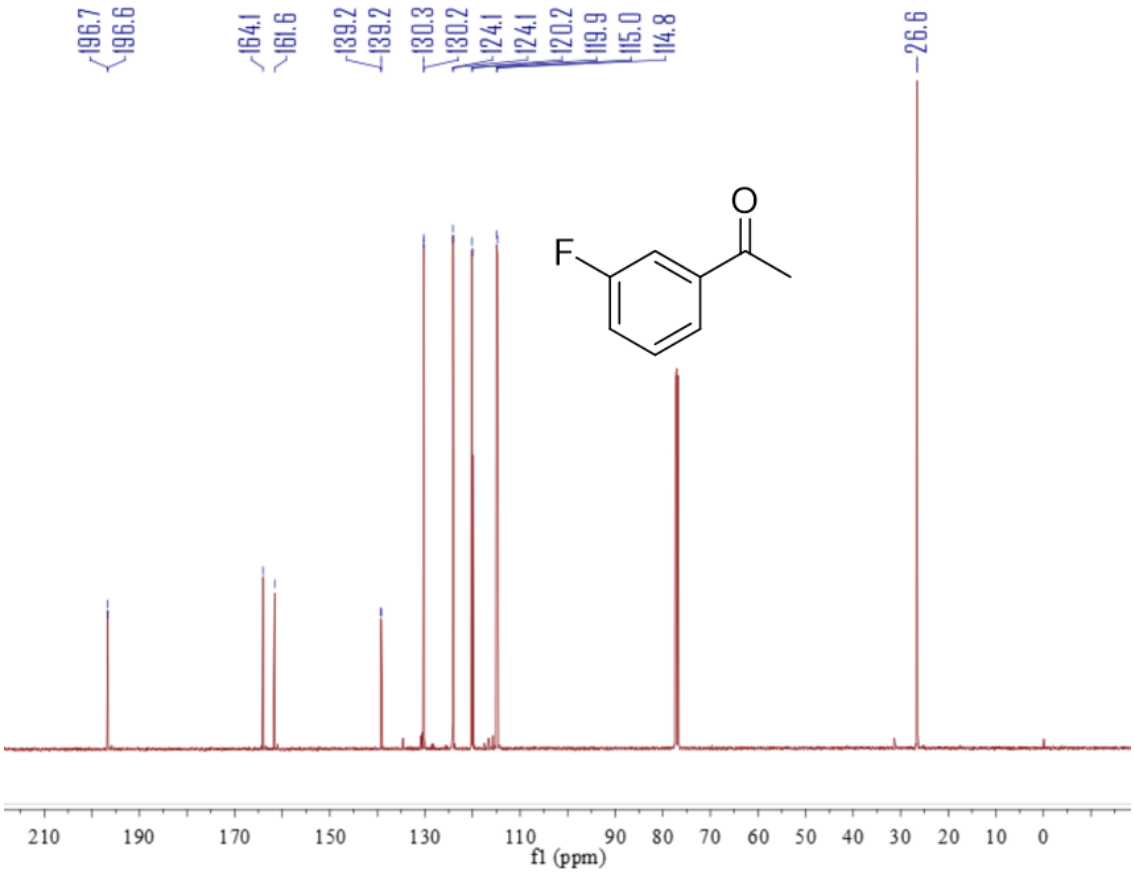
196.7
196.6
164.1
161.6
139.2
139.2
130.3
130.2
124.1
124.1
120.2
119.9
115.0
114.8
26.6
F
O
210
190
170
150
130
110
90
80
70
60
50
40
30
20
10
0
f1 (ppm)

Compound 4d

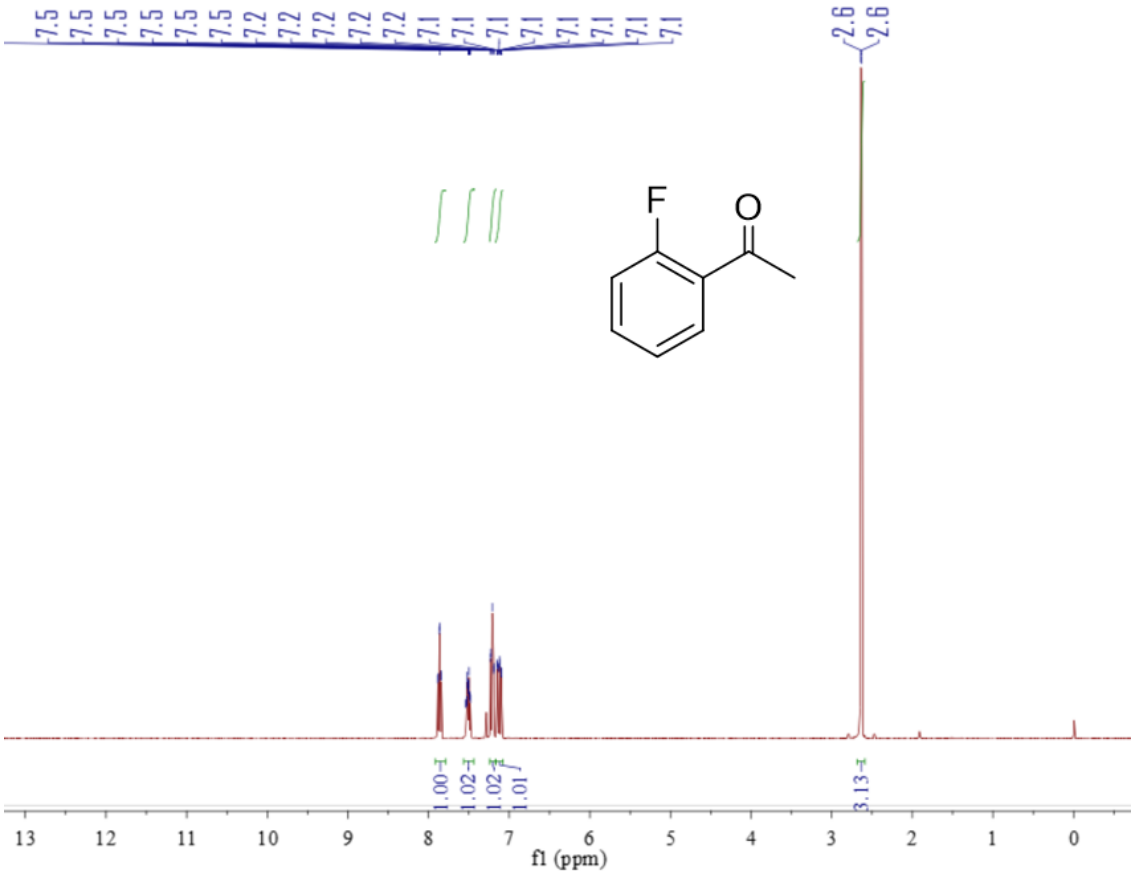
7.5
7.5
7.5
7.5
7.5
7.5
7.2
7.2
7.2
7.2
7.2
7.1
7.1
7.1
7.1
7.1
7.1
7.1
7.1
2.6
2.6
F
O
1.00
1.02
1.02
1.01
3.13
13
12
11
10
9
8
7
6
5
4
3
2
1
0
f1 (ppm)

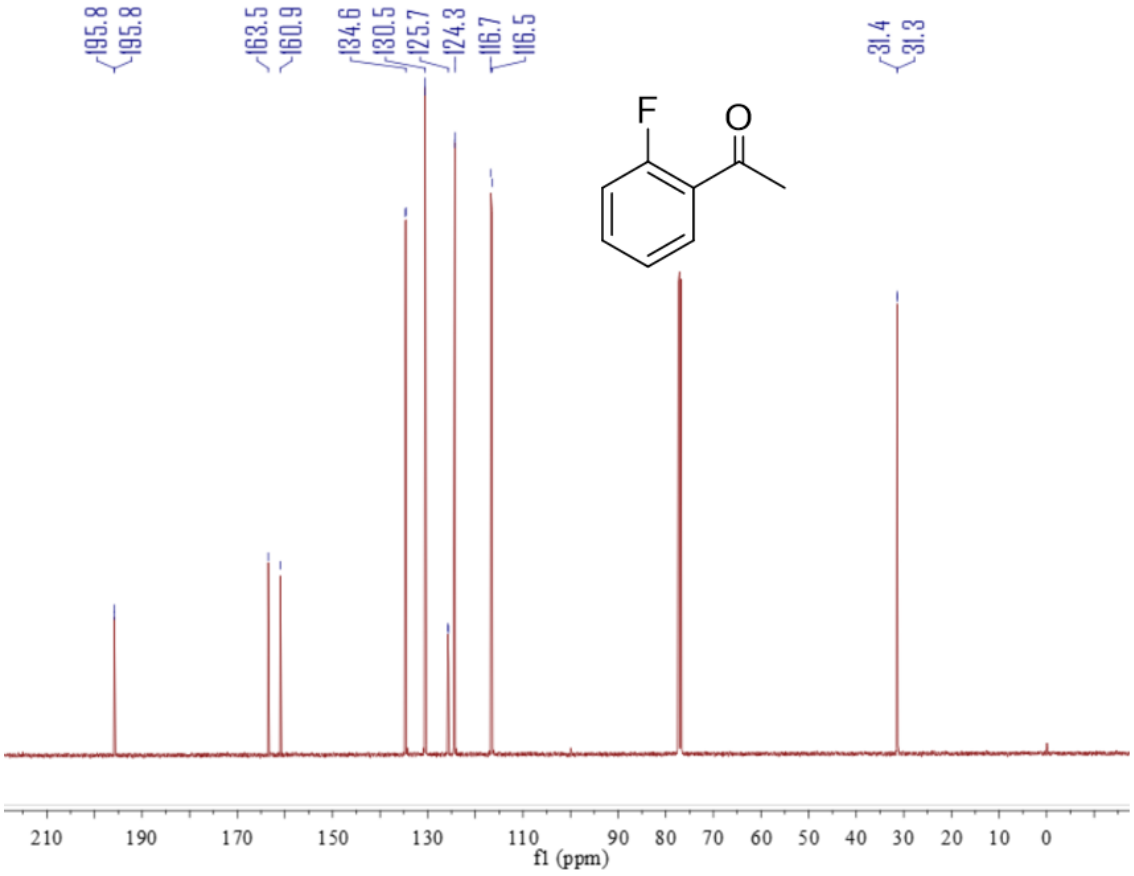
195.8
195.8
163.5
160.9
134.6
130.5
125.7
124.3
116.7
116.5
31.4
31.3
F
O
210
190
170
150
130
110
90
80
70
60
50
40
30
20
10
0
f1 (ppm)

Compound 4e

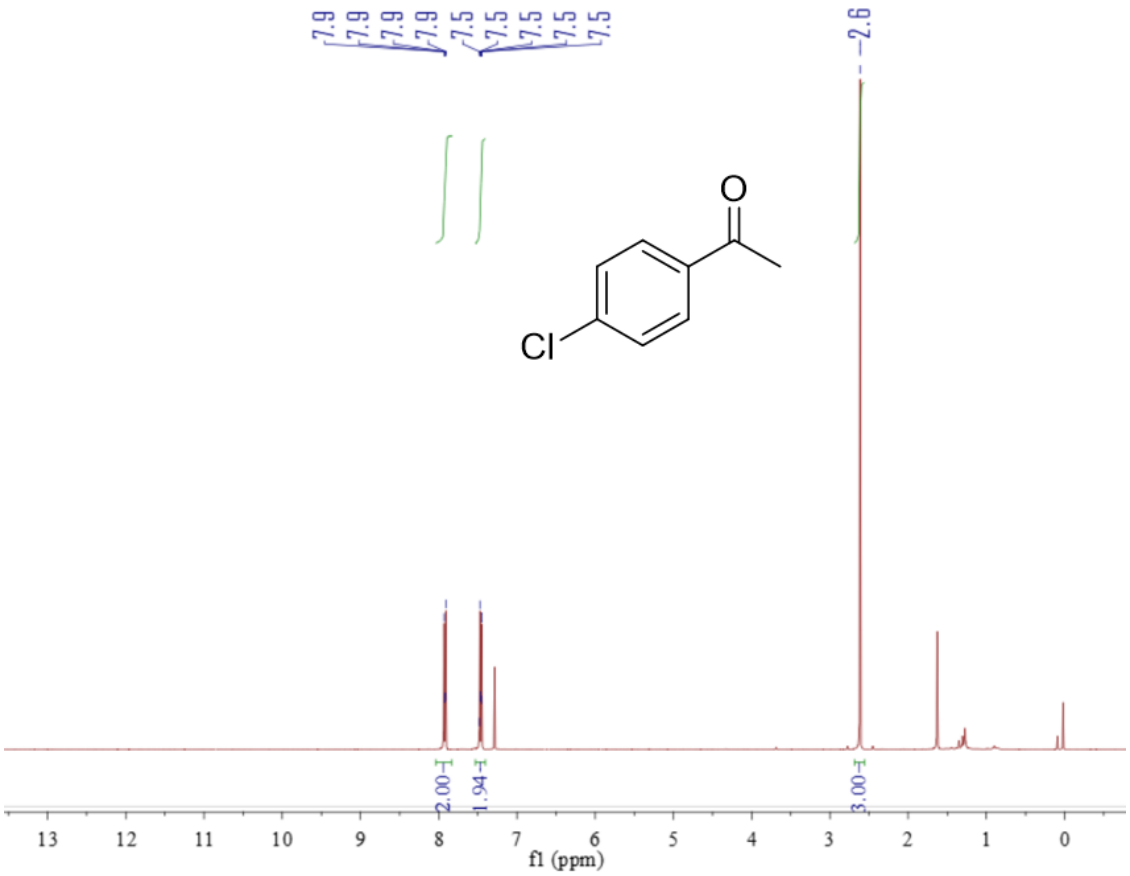
7.9
7.9
7.9
7.9
7.5
7.5
7.5
7.5
7.5
2.6
O
Cl
2.00
1.94
3.00
13 12 11 10 9 8 7 6 5 4 3 2 1 0
f1 (ppm)

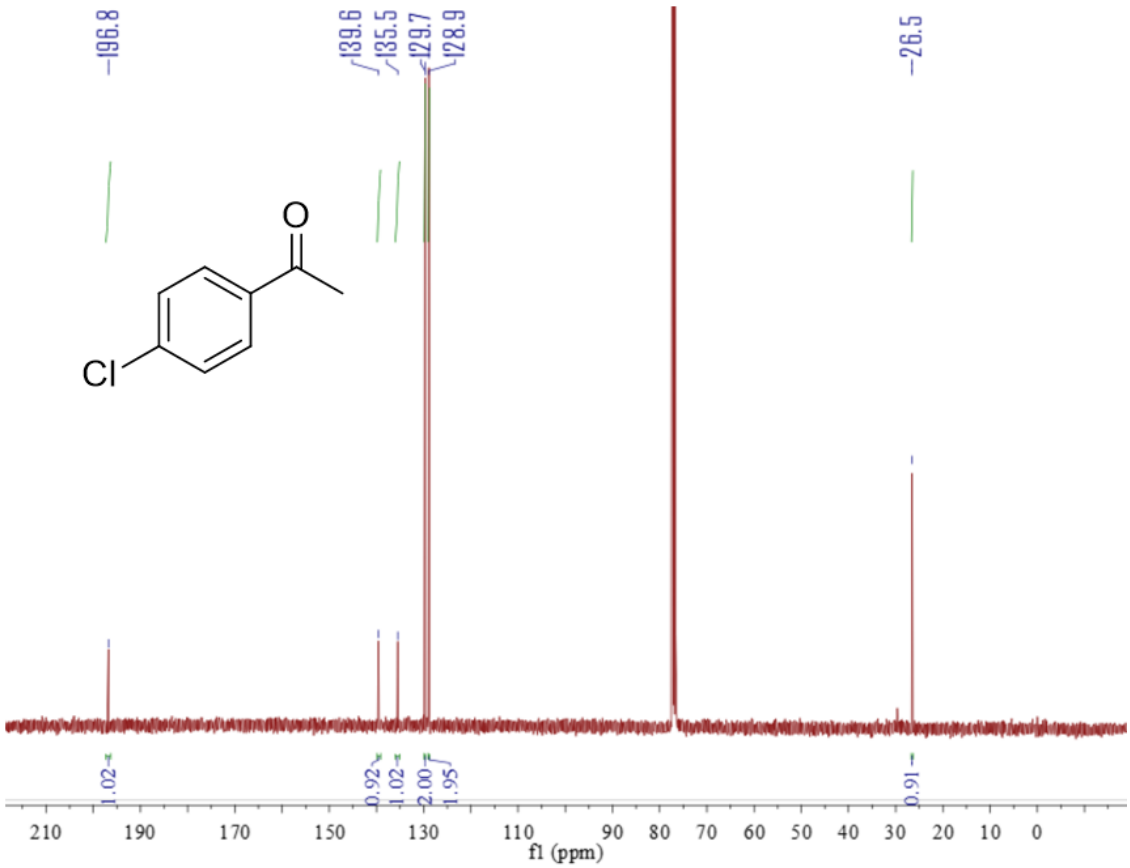
196.8
139.6
135.5
129.7
128.9
26.5
O
Cl
1.02
0.92
1.02
2.00
1.95
0.91
210 190 170 150 130 110 90 80 70 60 50 40 30 20 10 0
f1 (ppm)

Compound 4f

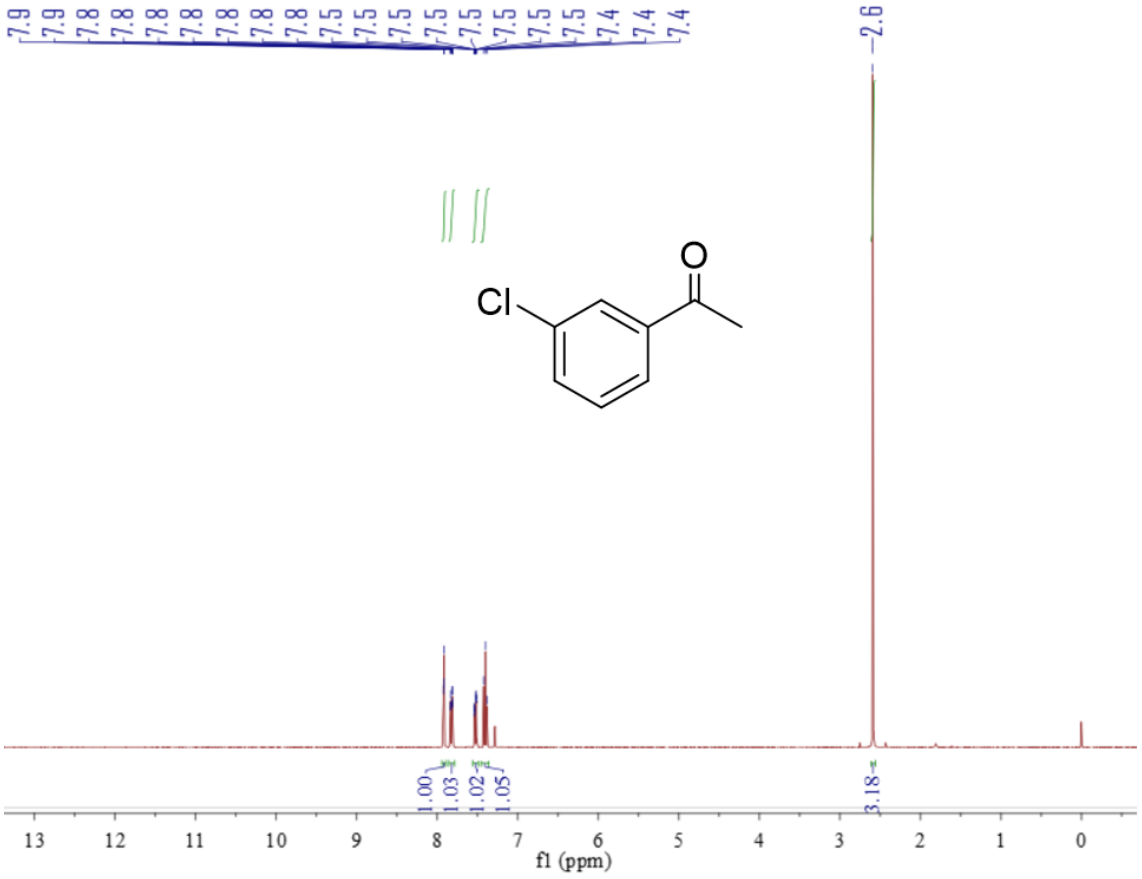
7.9
7.9
7.8
7.8
7.8
7.8
7.8
7.8
7.8
7.5
7.5
7.5
7.5
7.5
7.5
7.5
7.5
7.4
7.4
7.4
2.6
Cl
O
1.00
1.03
1.02
1.05
3.18
13
12
11
10
9
8
7
6
5
4
3
2
1
0
f1 (ppm)

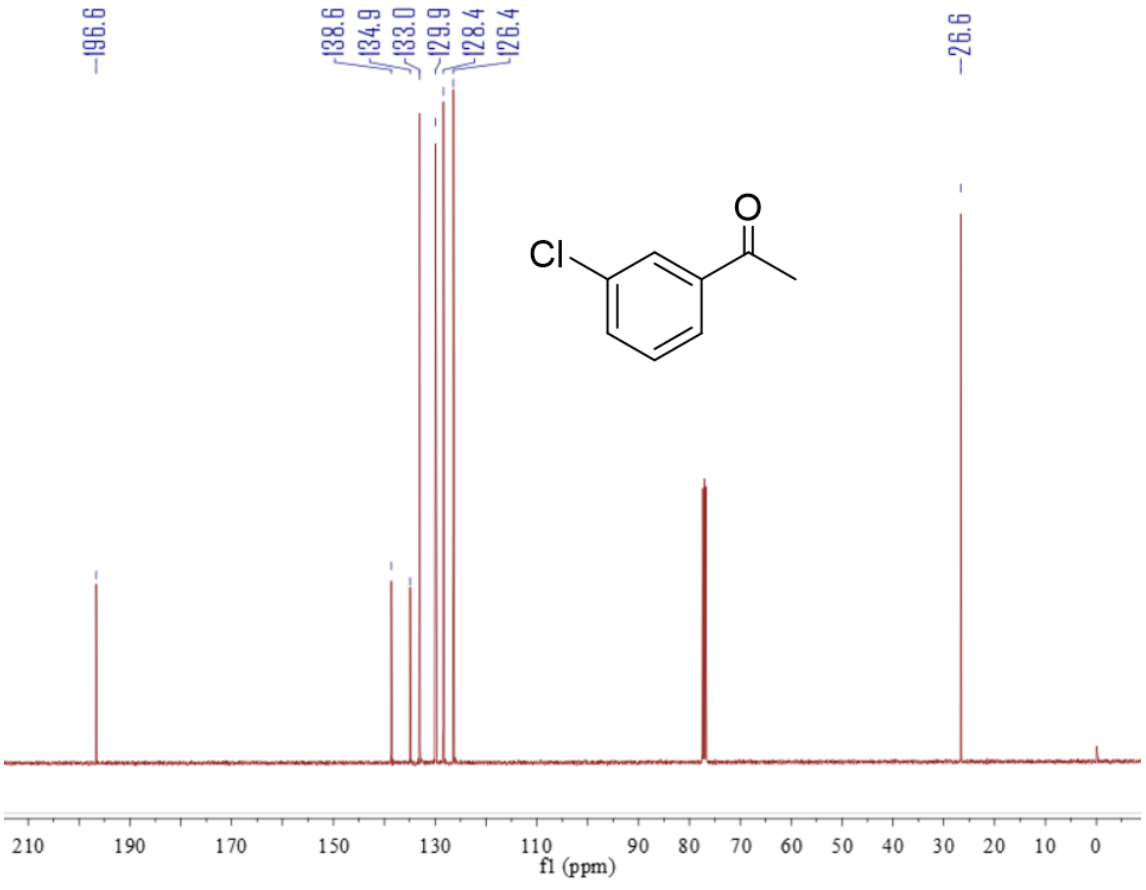
196.6
138.6
134.9
133.0
129.9
128.4
126.4
26.6
Cl
O
210
190
170
150
130
110
90
80
70
60
50
40
30
20
10
0
f1 (ppm)

Compound 4g

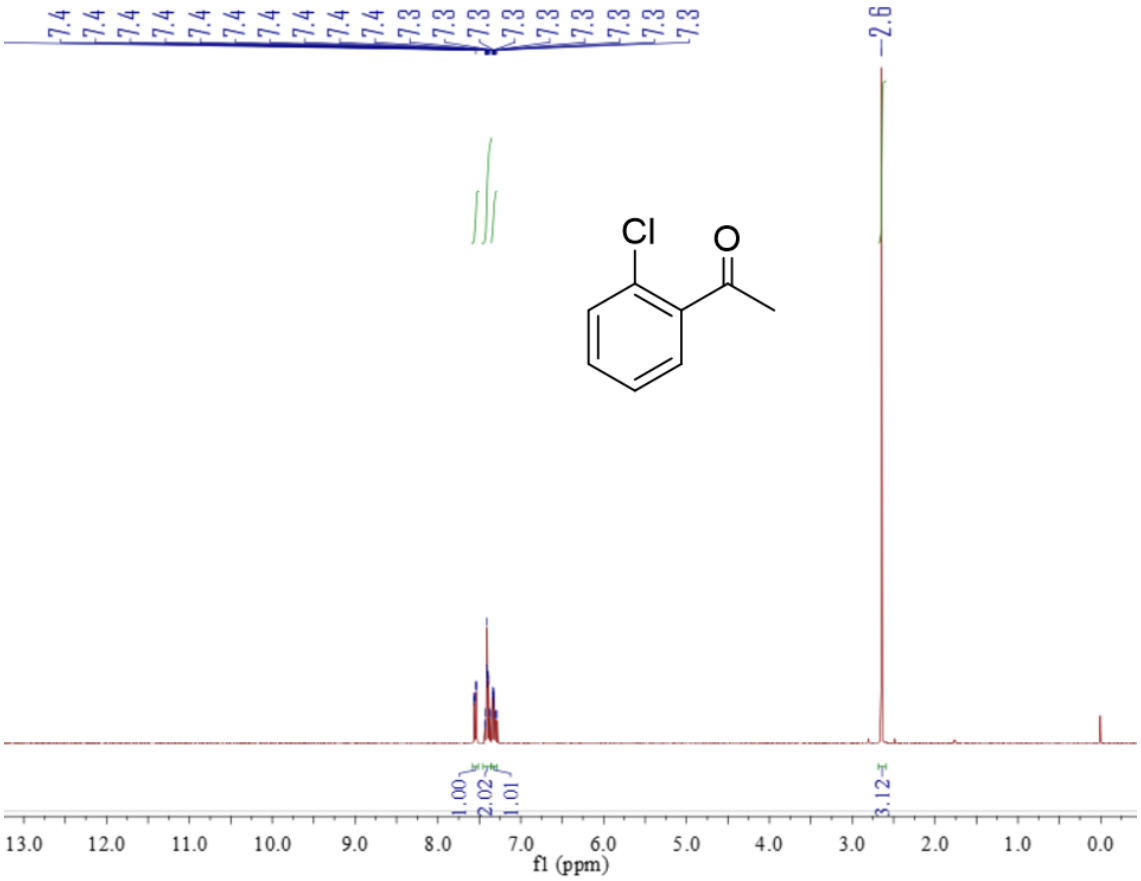
7.4
7.4
7.4
7.4
7.4
7.4
7.4
7.4
7.4
7.4
7.3
7.3
7.3
7.3
7.3
7.3
7.3
7.3
2.6
Cl
O
1.00
2.02
1.01
3.12
13.0
12.0
11.0
10.0
9.0
8.0
7.0
6.0
5.0
4.0
3.0
2.0
1.0
0.0
f1 (ppm)

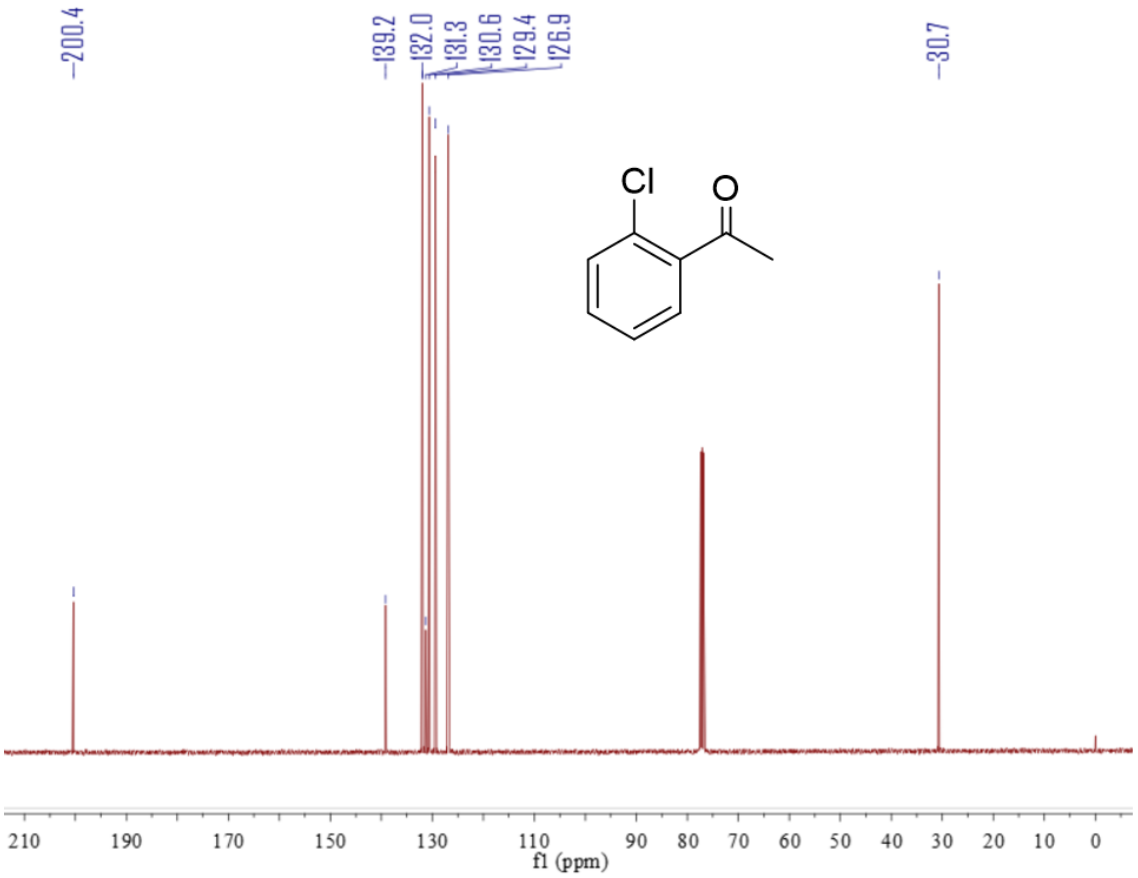
200.4
139.2
132.0
131.3
130.6
129.4
126.9
30.7
Cl
O
210
190
170
150
130
110
90
80
70
60
50
40
30
20
10
0
f1 (ppm)

Compound 4h

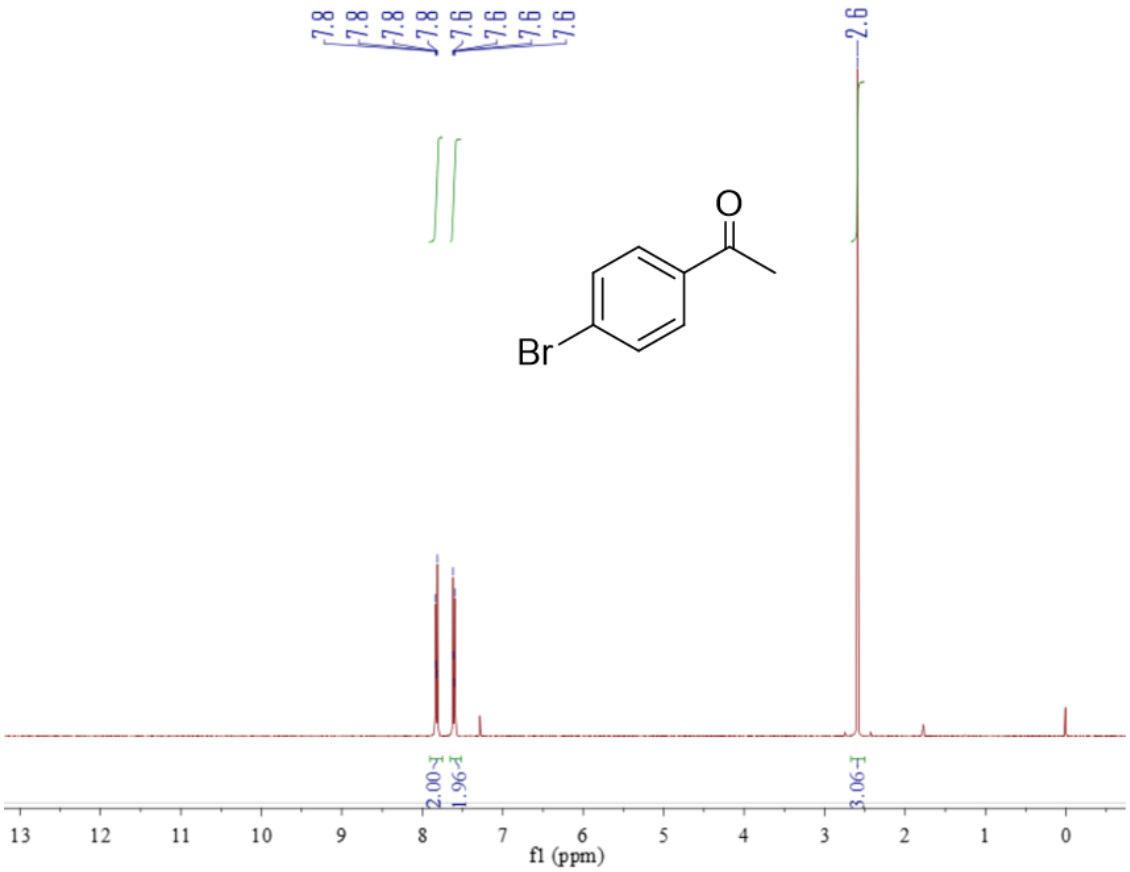
7.8
7.8
7.8
7.8
7.6
7.6
7.6
7.6
2.6
O
Br
2.00
1.96
3.06
13 12 11 10 9 8 7 6 5 4 3 2 1 0
f1 (ppm)

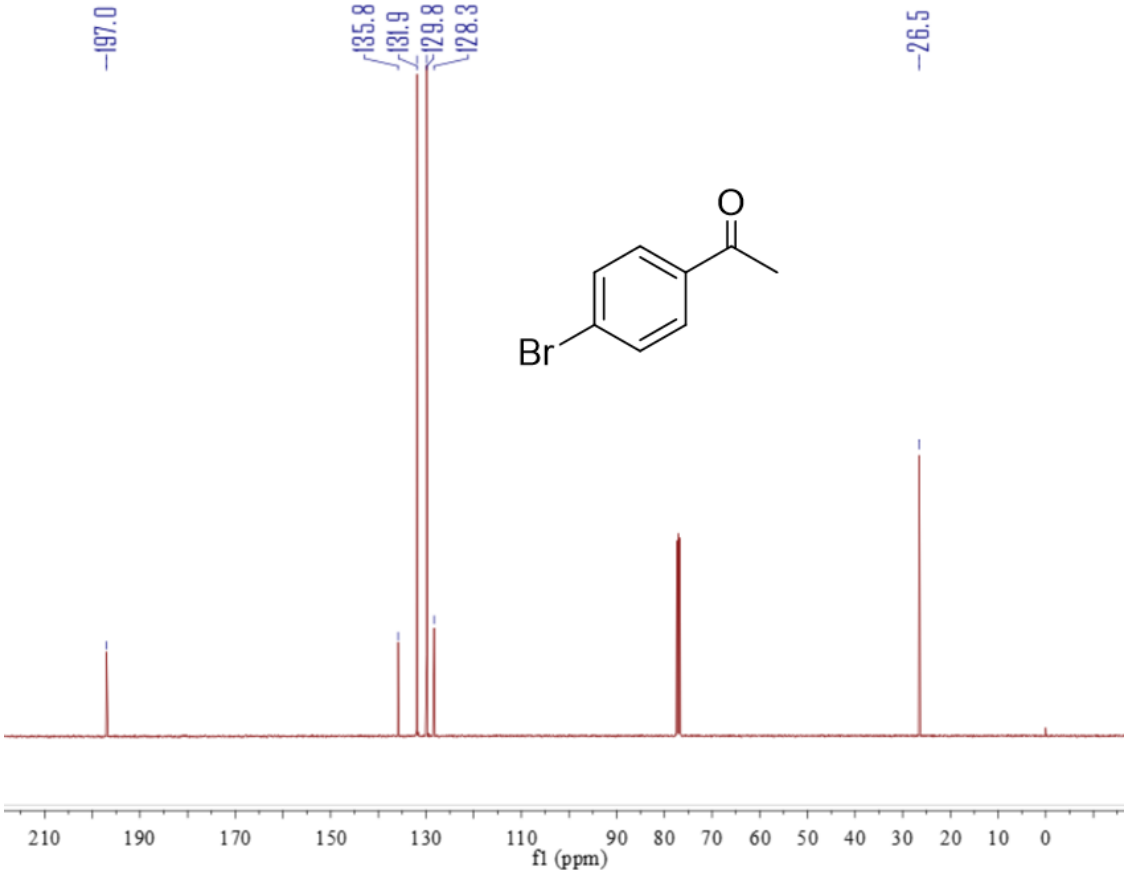
197.0
135.8
131.9
129.8
128.3
26.5
O
Br
210 190 170 150 130 110 90 80 70 60 50 40 30 20 10 0
f1 (ppm)

Compound 4i

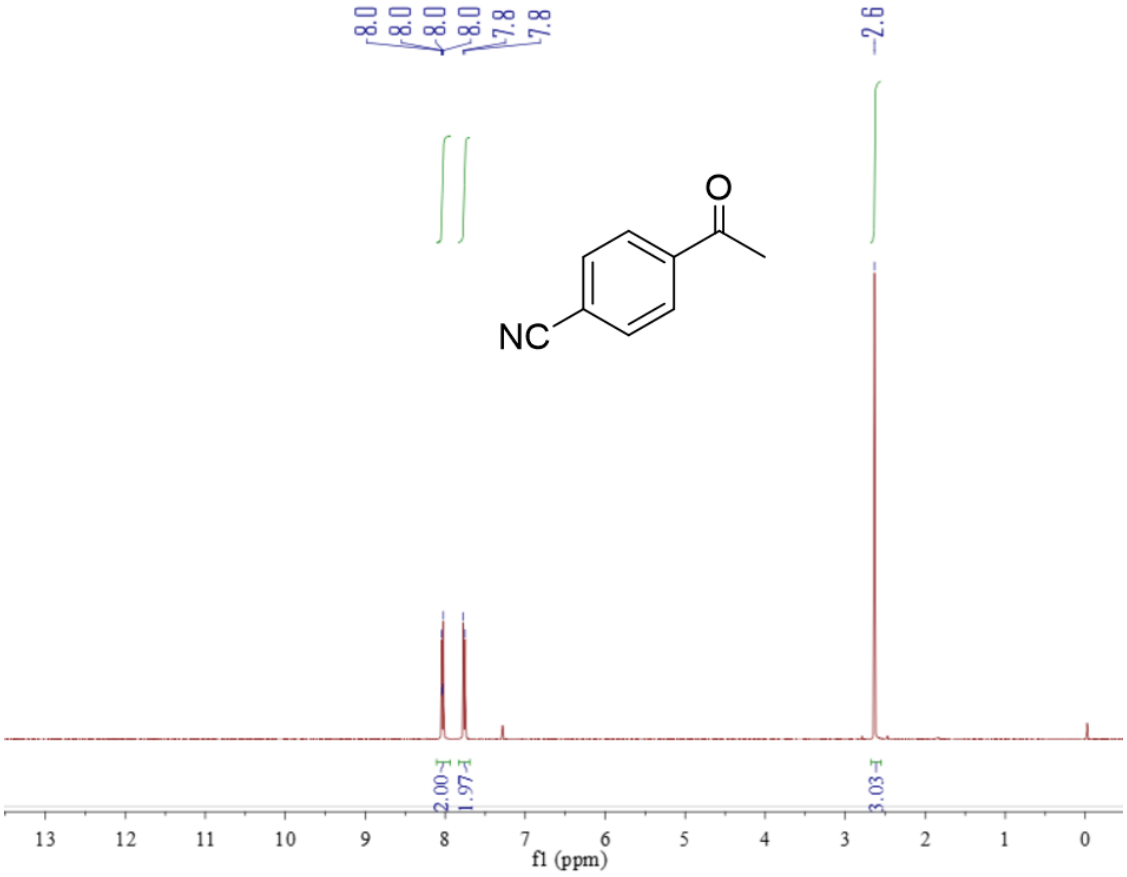
8.0
8.0
8.0
8.0
7.8
7.8
2.6
O
NC
2.00
1.97
3.03
13 12 11 10 9 8 7 6 5 4 3 2 1 0
f1 (ppm)

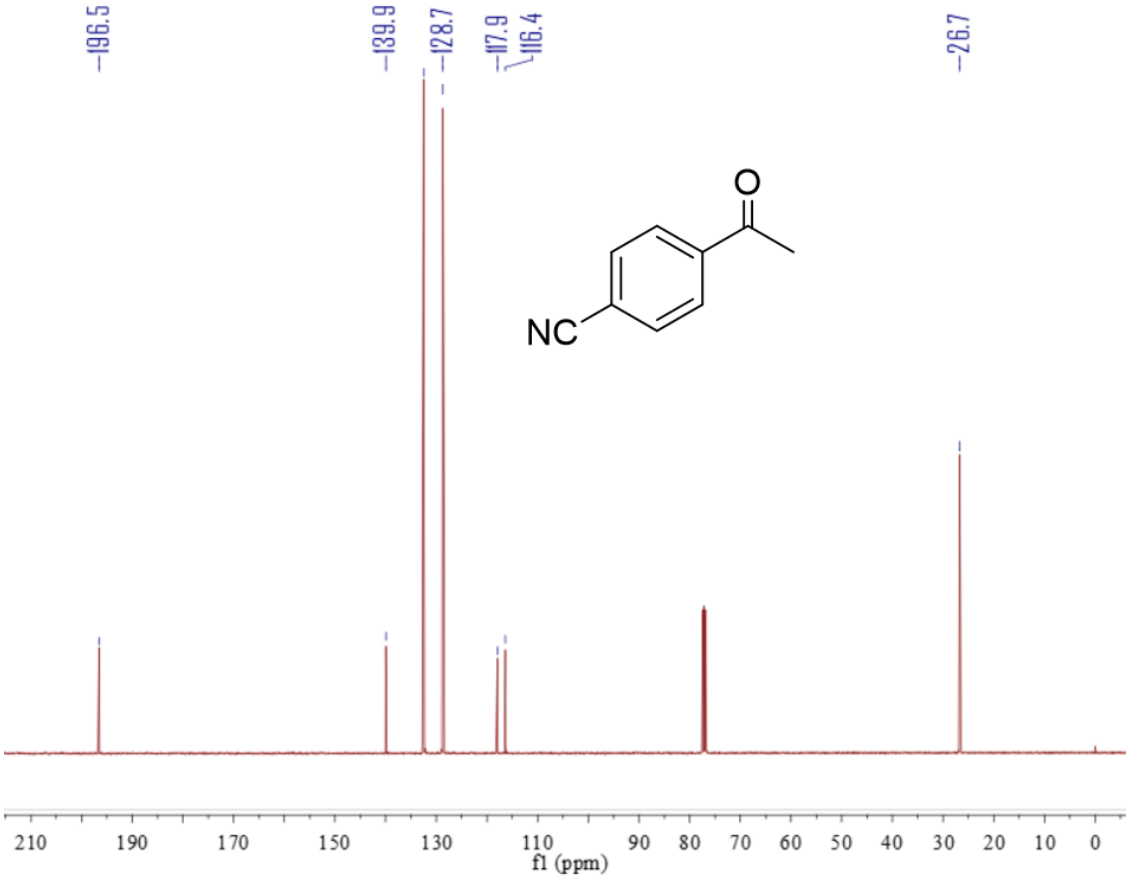
196.5
139.9
128.7
117.9
116.4
26.7
O
NC
210 190 170 150 130 110 90 80 70 60 50 40 30 20 10 0
f1 (ppm)

Compound 4j

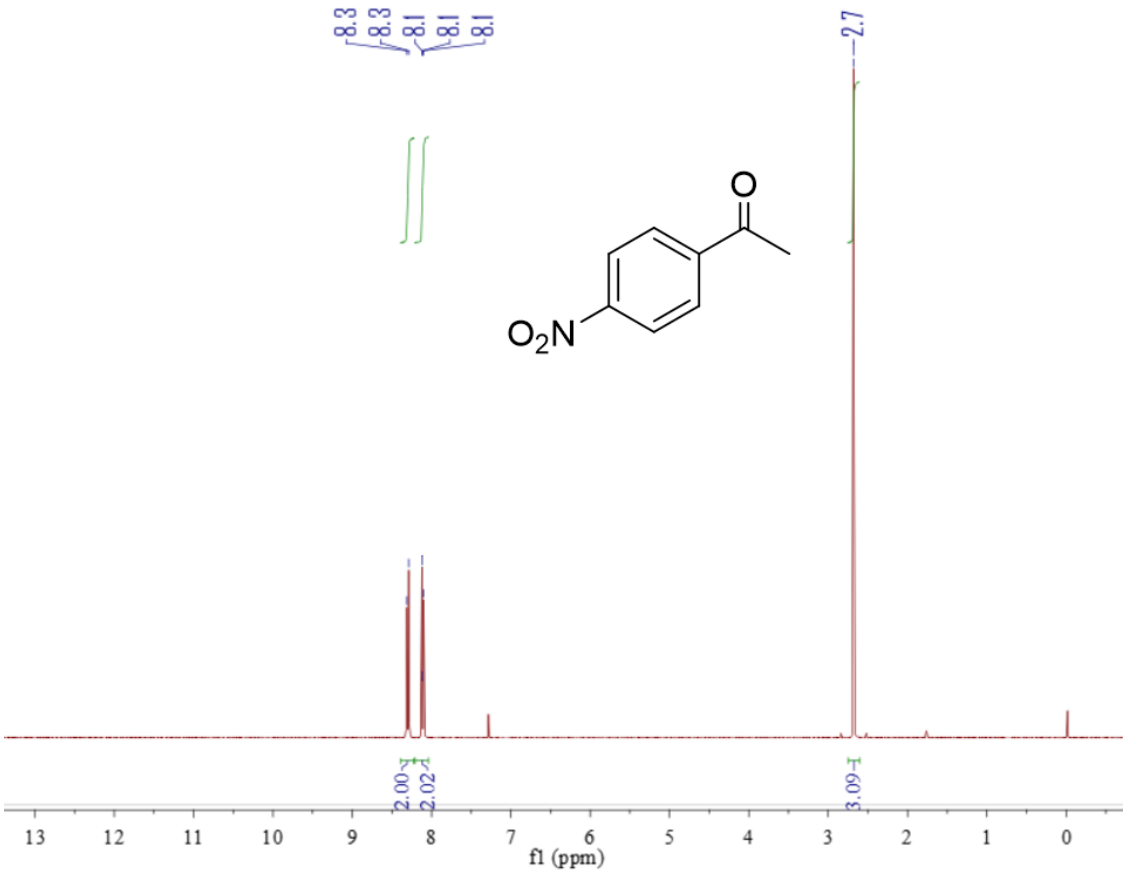
8.3
8.3
8.1
8.1
8.1
2.7
O
O2N
2.00
2.02
3.09
13 12 11 10 9 8 7 6 5 4 3 2 1 0
f1 (ppm)

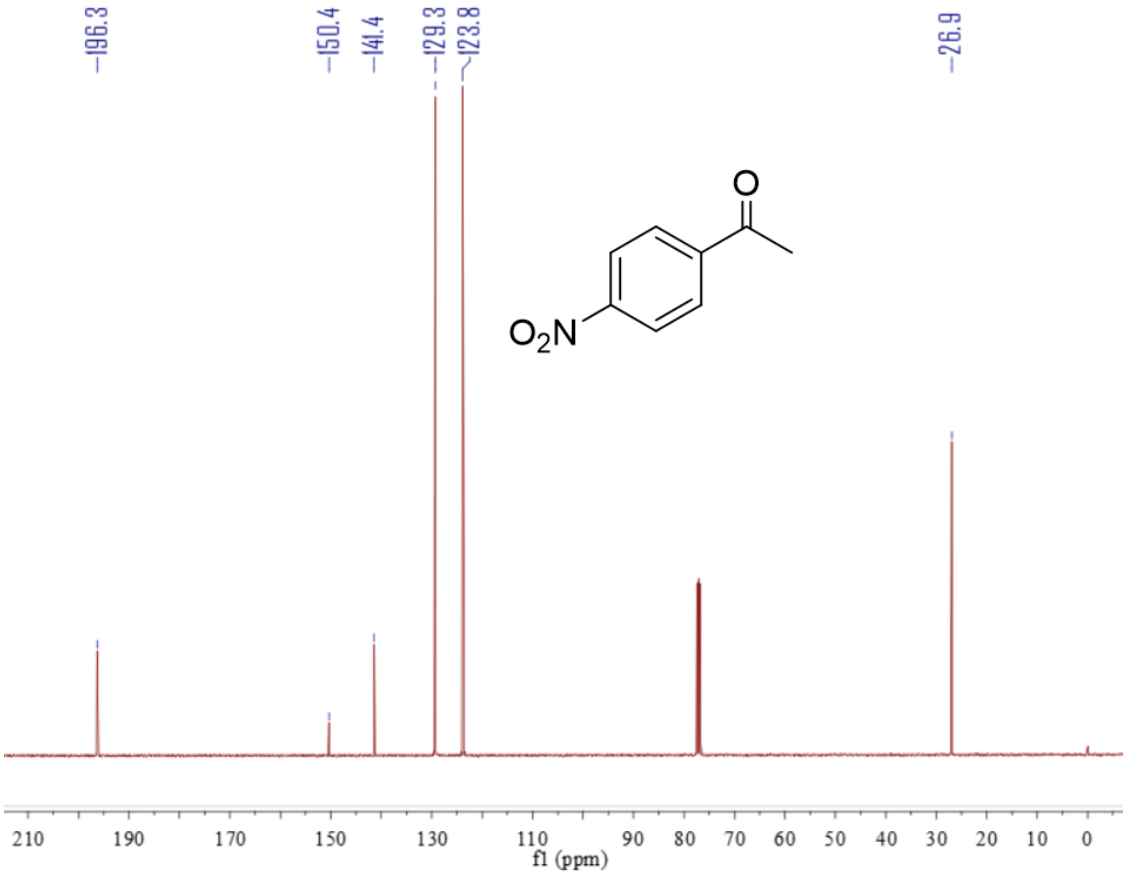
196.3
150.4
141.4
129.3
123.8
26.9
O
O2N
210 190 170 150 130 110 90 80 70 60 50 40 30 20 10 0
f1 (ppm)

Compound 4k

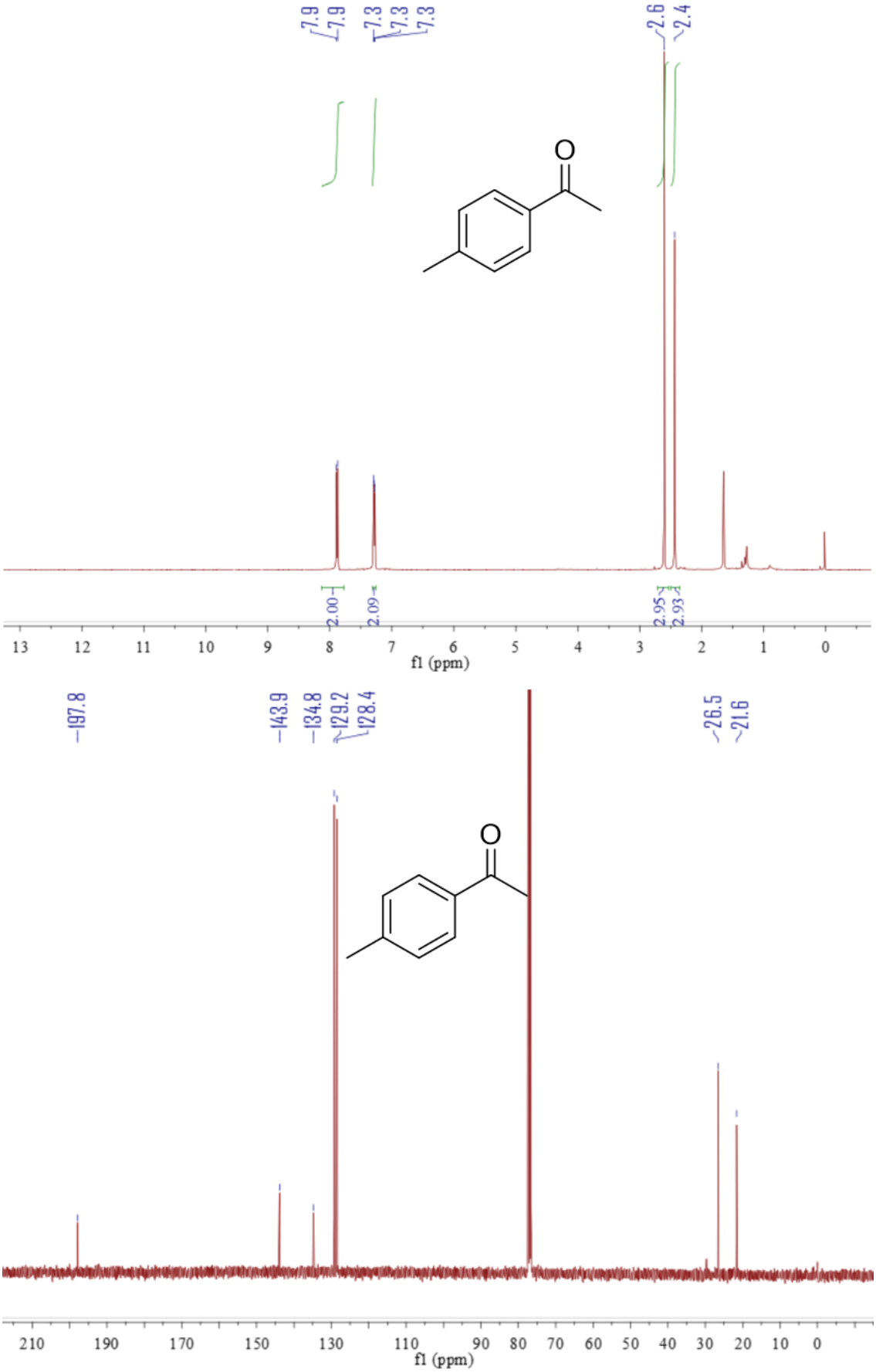
7.9
7.9
7.3
7.3
7.3
2.6
2.4
O
2.00
2.09
2.95
2.93
13 12 11 10 9 8 7 6 5 4 3 2 1 0
f1 (ppm)
197.8
143.9
134.8
129.2
128.4
26.5
21.6
O
210 190 170 150 130 110 90 80 70 60 50 40 30 20 10 0
f1 (ppm)

Compound 4l

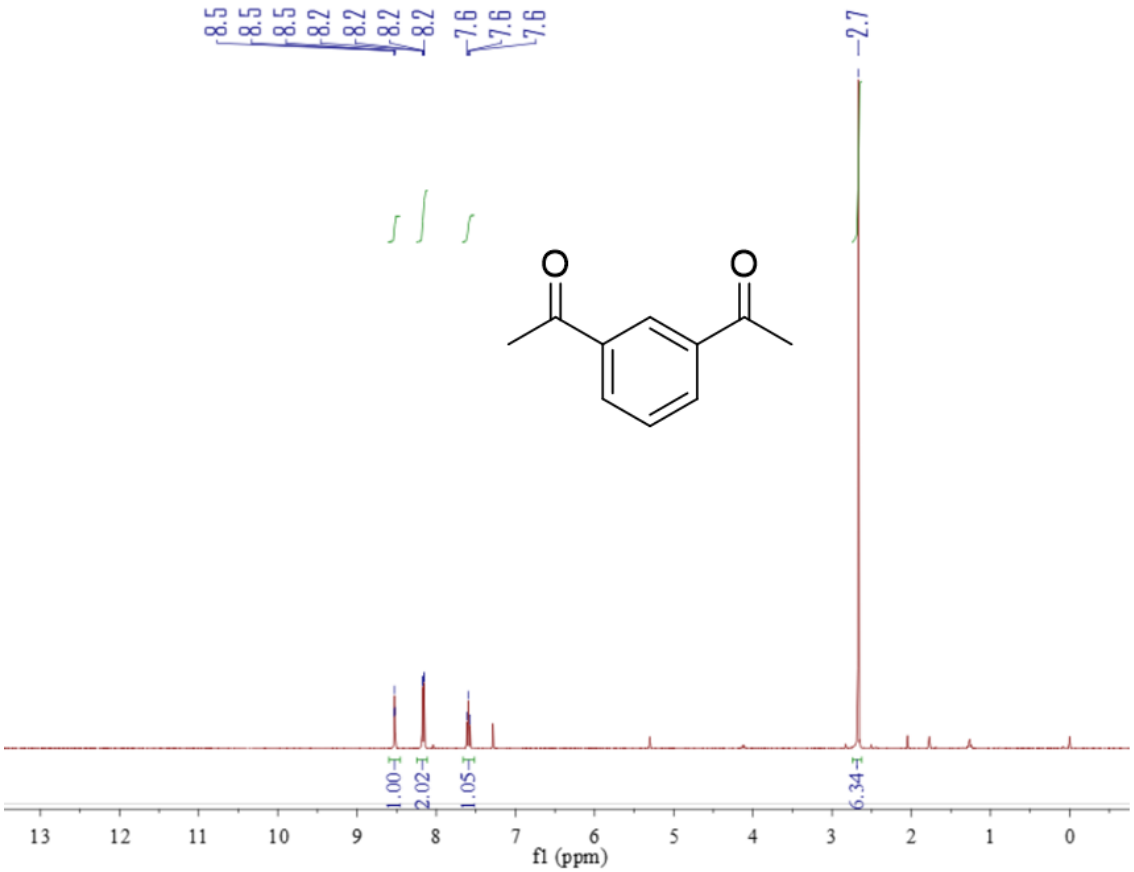
8.5
8.5
8.5
8.2
8.2
8.2
8.2
7.6
7.6
7.6
2.7
1.00
2.02
1.05
6.34
13 12 11 10 9 8 7 6 5 4 3 2 1 0
f1 (ppm)


197.3
137.4
132.5
129.0
128.0
26.7
210 190 170 150 130 110 90 80 70 60 50 40 30 20 10 0
f1 (ppm)

Compound 4m

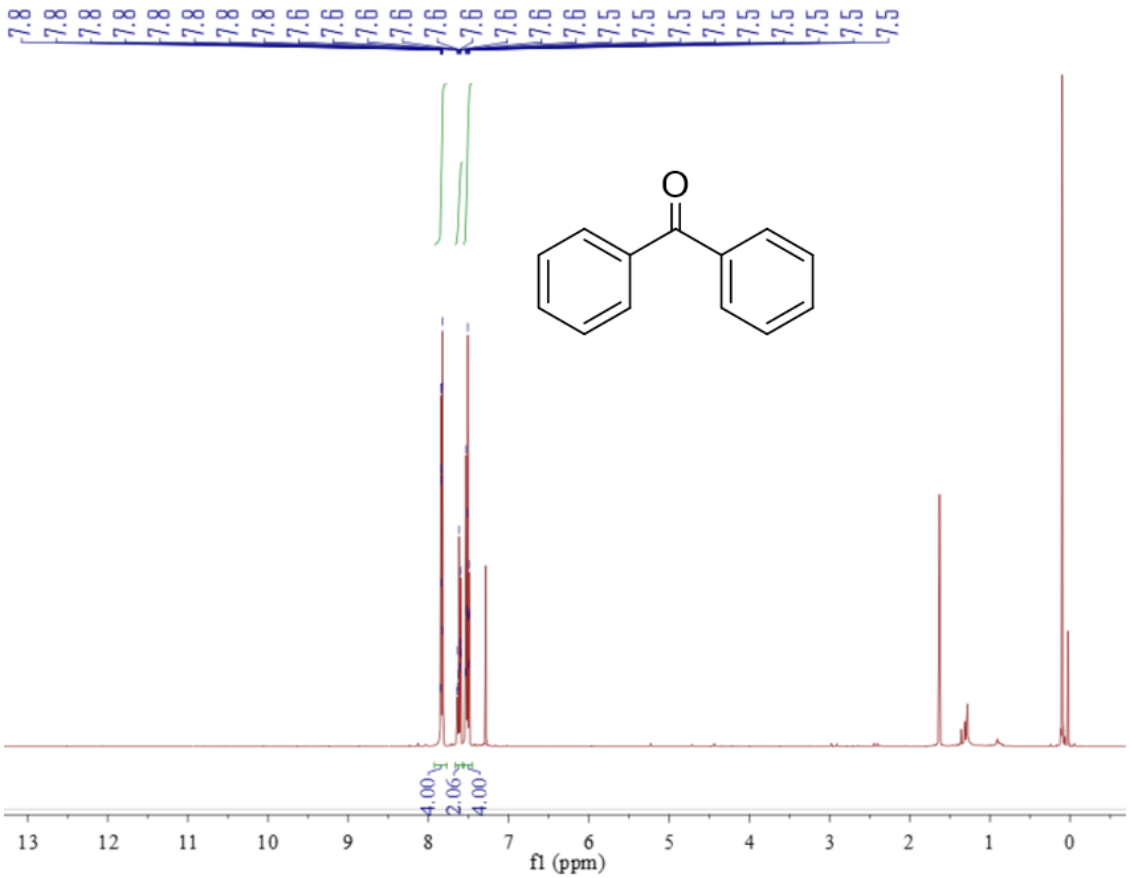
7.8
7.8
7.8
7.8
7.8
7.8
7.8
7.8
7.6
7.6
7.6
7.6
7.6
7.6
7.6
7.6
7.5
7.5
7.5
7.5
7.5
7.5
7.5
7.5
O
4.00
2.06
4.00
13
12
11
10
9
8
7
6
5
4
3
2
1
0
f1 (ppm)

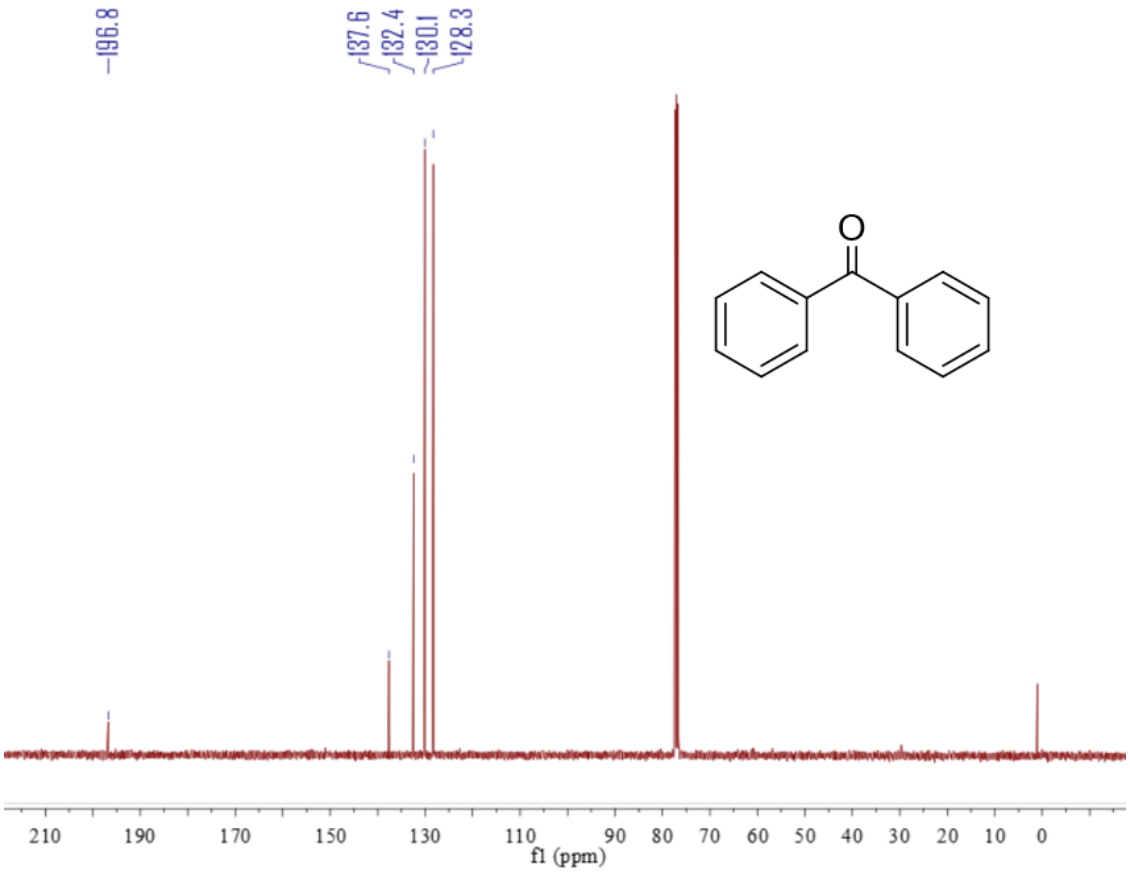
196.8
137.6
132.4
130.1
128.3
O
210
190
170
150
130
110
90
80
70
60
50
40
30
20
10
0
f1 (ppm)

Compound 4n

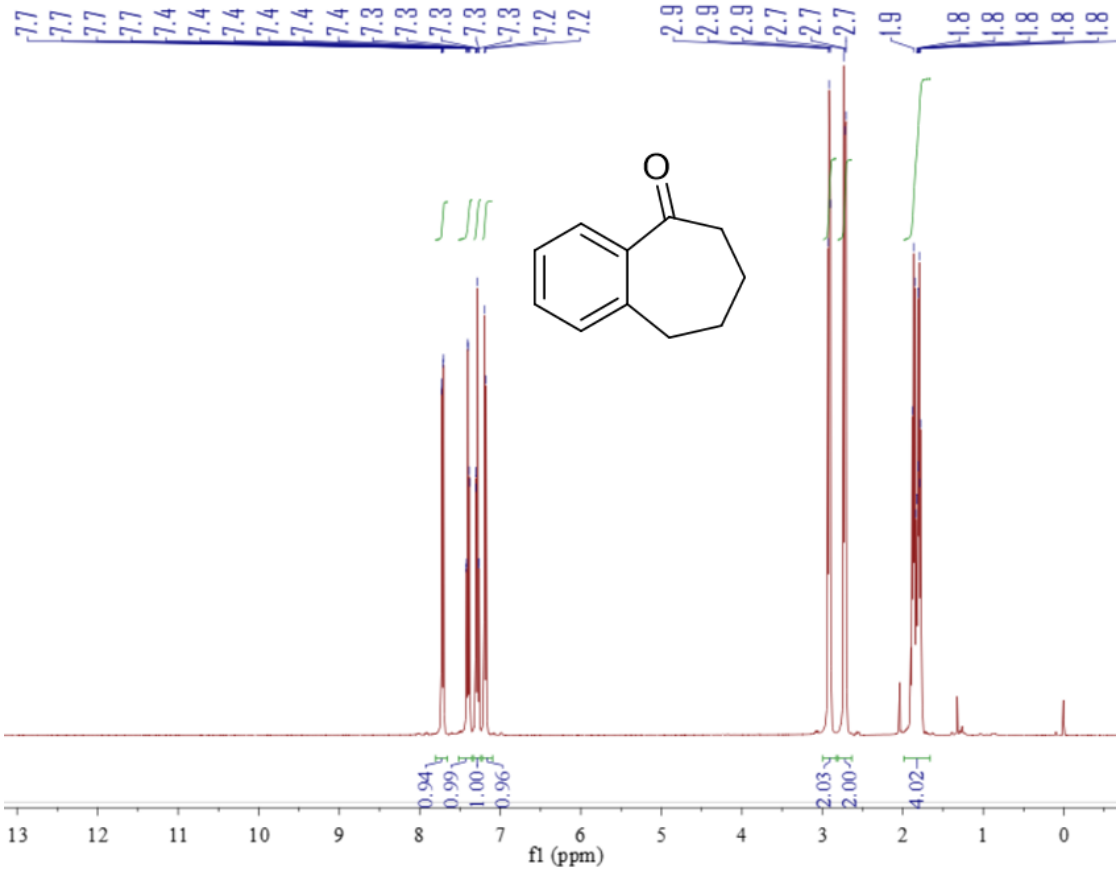
7.7
7.7
7.7
7.7
7.4
7.4
7.4
7.4
7.4
7.4
7.3
7.3
7.3
7.3
7.3
7.2
7.2
2.9
2.9
2.9
2.7
2.7
2.7
1.9
1.8
1.8
1.8
1.8
1.8
O
0.94
0.99
1.00
0.96
2.03
2.00
4.02
13
12
11
10
9
8
7
6
5
4
3
2
1
0
f1 (ppm)

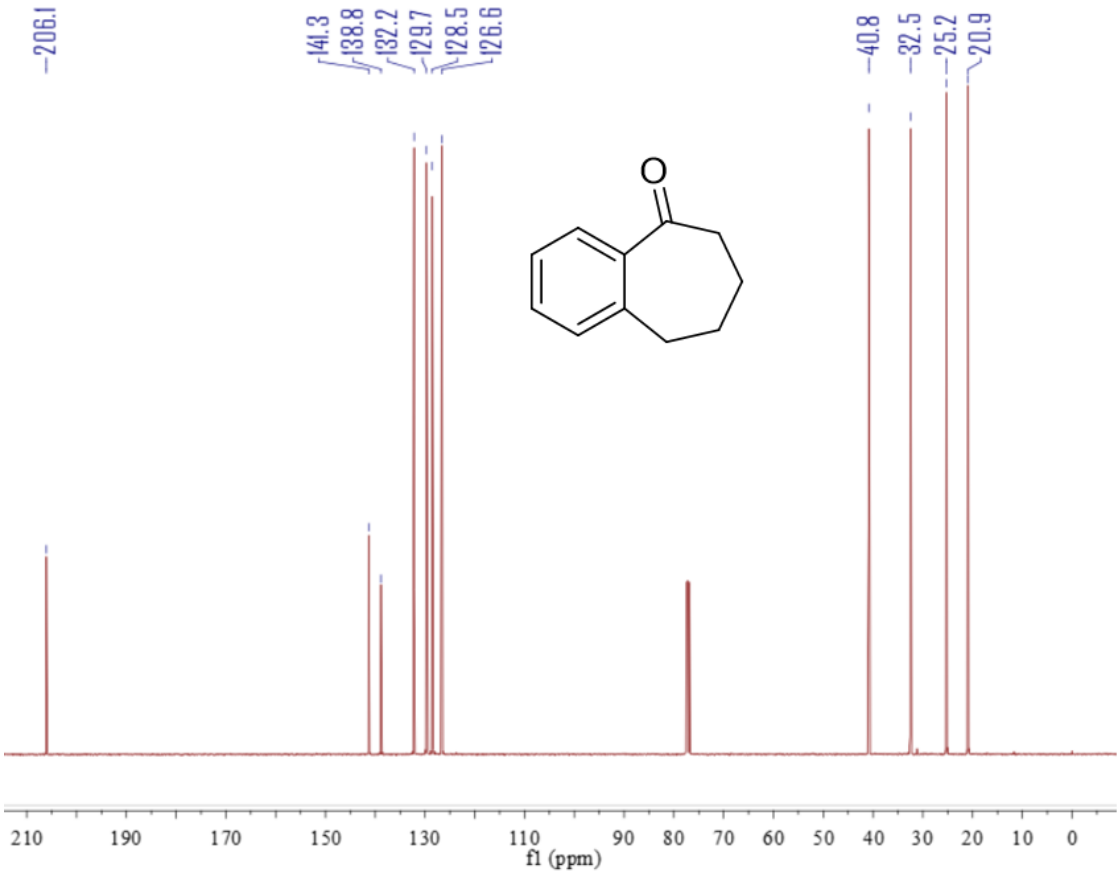
206.1
141.3
138.8
132.2
129.7
128.5
126.6
40.8
32.5
25.2
20.9
O
210
190
170
150
130
110
90
80
70
60
50
40
30
20
10
0
f1 (ppm)

Compound 4o

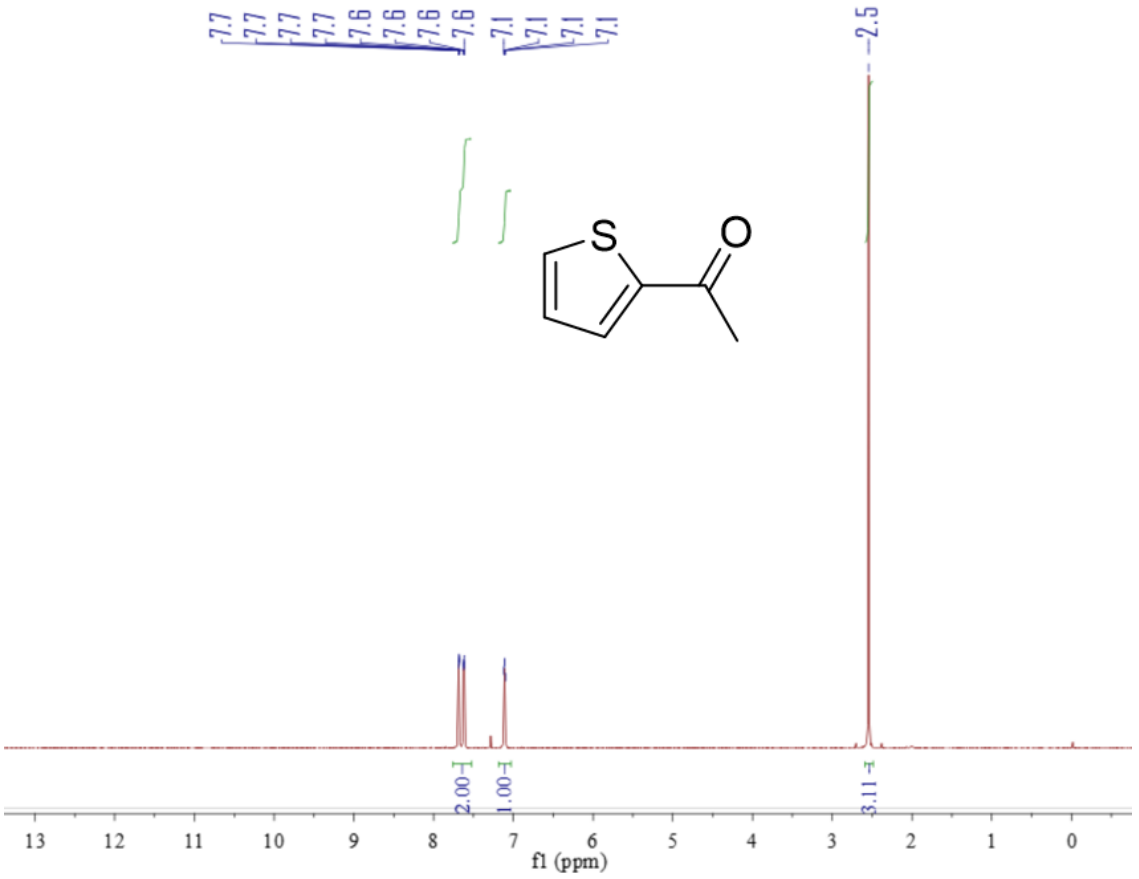
7.7
7.7
7.7
7.7
7.6
7.6
7.6
7.6
7.1
7.1
7.1
7.1
2.5
S
O
2.00
1.00
3.11
13
12
11
10
9
8
7
6
5
4
3
2
1
0
f1 (ppm)

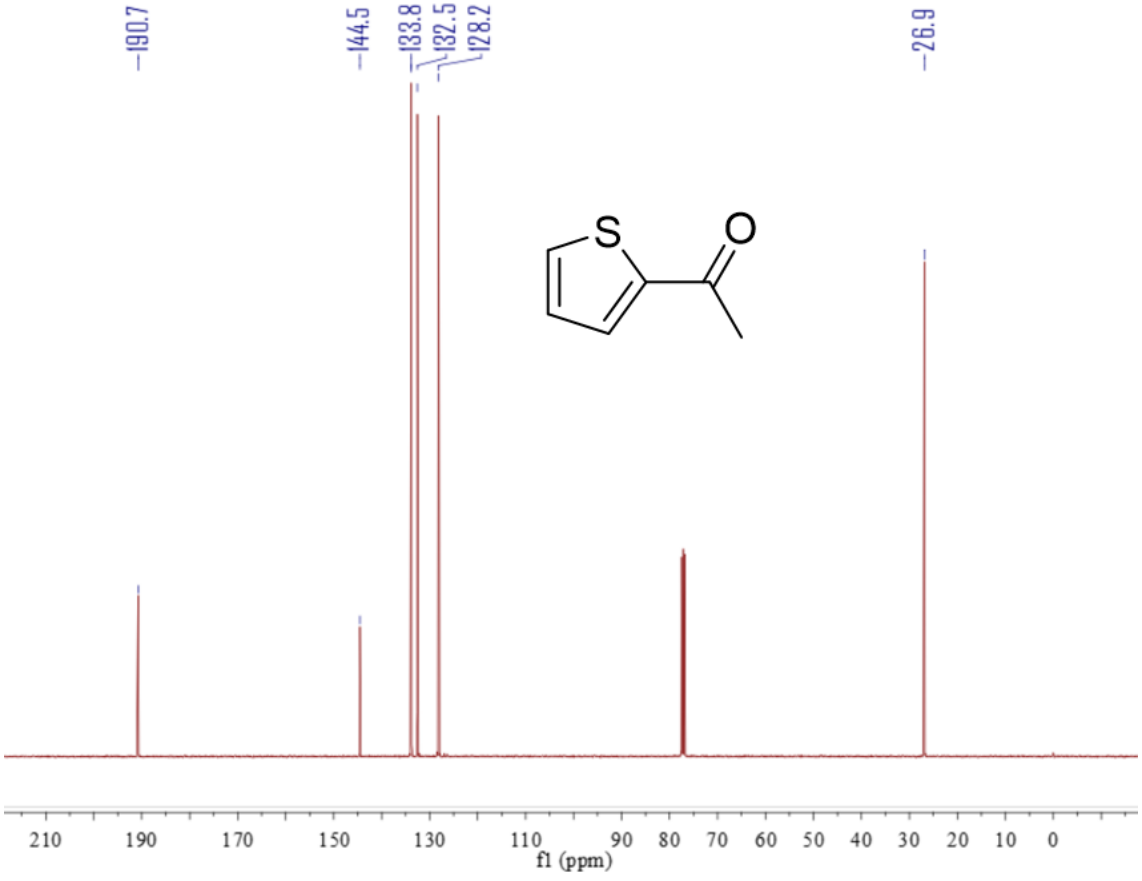
190.7
144.5
133.8
132.5
128.2
26.9
S
O
210
190
170
150
130
110
90
80
70
60
50
40
30
20
10
0
f1 (ppm)

Compound 4p

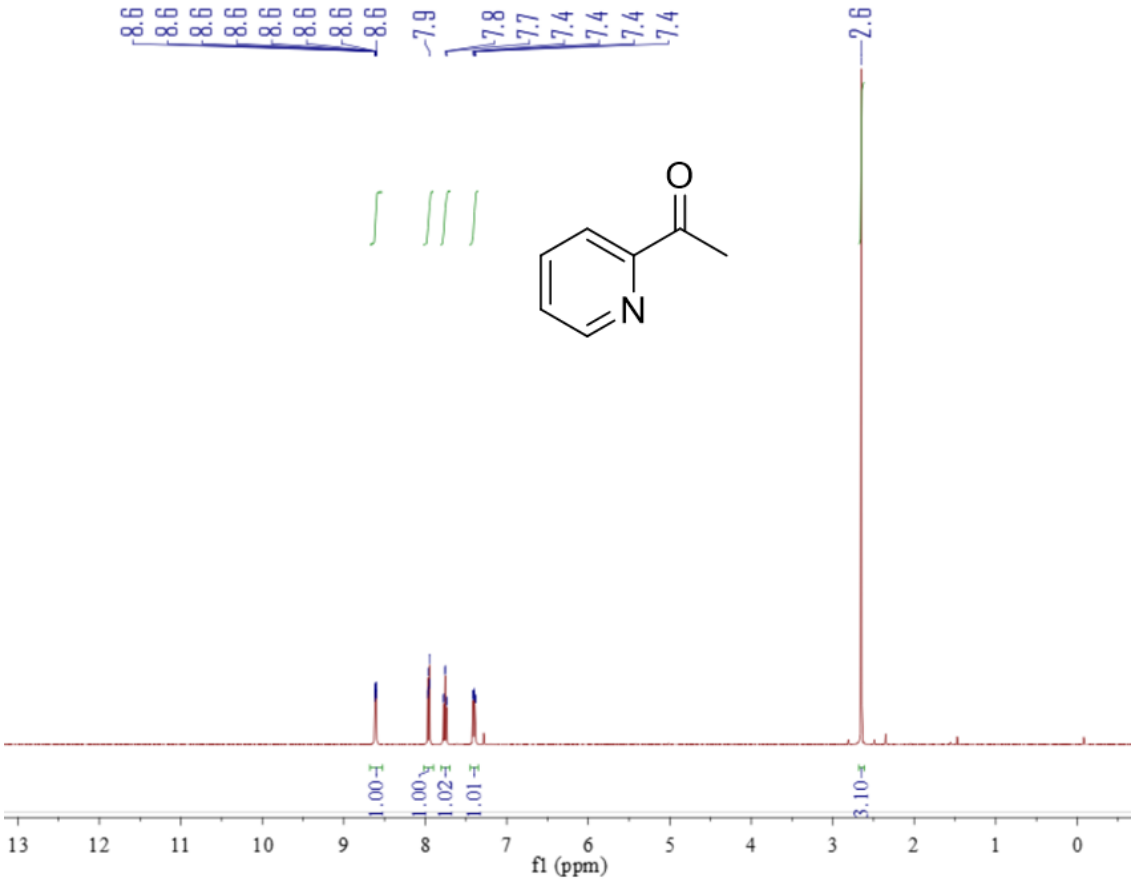
8.6
8.6
8.6
8.6
8.6
8.6
8.6
8.6
7.9
7.8
7.7
7.4
7.4
7.4
7.4
2.6
O
N
1.00
1.00
1.02
1.01
3.10
13
12
11
10
9
8
7
6
5
4
3
2
1
0
f1 (ppm)

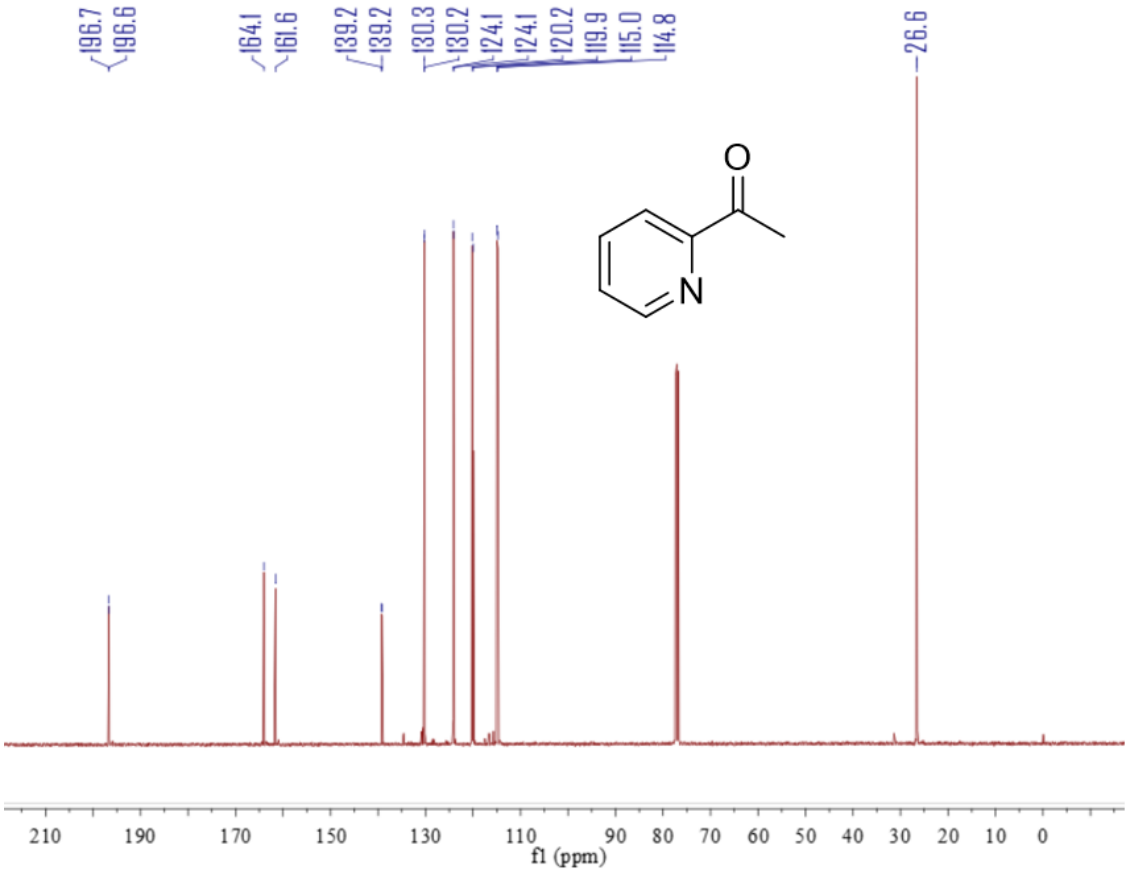
196.7
196.6
164.1
161.6
139.2
139.2
130.3
130.2
124.1
124.1
120.2
119.9
115.0
114.8
26.6
O
N
210
190
170
150
130
110
90
80
70
60
50
40
30
20
10
0
f1 (ppm)

Compound 4q

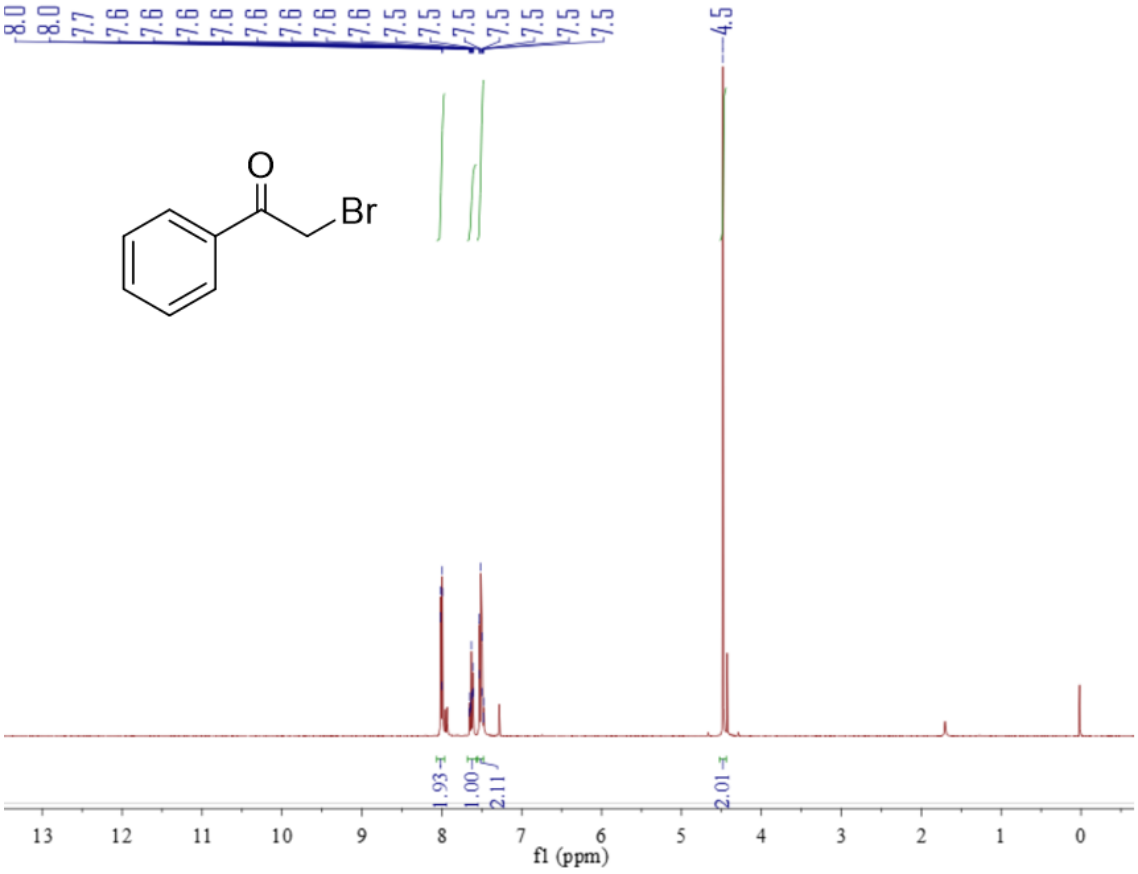
8.0
8.0
7.7
7.6
7.6
7.6
7.6
7.6
7.6
7.6
7.6
7.5
7.5
7.5
7.5
7.5
7.5
7.5
4.5
O
Br
1.93
1.00
2.11
2.01
13
12
11
10
9
8
7
6
5
4
3
2
1
0
f1 (ppm)

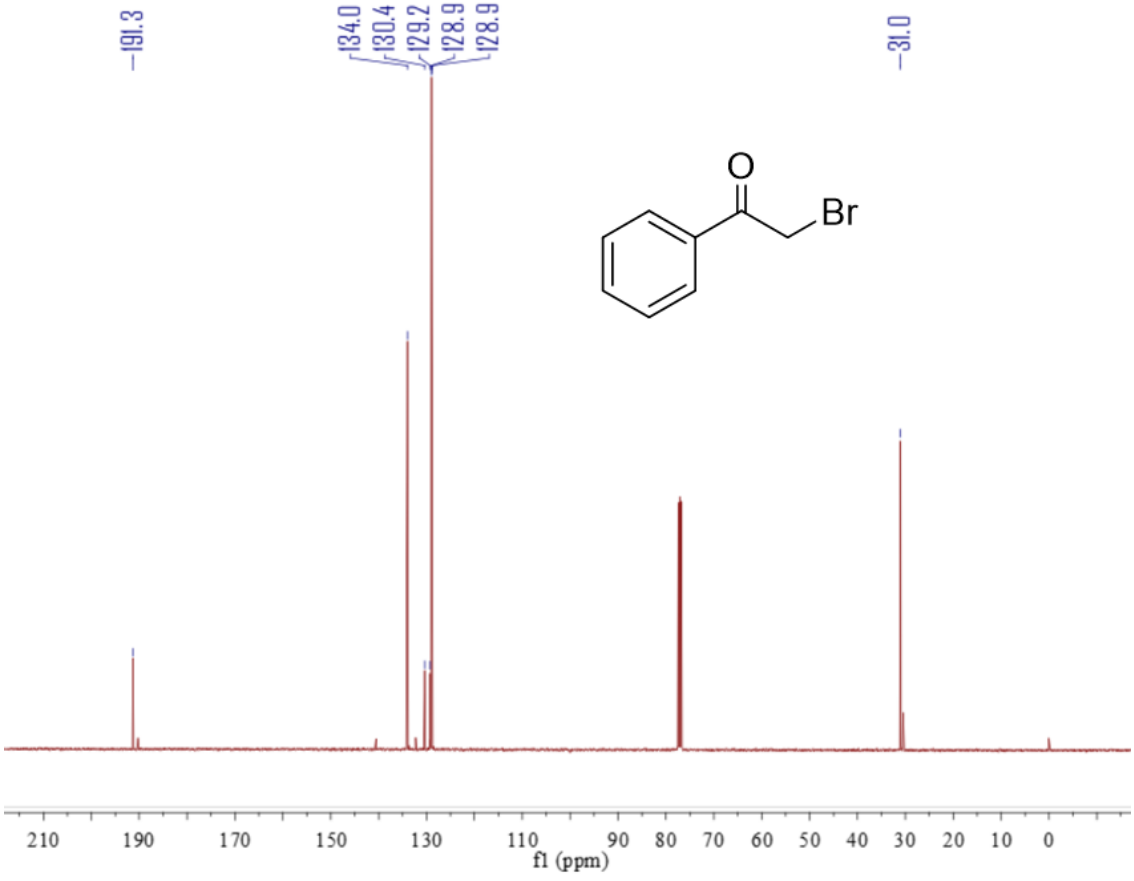
191.3
134.0
130.4
129.2
128.9
128.9
31.0
O
Br
210
190
170
150
130
110
90
80
70
60
50
40
30
20
10
0
f1 (ppm)

Compound 4r

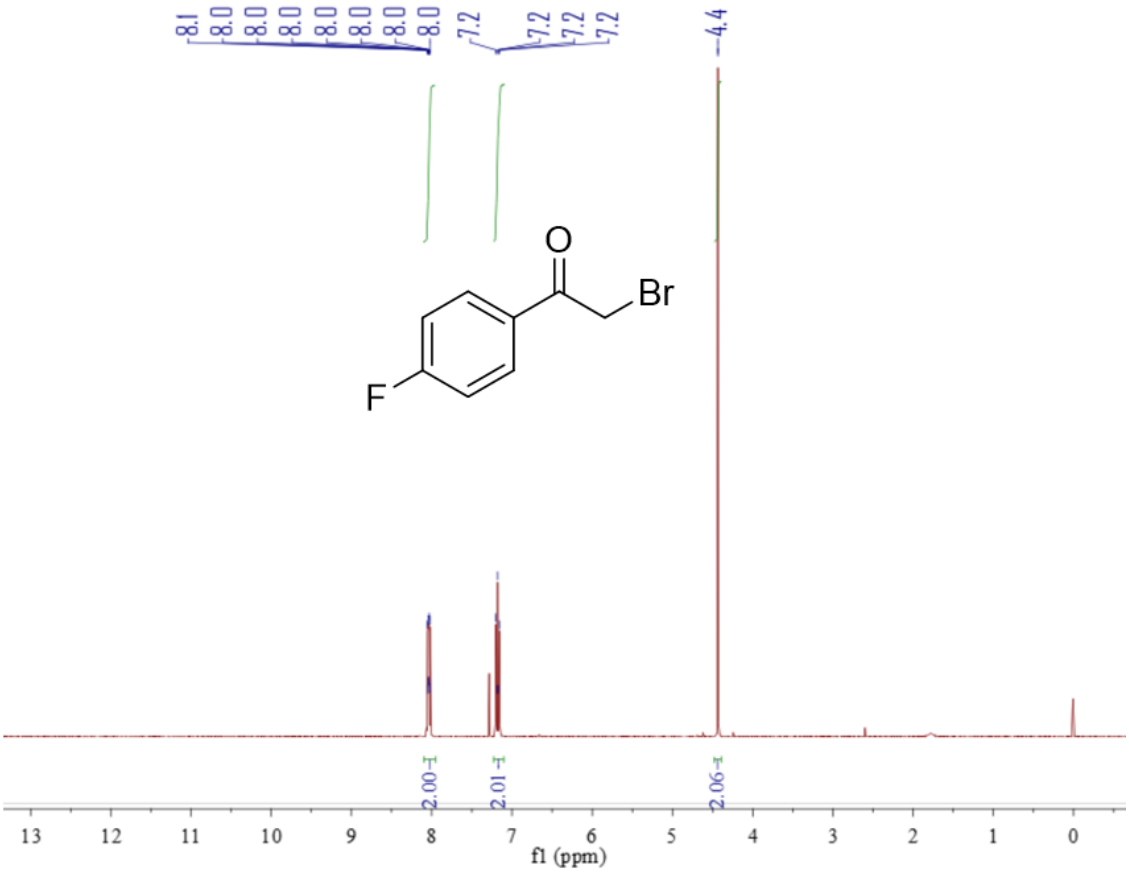
8.1
8.0
8.0
8.0
8.0
8.0
8.0
8.0
7.2
7.2
7.2
7.2
4.4
O
Br
F
2.00
2.01
2.06
13
12
11
10
9
8
7
6
5
4
3
2
1
0
f1 (ppm)

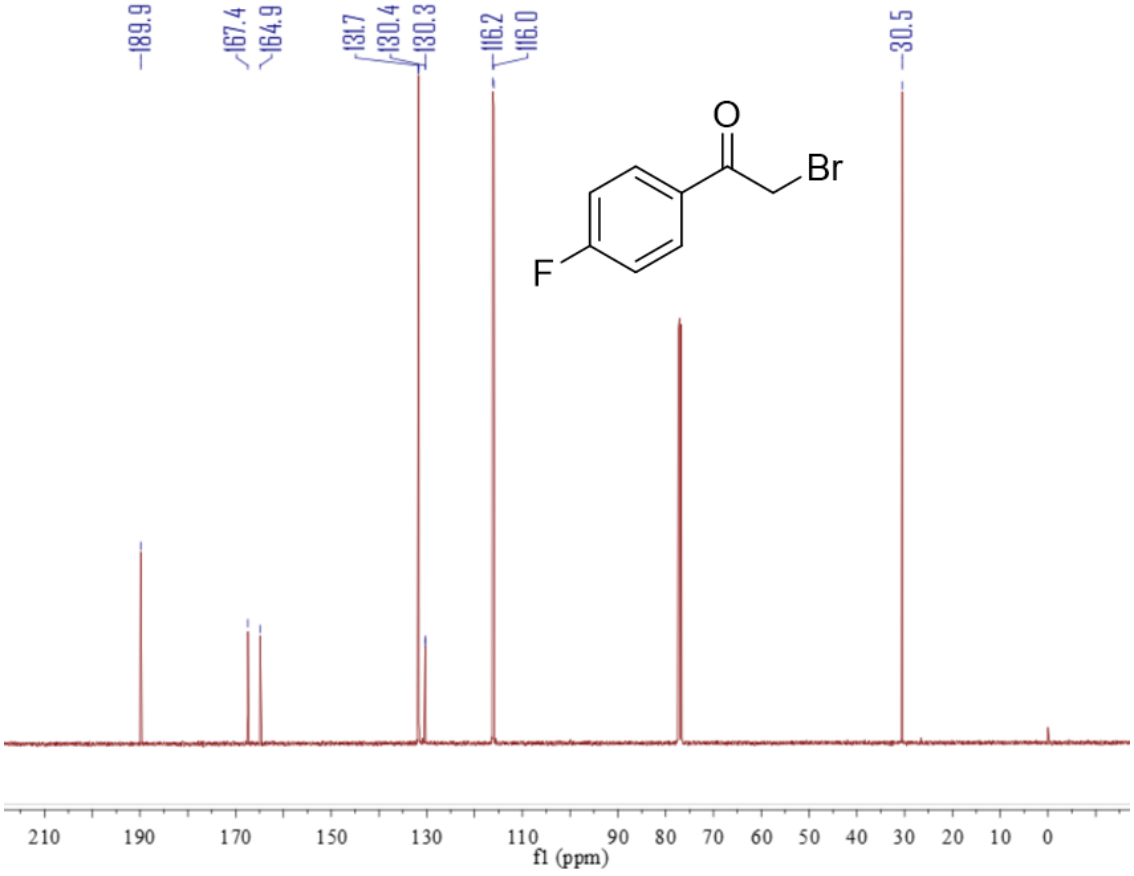
189.9
167.4
164.9
131.7
130.4
130.3
116.2
116.0
30.5
O
Br
F
210
190
170
150
130
110
90
80
70
60
50
40
30
20
10
0
f1 (ppm)

Compound 4s

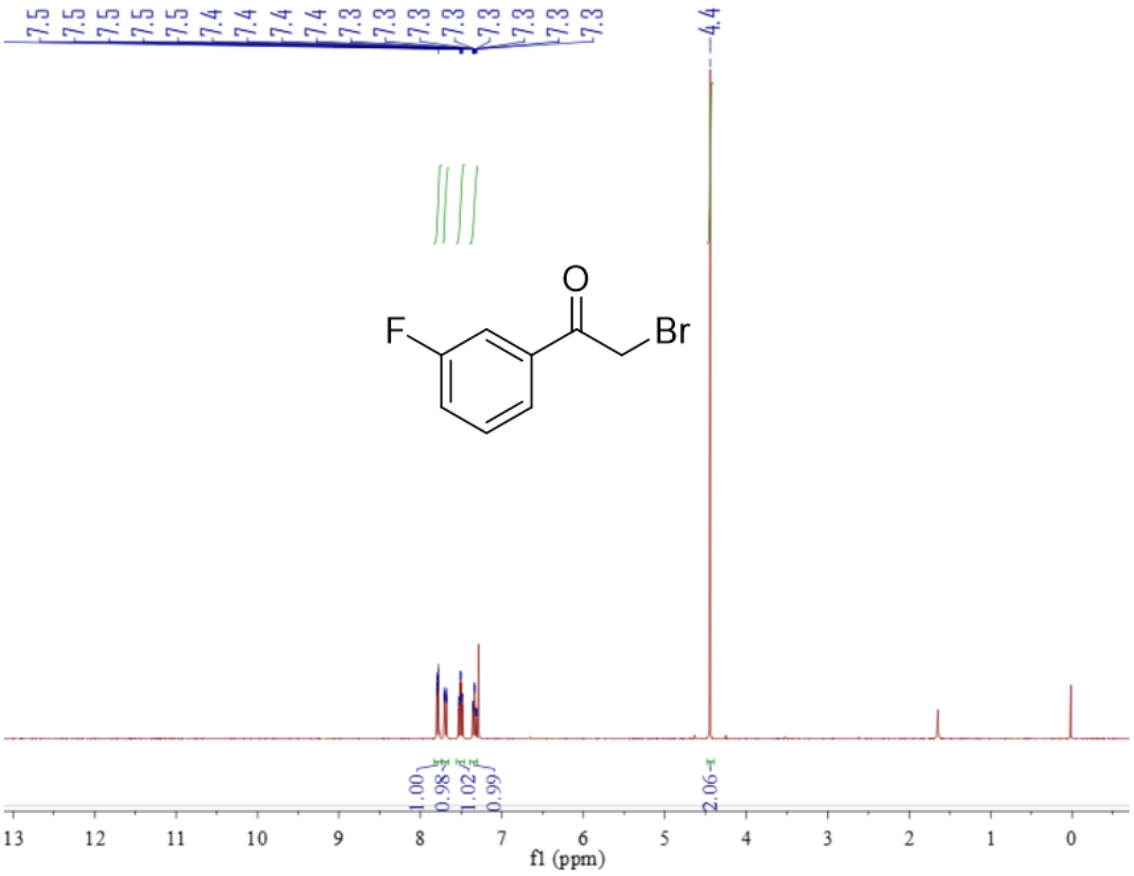
7.5
7.5
7.5
7.5
7.5
7.4
7.4
7.4
7.4
7.3
7.3
7.3
7.3
7.3
7.3
7.3
4.4
O
F
Br
1.00
0.98
1.02
0.99
2.06
13
12
11
10
9
8
7
6
5
4
3
2
1
0
f1 (ppm)

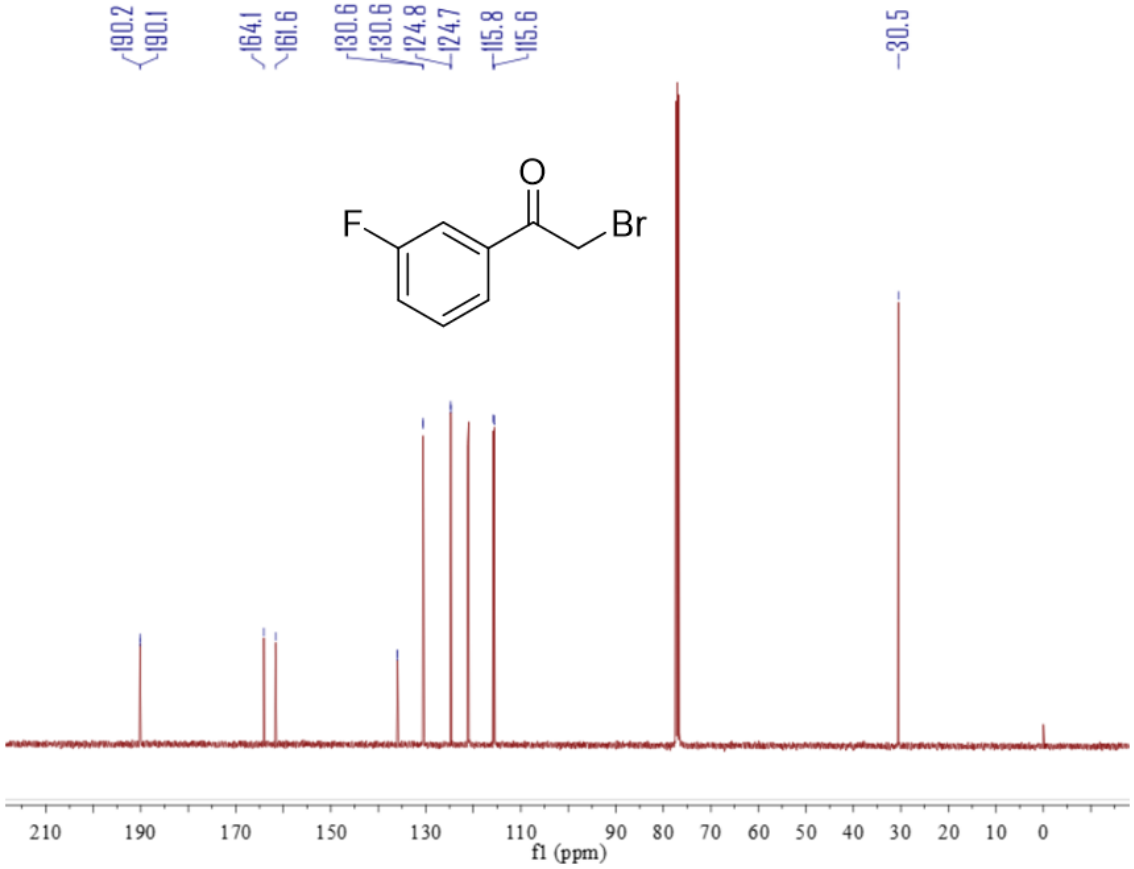
190.2
190.1
164.1
161.6
130.6
130.6
124.8
124.7
115.8
115.6
30.5
O
F
Br
210
190
170
150
130
110
90
80
70
60
50
40
30
20
10
0
f1 (ppm)

Compound 4t

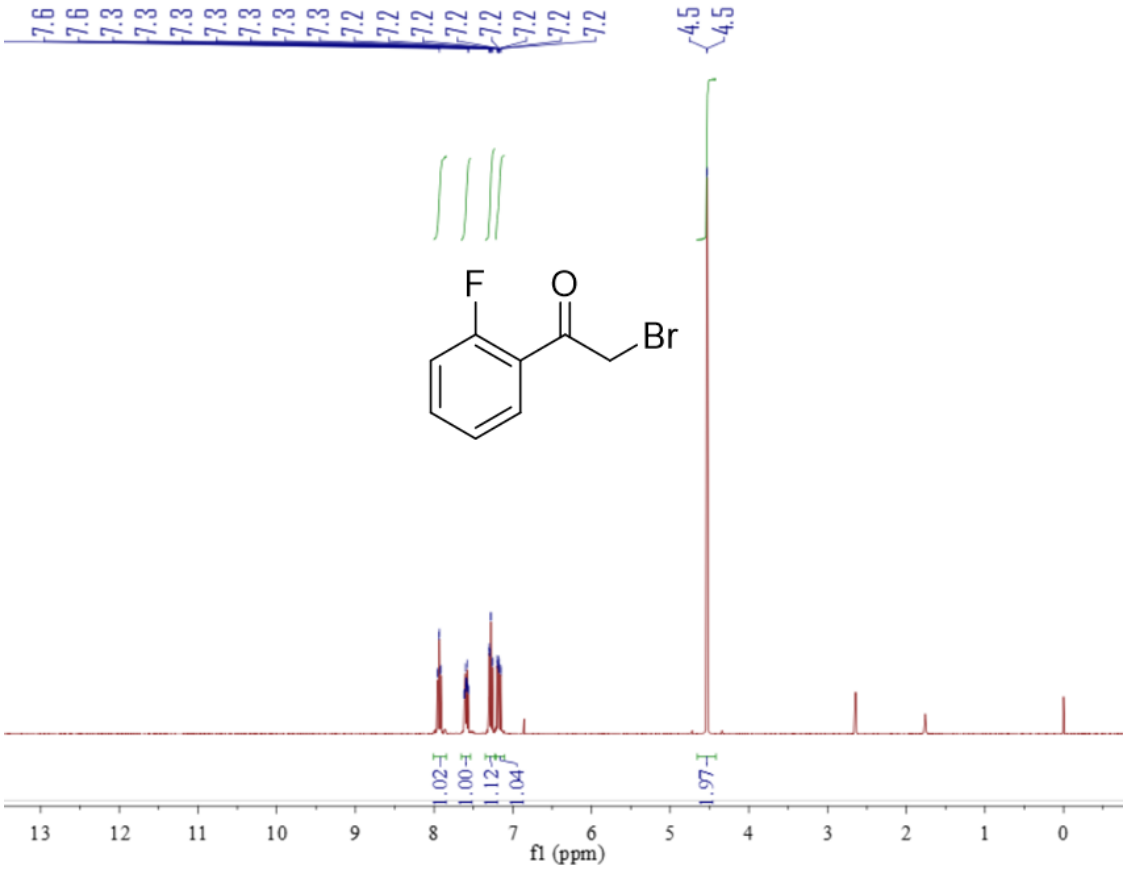
7.6
7.6
7.3
7.3
7.3
7.3
7.3
7.3
7.3
7.2
7.2
7.2
7.2
7.2
7.2
7.2
4.5
4.5
F
O
Br
1.02
1.00
1.12
1.04
1.97
13
12
11
10
9
8
7
6
5
4
3
2
1
0
f1 (ppm)

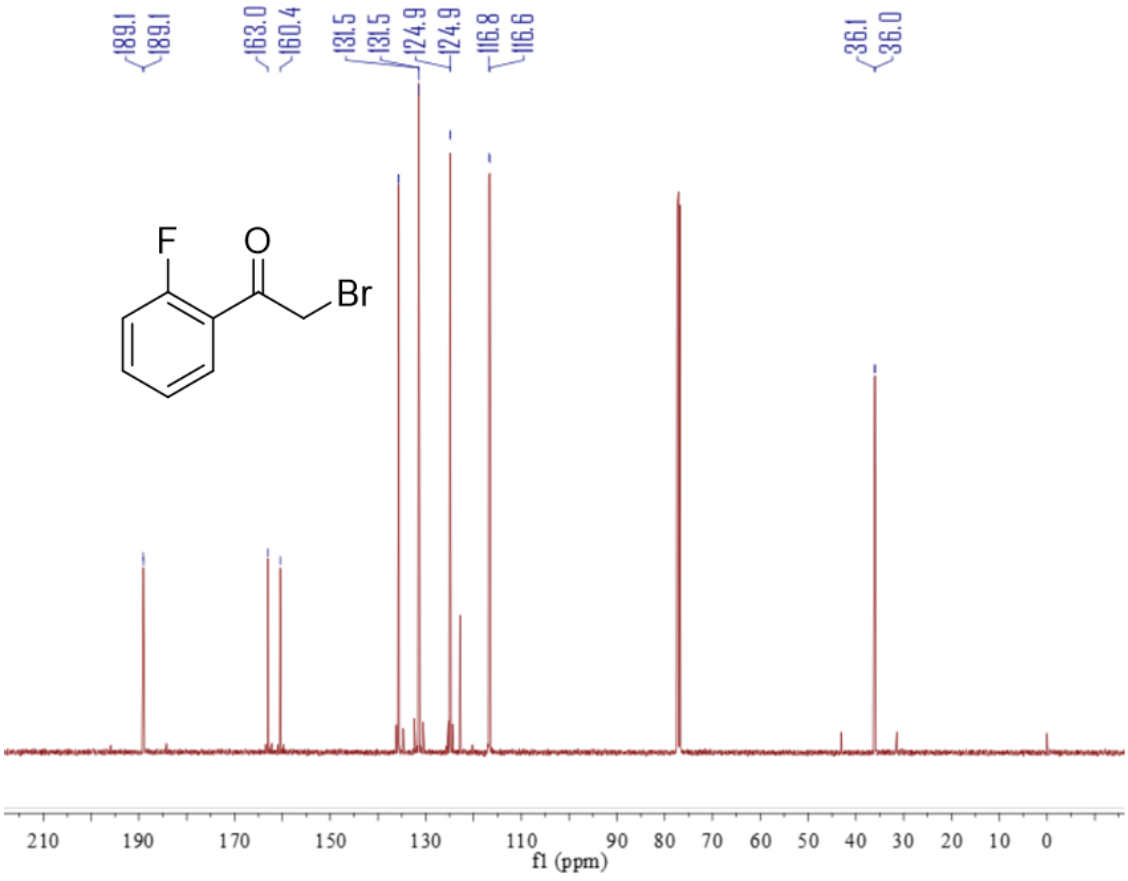
189.1
189.1
163.0
160.4
131.5
131.5
124.9
124.9
116.8
116.6
36.1
36.0
F
O
Br
210
190
170
150
130
110
90
80
70
60
50
40
30
20
10
0
f1 (ppm)

Compound 4u

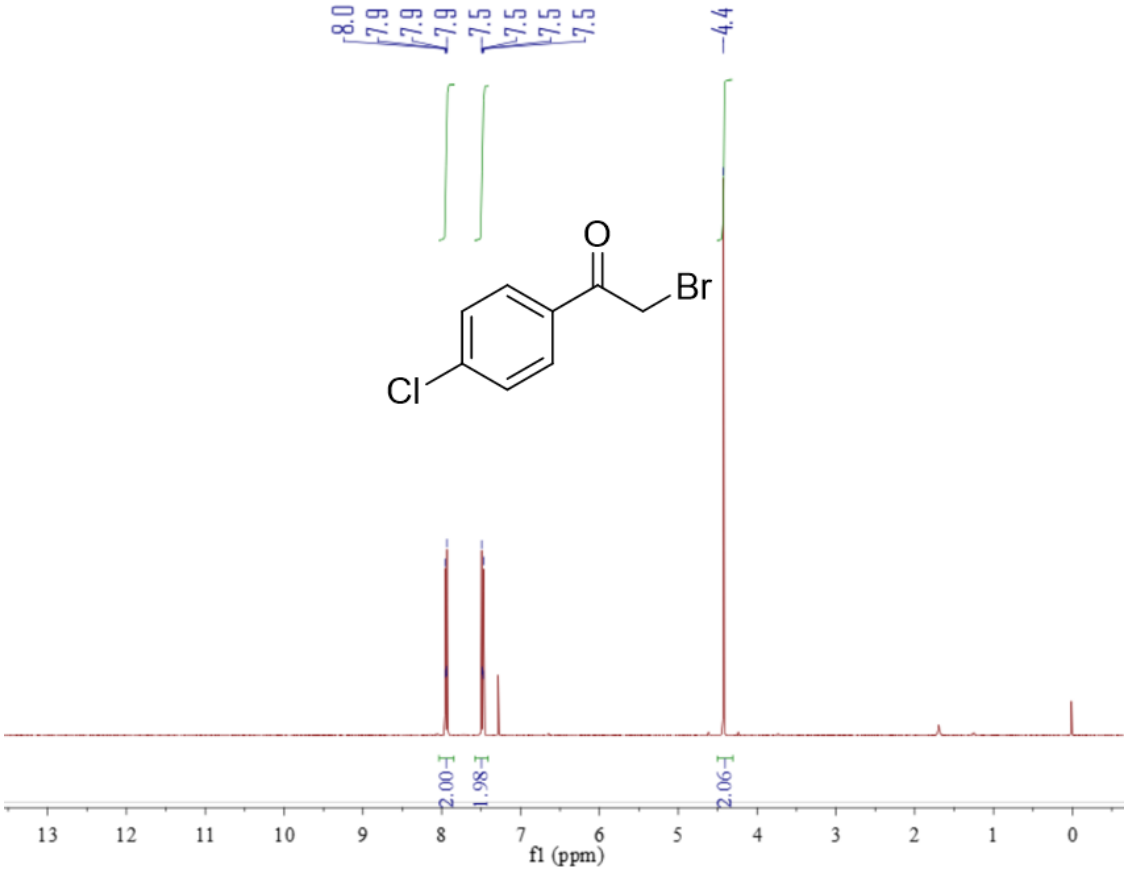
8.0
7.9
7.9
7.9
7.5
7.5
7.5
7.5
4.4
O
Br
Cl
2.00
1.98
2.06
13 12 11 10 9 8 7 6 5 4 3 2 1 0
f1 (ppm)

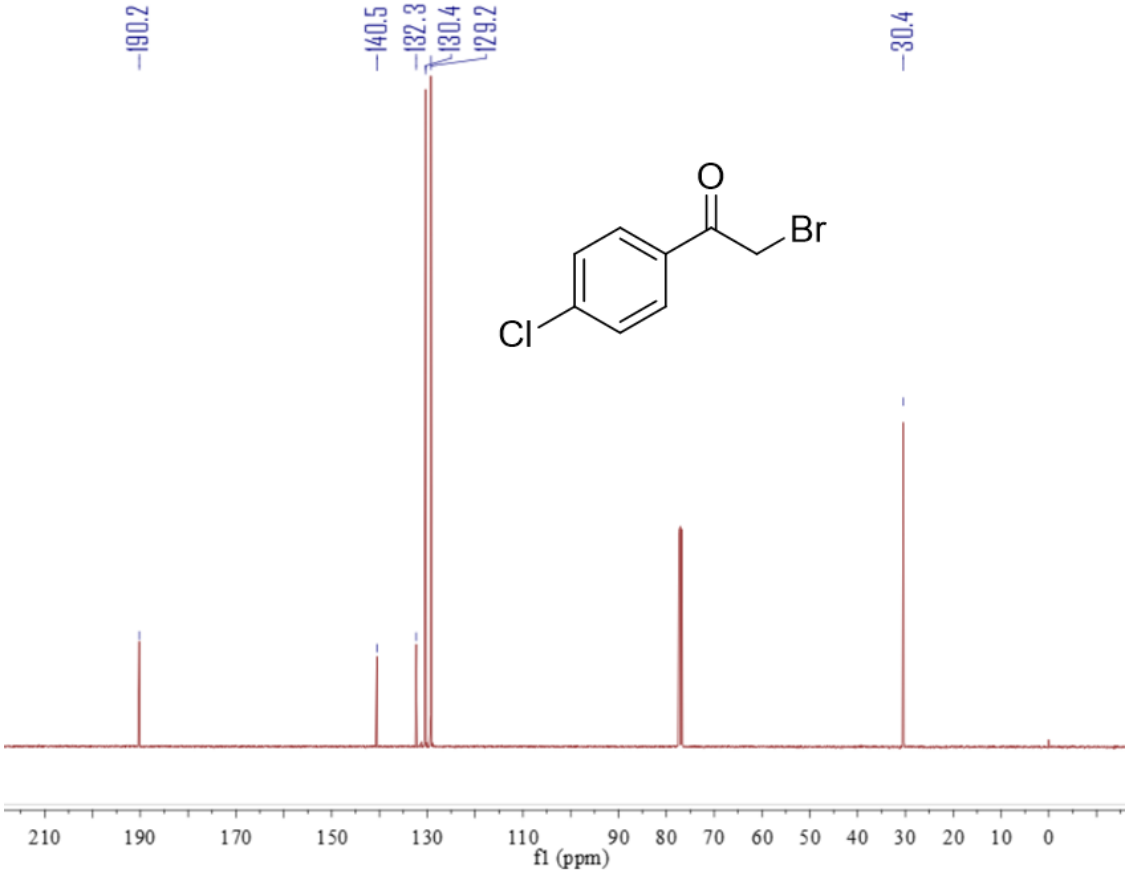
190.2
140.5
132.3
130.4
129.2
30.4
O
Br
Cl
210 190 170 150 130 110 90 80 70 60 50 40 30 20 10 0
f1 (ppm)

Compound 4v

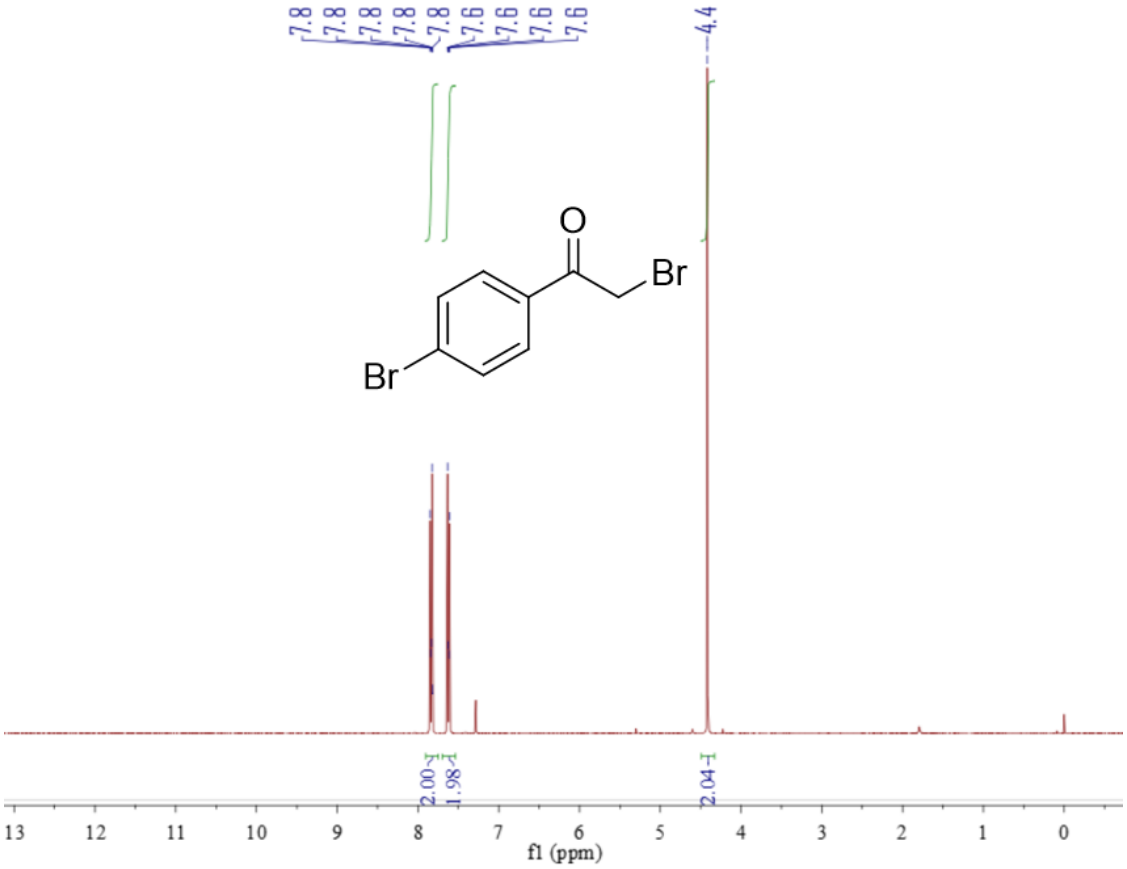
7.8
7.8
7.8
7.8
7.8
7.6
7.6
7.6
7.6
4.4
O
Br
Br
2.00
1.98
2.04
13
12
11
10
9
8
7
6
5
4
3
2
1
0
f1 (ppm)

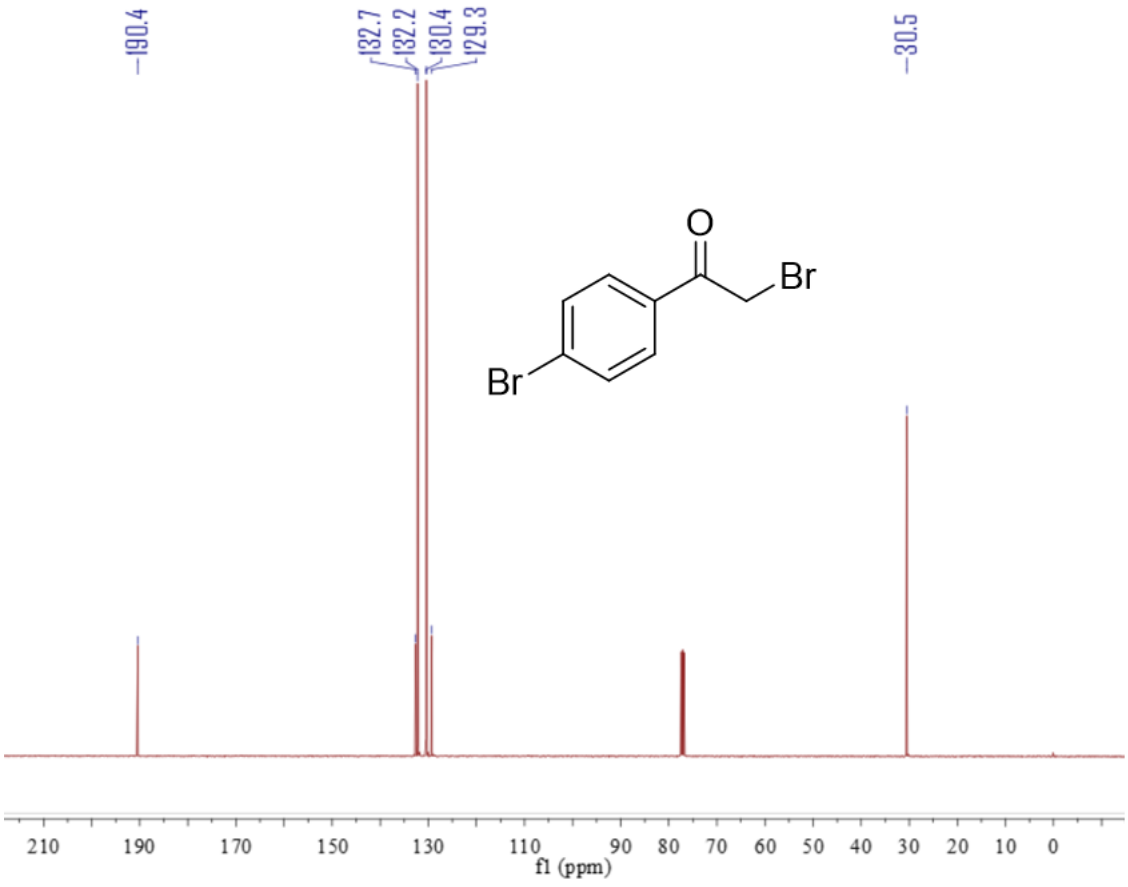
190.4
132.7
132.2
130.4
129.3
30.5
O
Br
Br
210
190
170
150
130
110
90
80
70
60
50
40
30
20
10
0
f1 (ppm)

Compound 4w

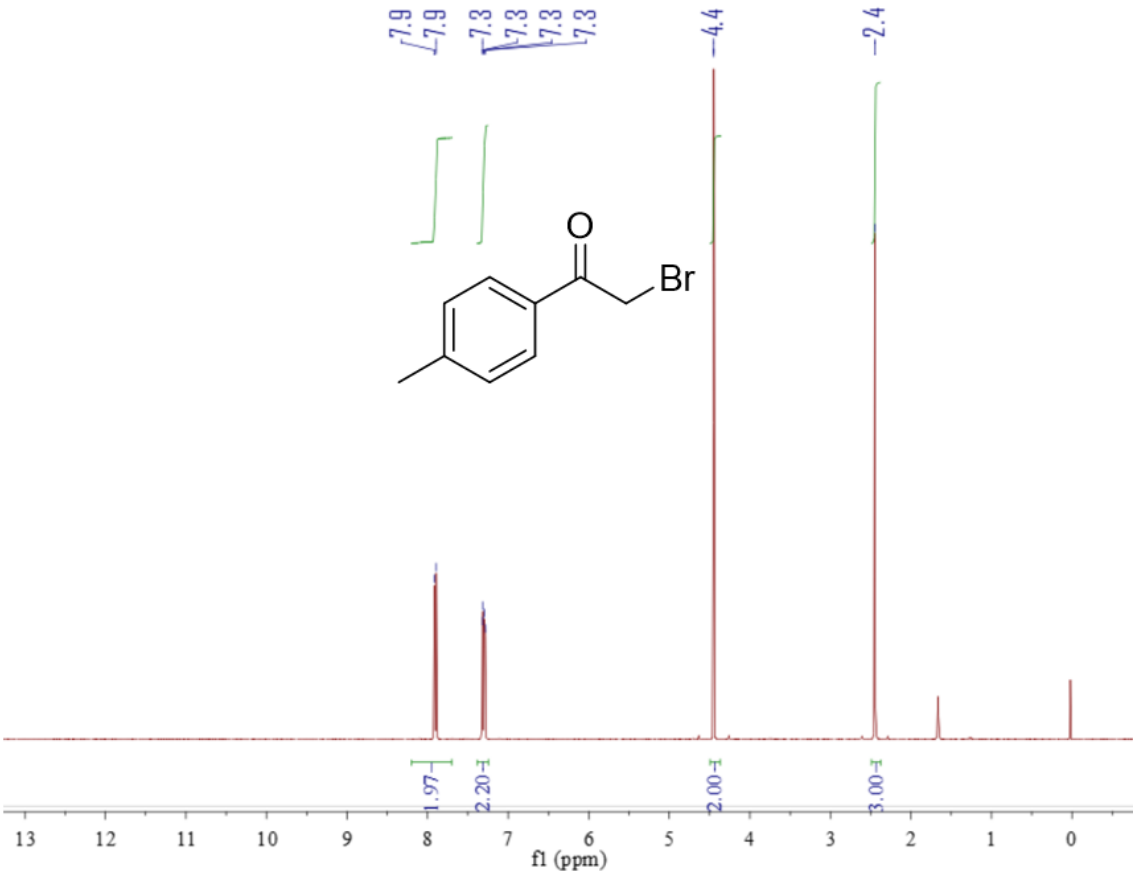
7.9
7.9
7.3
7.3
7.3
7.3
4.4
2.4
O
Br
1.97
2.20
2.00
3.00
13 12 11 10 9 8 7 6 5 4 3 2 1 0
f1 (ppm)

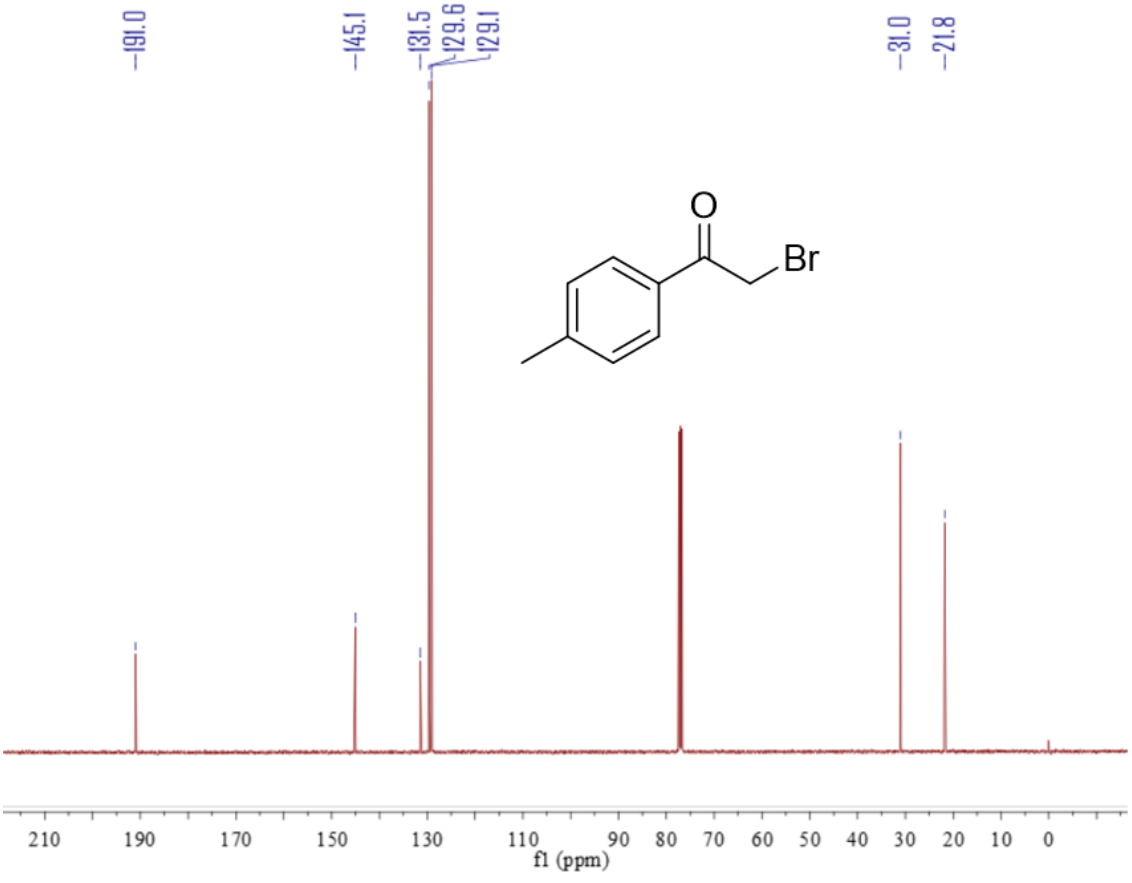
191.0
145.1
131.5
129.6
129.1
31.0
21.8
O
Br
210 190 170 150 130 110 90 80 70 60 50 40 30 20 10 0
f1 (ppm)